

Durham E-Theses

The crustal structure of the east Africa through earthquake seismology

P. K. H. Maguire

How to cite:

Maguire, P. K. H. (1974) The crustal structure of the east Africa through earthquake seismology. Doctoral thesis, Durham University.

Use policy

The full-text may be used and/or reproduced, and given to third parties in any format or medium, without prior permission or charge, for personal research or study, educational, or not-for-profit purposes provided that:

- a full bibliographic reference is made to the original source
- a <https://etheses.durham.ac.uk/id/eprint/10509/> is made to the metadata record in Durham E-Theses
- the full-text is not changed in any way

The full-text must not be sold in any format or medium without the formal permission of the copyright holders.

Please consult the [full Durham E-Theses policy](#) for further details.

EFFATA

Page A12 Line 6 'i' to read 'j'
Page A13 Lines 21, 22, 23 'δ' to read 'δ'
Page A14 Lines 1, 5, 6 'δ' to read 'δ'
Page A31 Line 22 'intergral' to read 'integral'
Page A49 Line 17 'headwaves' to read 'headwaves'



APPENDIX 1
THEORY

GENERAL SOLUTION OF THE WAVE EQUATION IN AN AXIALLY
SYMMETRIC CO-ORDINATE SYSTEM.

Consider a disturbance propagated in an elastic medium. If r , z and χ are the cylindrical co-ordinates, the z -axis vertically downward through the origin, and u and w are the displacements in the r and z directions, the resulting equations of motion will be independent of χ for an axially symmetric system.

Consider a compressional point source (i. e. SH waves will not be considered in the analysis. SV waves may be generated at interfaces in the medium.)

Defining a scalar potential ϕ and a vector potential ψ as follows:

$$u = \frac{\partial \phi}{\partial r} + \frac{\partial^2 \psi}{\partial r \partial z}$$

and
$$w = \frac{\partial \phi}{\partial z} + \frac{1}{r} \frac{\partial}{\partial r} \left(-r \frac{\partial \psi}{\partial r} \right)$$

The equations of motion are satisfied if ϕ and ψ are the solutions of the wave equations

$$\nabla^2 \phi = \frac{1}{\alpha^2} \frac{\partial^2 \phi}{\partial t^2} \quad \text{A1}$$

and
$$\nabla^2 \psi = \frac{1}{\rho^2} \frac{\partial^2 \psi}{\partial t^2}$$

where $\alpha = \sqrt{(\lambda + 2\mu) / \rho}$: the compressional wave velocity

and $\rho = \sqrt{(\mu / \rho)}$: the shear wave velocity.



λ and μ are Lame constants, while ρ is the density of the homogeneous medium. Only the potential $\phi(z, r, t)$ will be considered. The final required solutions to the wave equations A1 are in fact identical in form, although the intervening theory is slightly different. (see BERRY and WEST 1966)

$\phi(z, r, t)$ is defined in the time interval $(-\infty, \infty)$.

Taking Fourier Transforms with respect to t

$$\begin{aligned}\bar{\Phi}(z, r, w) &= \int_{-\infty}^{\infty} \phi(z, r, t) e^{iwt} dt \\ \phi(z, r, t) &= \int_{-\infty}^{\infty} \bar{\Phi}(z, r, w) e^{-iwt} dw\end{aligned}\quad \text{A2}$$

By substituting A2 into A1, it can be seen that $\bar{\Phi}(z, r, w)$ satisfies

$$\nabla^2 \bar{\Phi} = -k_{\nu}^2 \bar{\Phi} \quad \text{A3}$$

the time independent wave equation

$$\text{where } k_{\nu} = w/\nu$$

Now r is defined from 0 to $+\infty$.

Taking the Fourier-Bessel Transform with respect to r .

$$\begin{aligned}\bar{\bar{\Phi}}(z, k, w) &= \int_0^{\infty} \bar{\Phi}(z, r, w) J_n(kr) r dr \\ \bar{\Phi}(z, r, w) &= \int_0^{\infty} \bar{\bar{\Phi}}(z, k, w) J_n(kr) k dk.\end{aligned}\quad \text{A4}$$

(In an axially symmetric system $n = 0$).

Substituting A4 into A3

$$\left(\frac{\partial^2}{\partial r^2} + \frac{1}{r} \frac{\partial}{\partial r} + \frac{\partial^2}{\partial z^2} \right) \left(\int_0^\infty \bar{\Phi}(z, k, w) J_0(kr) k dk \right) \\ = -k_n^2 \int_0^\infty \bar{\Phi}(z, k, w) J_0(kr) k dk.$$

Hence since
$$\frac{\partial^2 J_0(kr)}{\partial r^2} + \frac{1}{r} \frac{\partial J_0(kr)}{\partial r} = -k^2 J_0(kr)$$

$$\frac{\partial^2 \bar{\Phi}}{\partial z^2} + (k_n^2 - k^2) \bar{\Phi} = 0$$

Hence
$$\bar{\Phi} = A(w, k) \exp[\pm i(k_n^2 - k^2)^{\frac{1}{2}} z]$$

Therefore

$$\bar{\Phi}(z, r, w) = \int_0^\infty A(w, k) \exp(\pm i k_n a z) J_0(kr) k dk \quad \text{A5}$$

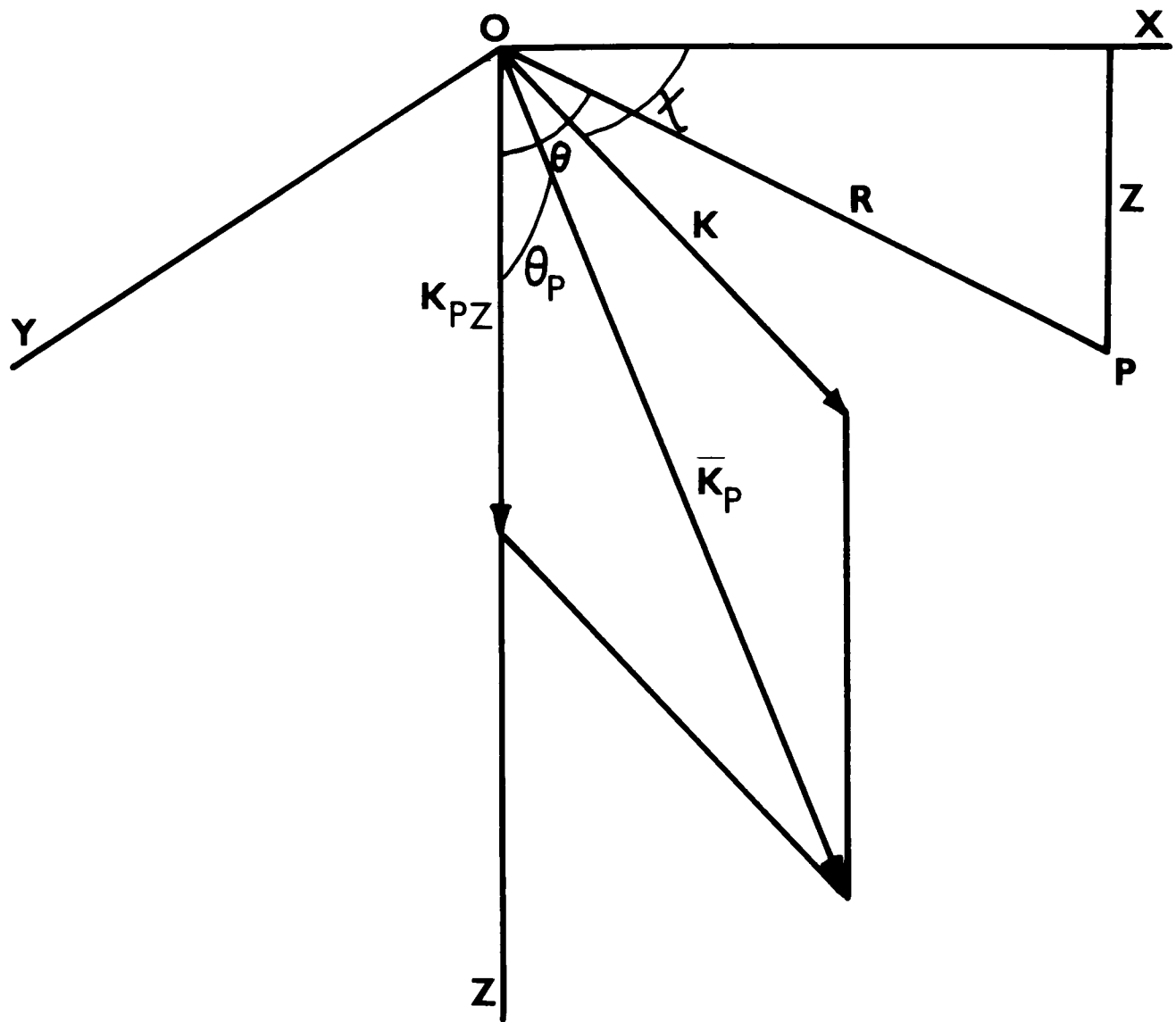
$$\text{where } a = (k_n^2 - k^2)^{\frac{1}{2}} / k_n^2$$

Since r is the radial co-ordinate k may be visualized as the radial component of the vector wave number \underline{k}_n (Fig. 53 from BERRY and WEST 1966).

i. e.
$$a = \frac{k_{\alpha z}}{k_n} \\ = \cos \theta_n$$

A5 is the general solution of the wave equation for an axially symmetric system.

Fig. 53. Coordinates of the field point P and wave vector \underline{k}_P .



INTERPRETATION OF THE GENERAL SOLUTION.

The integral representation of $J_n(x)$

$$J_n(x) = \frac{x^n}{2^{n-1} \Gamma(\frac{1}{2}) \Gamma(n+\frac{1}{2})} \int_0^{\pi/2} \cos(x \cos \theta) \sin^{2n} \theta \, d\theta$$

For $n = 0$

$$J_0(x) = \frac{2}{\pi} \int_0^{\pi/2} \cos(x \cos \theta) \, d\theta$$

or since $\int_0^{2\pi} \sin(x \cos \theta) \, d\theta = 0$

$$J_0(x) = \frac{1}{2\pi} \int_0^{2\pi} e^{ix \cos \theta} \, d\theta$$

Hence A5 may be written as

$$(z, r, w) = \frac{1}{2\pi} \int_0^{\infty} \int_0^{2\pi} A(w, k) \exp i(kr \cos \chi \left[\frac{1}{\alpha} + k \alpha z \right] k d \chi \left[\frac{1}{\alpha} \right] dk$$

$$\phi_1 = A(w, k) \exp i(kr \cos \chi \left[\frac{1}{\alpha} + k \alpha z \cos \theta \right] \alpha) \quad \text{A6}$$

when $\chi=0$ ϕ is the potential due to a plane wave travelling in the x - z plane. Therefore A6 may be considered to be the contribution to the potential at a point P in the x - z plane, due to a plane wave with wave vector \underline{k}_0 (Fig. 53).

THE SOURCE.

Assume a compressional point source. A difficulty arises if plane-layered media are to be considered in that the symmetry of the source and media are different. It is necessary to expand the initial spherical waves into a plane wave formulation.

Consider a source acting in a finite domain situated at the origin. Firstly the disturbance must vanish at infinity. Secondly no energy may be radiated from infinity into the region of the source.

A solution of the wave equation A3 satisfying these conditions is

$$\bar{\Phi}_0 = V_0(w) \frac{e^{-ik_\alpha R}}{R}$$

In cartesian wave-vector space

$$\bar{\Phi}_0 = \frac{iV_0(w)}{2\pi} \iiint_{-\infty}^{\infty} e^{i(k_{\alpha x} x + k_{\alpha y} y \pm k_{\alpha z} z)} \frac{dk_{\alpha x} dk_{\alpha y}}{k_{\alpha z}} \quad A7$$

(BATH 1968)

$$\begin{aligned} \text{Now } k_{\alpha x} &= k_\alpha \sin \theta_\alpha \cos \chi \\ k_{\alpha y} &= k_\alpha \sin \theta_\alpha \sin \chi \\ k_{\alpha z} &= k_\alpha \cos \theta_\alpha \end{aligned}$$

Integration with respect to χ is between 0 and 2π

Since, if 1) $k_{\alpha x} = k_{\alpha y} = 0$

$$k_{\alpha z} = k_\alpha$$

and 2) $k_{\alpha x}$ or $k_{\alpha y} = \pm k_\alpha$

$$k_{\alpha z} = i k_\alpha$$

Then, because $\cos \theta_\alpha = \frac{k_{\alpha z}}{k_\alpha}$

$$\theta_{\alpha'} \text{ will vary from } \theta_{\alpha'} = 0 \\ \text{to } \theta_{\alpha'} = \pi/2 - i\infty$$

Choosing the path of integration from 0 to $\pi/2$ along the real $\theta_{\alpha'}$ axis and then from $\pi/2$ to $-i\infty$ (see BATH 1968), A7 may be written

$$\Phi_0 = \frac{V_0(w)}{2\pi} i k_{\alpha'} \int_0^{\pi/2-i} \int_0^{2\pi} e^{i(k_{\alpha'x} x + k_{\alpha'y} y + k_{\alpha'z} z)} \sin\theta_{\alpha'} \delta\theta_{\alpha'} \delta\chi' \quad \text{A8}$$

Thus in addition to the waves propagated in all directions, there will also be waves corresponding to complex values of $\theta_{\alpha'}$. These waves propagate in the x-y plane with a wavelength tending to zero and simultaneously attenuating in the z-direction.

Introducing polar coordinates in the x-y plane

$$x = r \cos \xi \\ y = r \sin \xi$$

Then since

$$\sin \theta_{\alpha'} d\theta_{\alpha'} = \frac{k dk}{k_{\alpha'}^2 a}$$

$$\text{and } \frac{1}{2\pi} \int_0^{2\pi} e^{ikr \cos(\chi^1 - \xi)} d\chi^1 \\ = \frac{1}{2\pi} \int_0^{2\pi} e^{ikr \cos(\chi^1 - \xi)} d(\chi^1 - \xi)$$

Since the integration is over all wave numbers $k_{\alpha'}$ for a given direction ξ

$$= J_0(kr)$$

(see INTERPRETATION OF
GENERAL SOLUTION)

$$\bar{\Phi}_0 = \int_0^{\infty} \frac{V_0(w) J_0(kr) e^{\pm i k_{\nu} a z}}{(-i k_{\nu} a)} dk$$

This represents the potential due to a point source provided that wavelengths are small compared with the distance to the nearest boundary (EWING et al 1957).

A SINGLE INTERFACE.

Assume two semi-infinite media in welded contact, the plane of intersection being at a depth h below the origin (or source). Let the upper medium parameters be $\alpha_1, \beta_1, \rho_1$ and the lower medium parameters be $\alpha_2, \beta_2, \rho_2$. Imposing the conditions that since the disturbance acts in a finite domain, it must vanish at infinity, and also that no energy may be radiated from infinity into the region of the source.

For $z \leq h$

$$\begin{aligned} \bar{\Phi}_1 = & \int_0^{\infty} V_0(w) (-i k_{\alpha_1} a_1)^{-1} \exp(i k_{\alpha_1} a_1 |z|) k J_0(kr) dk \\ & + \int_0^{\infty} G_1(w, k) \exp(-i k_{\alpha_1} a_1 z) J_0(kr) k dk \end{aligned}$$

For $z > h$

$$\bar{\Phi}_2 = \int_0^{\infty} G_2(w, k) \exp(i k_{\alpha_2} a_2 z) J_0(kr) k dk$$

A9

where $\bar{\Phi}_1$ and $\bar{\Phi}_2$ are the displacement potentials in the two media. G_1 and G_2 are obtained by imposing the boundary conditions, continuity of displacement and stress, at the interface. These necessarily imply introduction of the potentials $\bar{\Psi}_1$ and $\bar{\Psi}_2$, as the

boundary conditions for two solid elastic media are dependent on both $\bar{\Phi}$ and $\bar{\Psi}$. On inserting the expressions for $\bar{\Phi}$ and $\bar{\Psi}$ into the boundary condition equations, a system of four linear equations is obtained for the functions

$$\hat{G}_1 = G_1 \exp(-i k_{\alpha_1} a_1 h)$$

$$\hat{G}_2 = G_2 \exp(i k_{\alpha_2} a_2 h)$$

and the equivalent two $\bar{\Psi}$ displacement coefficients.

We may write

$$G_1 = R_{p_1 p_1} \left\{ \frac{V_o(w)}{(-i k_{\alpha_1} a_1)} \exp(i k_{\alpha_1} a_1 h) \right\} \exp(i k_{\alpha_1} a_1 h)$$

$$\text{and } G_2 = T_{p_1 p_2} \left\{ \frac{V_o(w)}{(-i k_{\alpha_1} a_1)} \exp(i k_{\alpha_1} a_1 h) \right\} \exp(-i k_{\alpha_2} a_2 h)$$

Thus for $z \geq 0$

$$\begin{aligned} \bar{\Phi}_1 = & \int_0^{\infty} \frac{V_o(w)}{(-i k_{\alpha_1} a_1)} \exp(i k_{\alpha_1} a z) J_0(kr) k dk \\ & + \int_0^{\infty} \frac{V_o(w)}{(-i k_{\alpha_1} a_1)} \left[R_{p_1 p_1} \right] \exp i \left[k_{\alpha_1} a_1 h + k_{\alpha_1} a_1 (h-z) \right] J_0(kr) k dk \end{aligned}$$

$$\text{and } \bar{\Phi}_2 = \int_0^{\infty} \frac{V_o(w)}{(-i k_{\alpha_1} a_1)} \left[T_{p_1 p_2} \right] \exp i \left[k_{\alpha_1} a_1 h - k_{\alpha_2} a_2 (h-z) \right] J_0(kr) k dk$$

A10

The first term in equation A10 represents the direct compressional wave. The other terms (including also those in the $\bar{\Psi}$ potentials) represent waves generated in the two media by the

interaction of the direct wave with the interface.

If the integrands in A10 are interpreted as in the INTERPRETATION OF THE GENERAL SOLUTION, firstly it is seen that R and T are the reflection and transmission coefficients for plane waves. They are functions of k , the density of the two media and the compressional (and shear) wave velocities in the two media. Secondly, the individual integrals in equation A10 represent the displacement potentials due to all waves travelling from the source to the receiver, not only the ray following the least time path, but also headwaves and rays following non-least-time paths. For example the displacement potential, $\bar{\Psi}_1$, would be due to all waves travelling from a source in medium 1 as a compressional wave, incident on the interface, and subsequently radiated from the interface as an S wave.

N-LAYERED HALF SPACE.

From equation A10, it can be seen that at the interface, the integrands in the expressions for the transmitted and reflected P-waves, and the incident P wave differ only by a factor which is independent of the source. Thus the terms describing the reflected and transmitted waves may be constructed from the terms which describe the incident waves. Each time a wave component is incident on an interface, four new components are generated, and together these five components must completely satisfy the boundary conditions at that interface. If there is more than one boundary the total number of generated waves is infinite. SPENCER (1960) introduced the concept of a 'generalized ray path'. By starting with the source potential, the displacement potential at the receiver may be determined due to a generalized ray path, built up as a system of individual ray components in each layer of a multilayered medium. Each component is specified only by the mode and direction of propagation across adjacent pairs of interfaces. Thus for example, the displacement potential at the receiver, due to

a $P_1 P_2 P_3 P_3 S_2 P_1$ reflected wave (including all waves which fall into this category) originating from a source in the uppermost layer with focal depth z (see Fig. 54), is given by

$$\bar{\Phi} = \int_0^{\infty} \frac{V_0(w)}{(-ik \quad a_1)} \left(T_{P_1 P_2}(k) T_{P_2 P_3}(k) R_{P_3 P_3}(k) T_{P_3 S_2}(k) T_{S_2 P_1}(k) \right) \exp i \left(k \alpha_1 a_1 (h_1 - z) + k \alpha_2 a_2 h_2 + k \alpha_3 a_3 h_3 + k \alpha_3 a_3 h_3 + k \alpha_2 b_2 h_2 + k \alpha_1 a_1 h_1 \right) J_0(kr) k dk \quad A11$$

It is such an equation as A11 that needs to be evaluated in order to determine the displacement at the surface due to all the waves following a generalized ray path.

It is convenient to transform A11 by changing the limits of integration and replacing the Bessel Function by Hankel Functions.

$$J_0(kr) = \frac{1}{2} [H_0^{(1)}(kr) + H_0^{(2)}(kr)] \quad A12$$

Substituting A12 into A11 we obtain the potential as a sum of two integrals

In the integral containing $H_0^{(2)}(kr)$ replace k by $-k$.

$$\bar{\Phi} = \int_0^{\infty} f(k) dk - \int_{-\infty}^0 f^1(-k) dk$$

$$\begin{aligned} \text{But } H_0^{(2)}(-x) &= H_0^{(2)}(e^{-i\pi} x) \\ &= -H_0^{(1)}(x) \quad (\text{WATSON 1952}) \end{aligned}$$

$$\text{and } T(k) = T(-k), \quad R(k) = R(-k)$$

(BREKHOVSKIKH 1960)

Hence in the example A11

$$\begin{aligned}
&= \frac{1}{2} \int_{-\infty}^{\infty} \frac{V_o(w)}{(-ik a_1)} (T_{P_1 P_2}(k) T_{P_2 P_3}(k) R_{P_3 P_3}(k) T_{P_3 S_2}(k) T_{S_2 P_1}(k)) \\
&\exp i (k_{\alpha_1} a_1 (h-z) + k_{\alpha_2} a_2 h_2 + k_{\alpha_3} a_3 h_3 + k_{\alpha_3} a_3 h_3 + k_{\alpha_2} b_2 h_2 \\
&\quad + k_{\alpha_1} a_1 h) H_o^{(1)}(kr) k dk
\end{aligned} \tag{A13}$$

In order to solve A13, we assume that

$$k_{\alpha_1} r \gg 1$$

i. e. that the distance from the source to the point of observation (and the dimensions of the model) are large compared with the wavelength of the waves contributing to the integral.

In which case the Hankel function in A13 may be replaced by its asymptotic approximation.

$$H_o^{(1)}(kr) \longrightarrow \frac{2}{\sqrt{\pi kr}} \exp i(kr - \pi/4)$$

$$\text{Let } p = k/k_{\alpha_1} = \sin \theta_1$$

$$dp = \frac{dk}{k_{\alpha_1}}$$

By transferring the origin to the source, with h_1 the vertical distance from the source to the first boundary (renumbering the layers accordingly if the source is in a different layer from the receiver)

$$\text{since } \frac{k_{\alpha_n}}{k_{\alpha_1}} = \frac{\sin \theta_1}{\sin \theta_{\alpha_n}} = \frac{\alpha_1}{\alpha_n}$$

which shall be defined as V_n

Then we may say (for the case in question)

$$\begin{aligned} & \exp i(k_{\alpha_1} a_1 h_1 + k_{\alpha_2} a_2 h_2 + k_{\alpha_3} a_3 h_3 + k_{\alpha_3} a_3 h_3 + k_{\beta_2} b_2 h_2 \\ & \qquad \qquad \qquad + k_{\alpha_1} a_1 (h_1 + z)) \\ & = \exp i k_{\alpha_1} \sum_{i=1}^6 \frac{h_i (1-p^2 V_i^2)^{\frac{1}{2}}}{V_i} \end{aligned}$$

where

i = 1, 2, 3	i = 4	i = 5	i = 6
$V_j = \alpha_j / \alpha_1$	α_3 / α_1	β_2 / α_1	1
$h_j = h_j$	h_3	h_2	$h_1 + z$

$$\begin{aligned} \bar{\Phi} &= \frac{1}{2} \int_{-\infty}^{\infty} \frac{V_o(w)}{(-ik_{\alpha_1} a_1)} (T(p)R(p)) \exp i k_{\alpha_1} \left\{ \sum_{i=1}^6 \frac{h_i (1-p^2 V_i^2)^{\frac{1}{2}}}{V_i} \right\} \sqrt{\frac{2}{\pi k r}} \\ & \qquad \qquad \qquad \exp i(kr - \pi/4) k_{\alpha_1}^2 p dp \\ &= V_o(w) e^{i\pi/4} \sqrt{\frac{k_{\alpha_1}}{2\pi r}} \int_{-\infty}^{\infty} T(p)R(p) \exp i k_{\alpha_1} \left\{ \sum_{i=1}^6 h_i \frac{(1-p^2 V_i^2)^{\frac{1}{2}}}{V_i} + pr \right\} \\ & \qquad \qquad \qquad \left(\frac{p^2}{1-p^2} \right)^{\frac{1}{2}} dp \end{aligned}$$

A14

A14 may be evaluated at distances from the source which are large compared to the wavelength by the method of steepest descent. The integral is evaluated in such a way that only those waves travelling in the direction of the geometrical ray path contribute substantially to the integral. A14 may be represented as

$$I = \int_C \exp[\ell f(p)] F(p) dp \quad \text{A15}$$

where $\ell = k_{\alpha_1}$ is large, real and positive. $f(p)$, $F(p)$ are analytic functions of the complex variable p , and C is the path of integration in the complex plane.

This path can be deformed, without changing the value of the integral. Using this fact, we try to select a path such that the entire value of the integral is determined by a comparatively short portion of the path. Then the integrand is replaced by a simpler function which coincides sufficiently closely with the integrand over the essential portion of the path. The behaviour of the function over the remaining portions of the path is of no concern.

$$\text{Now } f(p) = f_1(p) + if_2(p)$$

$$p = x + iy$$

The integrand in A15, containing

$$\exp \ell f_1(p) \exp i \ell f_2(p)$$

will be large when $f_1(p)$ is large.

If we choose C such that the largest values of $f_1(p)$ are located as close to each other as possible, then an approximate value of the integral can be obtained by carrying out the integration only over the largest values of $f_1(p)$.

$$\frac{\delta f}{\delta x} = \frac{df}{dp} \cdot \frac{\delta p}{\delta x} = \frac{df}{dx} = \frac{\delta f_1}{\delta x} + i \frac{\delta f_2}{\delta x}$$

$$\frac{\delta f}{\delta y} = \frac{df}{dp} \cdot \frac{\delta p}{\delta y} = i \frac{df}{dx} = \frac{\delta f_1}{\delta y} + i \frac{\delta f_2}{\delta y}$$

$$\text{Hence } \frac{\delta f_1}{\delta x} = \frac{\delta f_2}{\delta y}$$

$$\frac{\delta f_1}{\delta y} = -\frac{\delta f_2}{\delta x}$$

The Cauchy-Riemann conditions.

We define the path of integration as

1) passing through the stationary (maximum) point of f_1 where $p = p_0$

$$\text{i. e. } df_1 = \frac{\delta f_1}{\delta x} dx + \frac{\delta f_2}{\delta y} dy = 0$$

or where $\frac{\delta f_1}{\delta x} = \frac{\delta f_2}{\delta y} = 0$ for any values of dx, dy .

(The point p_0 represents a saddle point in the space of the complex variable, since the modulus of an analytic function cannot have a local maximum within the region of analyticity of the function).

2) directed along the maximum negative gradient of f_1 . But the real and imaginary parts of an analytic function have the property that in the space of the complex variable, the lines of most rapid decrease of one part are lines of constant values of the other.

i. e. along the contour C

$$f_2 = \text{constant}$$

We wish to determine the point p_0 , which must be known for the evaluation of A15.

At this point

$$\left. \frac{df(p)}{dp} \right|_{p=p_0} = 0$$

Expanding $f(p)$ about p_0 as

$$\begin{aligned} f(p) &= f(p_0) + (p - p_0)f'(p_0) + \frac{1}{2}(p - p_0)^2 f''(p_0) + \dots \\ &= f(p_0) + \frac{1}{2}(p - p_0)^2 f''(p_0) + \dots \end{aligned}$$

$$\text{Let } p - p_0 = r e^{i\gamma}$$

$$\text{and } \frac{1}{2}f''(p_0) = F e^{i\delta}$$

Since f_2 is constant along the path of integration

$$\begin{aligned} \oint_m [f(p) - f(p_0)] &= \int_m (Rr^2 e^{i(2\gamma + \delta)}) \\ &= 0 \end{aligned}$$

$$\text{i. e. } \sin(2\gamma + \delta) = 0$$

$$\text{or } \gamma = -\frac{\delta}{2} + \frac{n\pi}{2}$$

A16 (n integer)

γ is defined as the direction the path of integration makes with the positive x -axis in the vicinity of the saddle point.

But A16 defines two lines at right angles (4 values of γ differing by $\pi/2$).

The path of the steepest descent is such that the second derivative of $f(p)$ $_{p=p_0}$ is real and negative (real, since along the path, f_2 is constant).

Hence $(p - p_0)^2 f''(p_0)$ is also real and negative along the path.

Hence from a similar analysis to that leading to A16, we find that $n = 2k + 1$ (k integer) defining one line (in two directions differing by π).

$$\begin{aligned} \text{Let } \chi^2 &= -\frac{1}{2}(p - p_0)^2 f''(p_0) \\ &= \frac{1}{2} \left| r^2 e^{2i\gamma} f''(p_0) \right| \\ &= \frac{1}{2} r^2 \left| f''(p_0) \right| \quad \text{since } \left| e^{2i\gamma} \right| = 1 \end{aligned}$$

$$\text{i. e. } = \frac{\pm r}{\sqrt{2}} \left| f''(p_0) \right|^{\frac{1}{2}}$$

$$\text{and } \frac{d\chi}{dp} = \pm \frac{e^{i\gamma}}{\sqrt{2}} \left| f''(p_0) \right|^{\frac{1}{2}}$$

Hence we may write equation A15

$$I = e^{f(p_0)} \int_C e^{-\chi^2} F(p) \frac{dp}{d\chi} d\chi$$

Assuming $F(p)$ is a slowly varying function in the region of interest, and taking only the first term in the series expansion

$$I = e^{f(p_0)} F(p_0) \sqrt{2} e^{i\gamma} \left| f''(p_0) \right|^{-\frac{1}{2}} \int_C e^{-\chi^2} d\chi$$

C extends from $-\infty$ to ∞

$$\text{but } \int_{-\infty}^{\infty} e^{-\chi^2} d\chi = \sqrt{\pi/e}$$

$$F(p_0) \sqrt{2\pi} e^{i\gamma} e^{f(p_0)}$$

$$\text{Hence } I = \frac{F(p_0) \sqrt{2\pi} e^{i\gamma} e^{f(p_0)}}{\left(e \left| f''(p_0) \right| \right)^{\frac{1}{2}}} \quad \text{A17}$$

$$\text{where } \gamma = -\delta/2 \pm \pi/2$$

In the present case, equation A14, since $\delta = \arg f''(p_0)$ and $f''(p_0)$ is real and negative and equal to $ig''(p_0)$

$$\delta = -\pi/2, 3\pi/2$$

Thus $\gamma = -\pi/4, 3\pi/4$ in the neighbourhood of p_0 .

As long as the contour of integration can be deformed to pass through the saddle point p_0 , defined by $f'(p_0) = 0$, along the path of steepest descent, inclined at an angle $-\pi/4$ to the Real p axis, equation A14 may be evaluated to give (from A17)

$$\bar{\Phi} = V_0(w) e^{i\pi/4} \sqrt{\left(\frac{k}{2\pi r} \right)} \left[T(p_0) R(p_0) \right] \left(\frac{p_0}{1-p_0} \right)^{\frac{1}{2}} \sqrt{2\pi} e^{-i\pi/4}$$

$$\begin{aligned}
& \exp k_{\alpha_1} \left[i \sum_{j=1}^6 \frac{h_j (1 - p_o^2 V_j^2)^{\frac{1}{2}}}{V_j} + p_o r \right] \\
& \left(k_{\alpha_1} \left| -i \sum_{j=1}^6 \frac{h_j V_j p_o (1 - p_o^2 V_j^2)^{-3/2}}{p_o} \right. \right)^{\frac{1}{2}} \\
& = V_o(w) [T(p_o)R(p_o)] \left[\frac{p_o^2}{(1-p_o^2)} \quad r \sum_{j=1}^6 \frac{1}{p_o V_j h_j (1-p_o^2 V_j^2)^{-3/2}} \right]^{\frac{1}{2}} \\
& \exp ik_{\alpha_1} \left(\sum_{j=1}^6 \frac{h_j (1 - p_o^2 V_j^2)^{\frac{1}{2}}}{V_j} + p_o r \right) \quad \text{A18}
\end{aligned}$$

where $r = \sum_{j=1}^6 h_j p_o V_j (1 - p_o^2 V_j^2)^{-\frac{1}{2}}$

since $f'(p_o) = 0$

In evaluating A14 to A18, no consideration has been taken of poles or branch points. (No account will be taken of the contributions to the integrals by poles, leading to interface and surface waves).

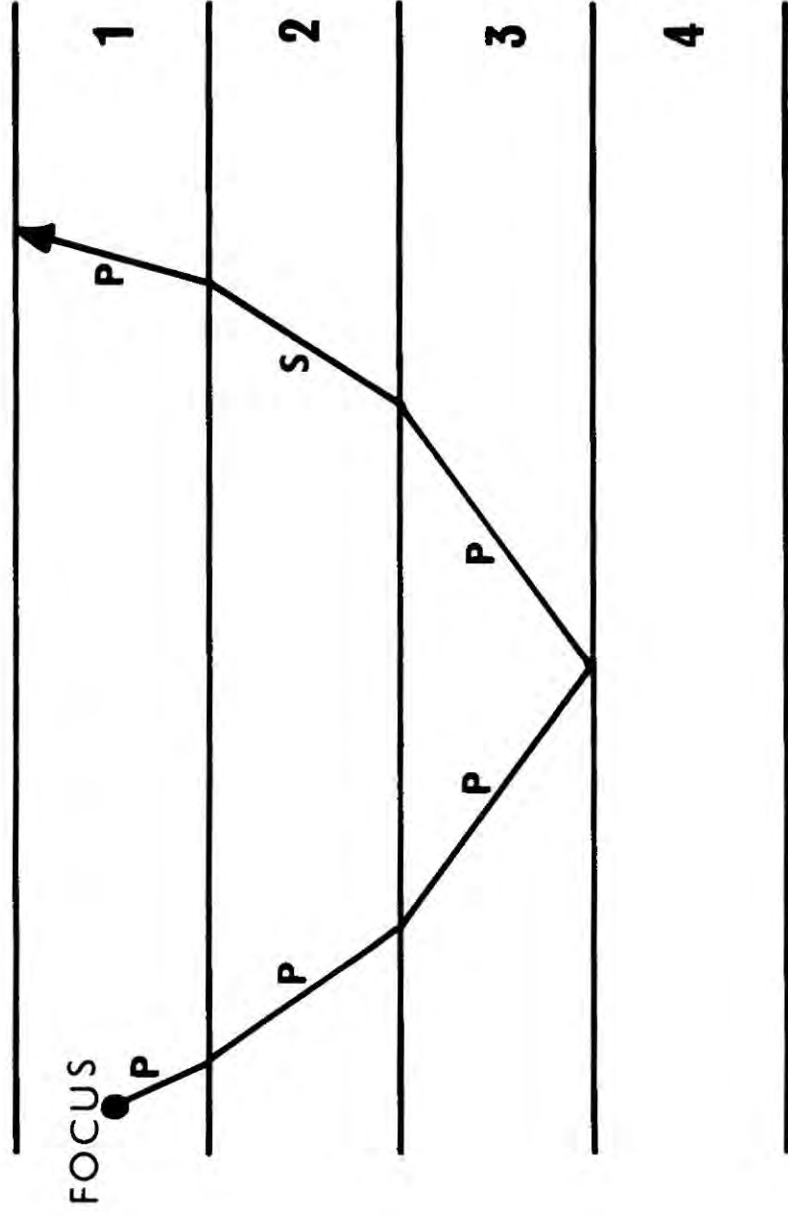
When $p_o < \alpha_1 / \alpha_{n+1}$, equation A18 is the final solution and represents the displacement potential at the receiver due to the geometrical or least time reflection path as in Fig. 54. The explicit expressions for the Reflection and Transmission coefficients may be obtained in a number of references. Consider the reflection coefficients, they contain the radicals

$$(1 - p^2 V_n^2)^{\frac{1}{2}}$$

where $V_n = \alpha_n / \alpha_1, \beta_n / \alpha_1$

(BERRY and WEST 1966)

Fig. 54. Generalized ray path for a $P_1 P_2 P_3 P_3 S_2 P_1$ wave originating in the upper layer and being observed in the upper layer of a four layered model.



As a result $p = \alpha_1 / \alpha_n$

$$\text{or } p = \alpha_1 / \alpha_n$$

will be branch points, since at each point p , the reflection coefficient can take two values, depending on which sign we choose for the radical. Thus, we have a two sheeted Riemann surface on each of which sheets the reflection coefficient will be single valued. The sheets will be joined along the branch lines starting at the branch point A_1 , where $p = 1/V_n$.

The branch points correspond to the values of p taken for the critically incident reflection when $p = p_c$. When p_0 , the saddle point, is less than p_c , as in the evaluation leading to equation A18, that equation is the complete solution. When the angle of incidence is greater than the critical angle, the branch points p_c , will interfere with the contour of integration, and the complete expression for the displacement potential will consist of two parts

$$\phi = \phi_{\text{REFL}} + \phi_{\text{HEAD}} \quad \text{A19}$$

where ϕ_{REFL} is the potential evaluated for the original contour, and the potential evaluated for that part of the contour which must be deformed around the cut, ϕ_{HEAD} , can be shown to be that due to the critically refracted headwave (BFEKHOVSKIKH, 1960).

The integral around the cut is evaluated as a single integral along the cut from A_1 to ∞ including $\Delta R = R_{\text{OUT}} - R_{\text{IN}}$.

R_{OUT} and R_{IN} are the values of the reflection coefficient on each side of the cut. As in the previous analysis, we again use the method of steepest descent to evaluate the integral. The integration path is deformed in such a way that it goes from the branch point A_1 along the line on which the exponential in the integrand decreases most rapidly. From A15 this will be the line on which the real part of $f(p)$ decreases most rapidly.

Introducing a new variable q , defined by

$$p = p_c + iq$$

and expanding the exponential in A15 as

$$\begin{aligned} f(p_c + iq) &= f(p_c) + iq f'(p_c) \\ &\approx ik_{\alpha_1} g(p_c + iq) = ik_{\alpha_1} g(p_c) - qk_{\alpha_1} g'(p_c) \end{aligned}$$

Since k_{α_1} is assumed to be large, and we have chosen the path of most rapid decrease, corresponding to the most rapid decrease in the Real part of $f(p) = qg(p_c)$ only small values of q will play an important role in the integrand (BREKHOVSKIKH, 1960).

Again we treat $F(p)$ (see A15) as a slowly varying function in the region of interest.

For small q , the difference in the reflection coefficient on the two sides of the cut can be shown to be related by a constant

$$H = (1 - p_c^2 V_n^2)^{\frac{1}{2}} \int_{p \rightarrow p_c}^{\infty} \frac{R^{\text{OUT}}(p) - R^{\text{IN}}(p)}{2(1 - p^2 V_{n+1}^2)^{\frac{1}{2}}} dp$$

where for small q

$$R = 2(-iq)^{\frac{1}{2}} p_c^{\frac{1}{2}} V_{n+1}^{\frac{1}{2}} (1 - p_c^2 V_n^2)^{\frac{1}{2}} H$$

(BERRY and WEST 1966)

where $V_n = \alpha_n / \alpha_1$

$R^{\text{IN}}(p)$ is the reflection coefficient as calculated when $p < p_0$

and $R^{\text{OUT}}(p)$ is the reflection coefficient when the radical $(1 - p^2 V_{n+1}^2)^{\frac{1}{2}}$ takes on its negative second value.

($n + 1$ is the headwave layer)

The integral around the cut may now be evaluated from 0 to ∞ over the variable q .

The integral corresponding to $\bar{\Phi}_{\perp \text{HEAD}}$ becomes

$$V_o(w) e^{i\pi/4} \sqrt{(k_{\alpha_1}/2\pi r)} \int_0^{\infty} F(p_c + iq) \exp(k_{\alpha_1} f(p_c + iq)) idq$$

or

$$\bar{\Phi}_{\perp \text{HEAD}} = V_o(w) e^{i\pi/4} \sqrt{(k_{\alpha_1}/2\pi r)} \int_0^{\infty} F(p_c) q^{\frac{1}{2}} e^{-(k_{\alpha_1} |f'(p_c)| q)} e^{k_{\alpha_1} f(p_c)} idq \tag{A21}$$

where $q^{\frac{1}{2}}$ has been included from the value for ΔF

For large k_{α_1} , A21 becomes

$$\frac{F(p_c) e^{k_{\alpha_1} f(p_c)} \pi^{\frac{1}{2}}}{(2(k_{\alpha_1} |f'(p_c)|)^3)^{\frac{1}{2}}} V_o(w) e^{i\pi/4} \sqrt{(k_{\alpha_1}/2\pi r)}$$

BERRY and WEST 1966

Thus $\bar{\Phi}_{\perp \text{HEAD}}$

$$= \frac{iV_o(w)}{k_{\alpha_1}} \left[i \left(r - \sum_{j=1}^6 h_j p_c V_j (1 - p_c^2 V_j^2)^{-\frac{1}{2}/3} \right)^{-\frac{1}{2}} \left(\frac{1 - p_c^2 V_n^2}{1 - p_c^2} \right)^{\frac{1}{2}} \right]$$

$$T_{p_1 p_2}(p_c) T_{p_2 p_3}(p_c) H_{p_3 p_3} T_{p_3 s_2}(p_c) T_{s_2 p_1}(p_c)$$

$$\exp i k_{\alpha_1} \left[\sum_{i=1}^6 \frac{h_j (1 - p_c^2 V_j^2)^{\frac{1}{2}}}{V_j} + p_c r \right]$$

where $p_c = \alpha_1 / \alpha_{n+1}$ (n+1 being the 4th layer)

The potentials for both the reflected and headwave terms for ray paths where certain legs are of shear type are identical, but with the relevant values of α and T_p, R_p changed to β, T_s, R_s

We have that for any ray

$$\bar{\Phi} = \bar{\Phi}_{\text{REFL}} + \bar{\Phi}_{\text{HEAD}}$$

and $\bar{\Psi} = \bar{\Psi}_{\text{REFL}} + \bar{\Psi}_{\text{HEAD}}$

depending on whether the final leg of the ray path is a compressional or shear wave.

The REFL terms will be present for all ray paths, but the head wave terms

$$= \bar{\Phi}_{\text{CP}} + \bar{\Phi}_{\text{CS}}$$

or $= \bar{\Psi}_{\text{CP}} + \bar{\Psi}_{\text{CS}}$

where CP denotes a P headwave

and CS denotes an S headwave

will only exist if p_o is greater than the relevant value of α_1 / α_{n+1} , α_1 / β_{n+1} .

8 such terms will exist corresponding to the four reflection coefficients and two branch points p_{CP} and p_{CS} .

SURFACE DISPLACEMENTS.

Having determined the displacement potential at the detector, it is necessary to calculate the amplitude of the displacement at the point of observation. Since the synthetic seismogram is to be compared with seismograms recorded on vertical seismometers, the vertical displacement at the surface will be calculated, making use of KNOPOFF'S et al (1957) coefficients.

Since the absolute intensity of the source is unknown, it is convenient to normalize the amplitude of the initial pulse at unit distance from the source. This amplitude is taken to be unity at a distance h from the source in an isotropic medium having the properties of the first layer.

The displacement amplitude

$$U_p = \nabla \bar{\Phi}$$

The normalizing amplitude is thus

$$U_{p_n} = \left. \frac{\delta \bar{\Phi}_{\text{SOURCE}}}{\delta r} \right|_{r=h}$$

However, since the assumption that $kr \gg 1$ must hold for the final amplitudes, it must also be applied to the normalized amplitude at a distance h from the source

Hence, since

$$\bar{\Phi}_{\text{SOURCE}} = \frac{A e^{ik_1 r}}{r}$$

$$U_{p_n} = \frac{ik_1 A e^{ik_1 r}}{r}$$

The final amplitude formulae are obtained as $U_p = \nabla_F \bar{\Phi}$

where ∇_F is in the direction of the final leg of the ray path.

Omitting the phase delay terms corresponding to propagation along the geometrical ray paths

$$Z_R = \left[\frac{(1 - p_o^2) \bar{r}_1}{p_o} \right]^{-\frac{1}{2}} \left[T_{P_1 P_2}(p_o) T_{P_2 P_3}(p_o) R_{P_3 P_3}(p_o) T_{P_3 S_2}(p_o) \right. \\ \left. T_{S_2 P_1}(p_o) S_{P_z}(p_o) \right]$$

and

$$Z_C = \left(\frac{i}{k_{\alpha_1} h} \right) \left(\frac{1 - p_c^2 V_n^2}{1 - p_c^2} \right)^{\frac{1}{2}} (\bar{r} \bar{L}^3)^{-\frac{1}{2}}$$

A22

$$[T_{P_1 P_2}(p_c) T_{P_2 P_3}(p_c) H_{P_3 P_3} T_{P_3 S_2}(p_c) T_{S_2 P_1}(p_c) S_{P_z}(p_c)]$$

where Z_R is the vertical ground displacement caused by a reflected wave and Z_C is that caused by a head wave.

$$\bar{r} = r/h = \sum_{j=1}^6 \bar{h}_j p_{oj} V_j (1 - p_{oj}^2 V_j^2)^{-\frac{1}{2}}$$

$$\bar{l} = \sum_{j=1}^6 h_j p_{oj} V_j (1 - p_{oj}^2 V_j^2)^{-3/2}$$

$$\bar{L} = \bar{r} - \sum_{j=1}^6 h_j p_{cj} V_j (1 - p_{cj}^2 V_j^2)^{-\frac{1}{2}}$$

$$\text{with } \bar{h}_j = h_j/h$$

(BERRY and WEST 1966)

Identical formulas hold for S-waves incident on the surface, with the appropriate values of α changed to β .

The coefficients S_{P_z} are the Knoppoff coefficients for incident P waves.

The values of the reflection and transmission coefficients are calculated from the Zoeppritz equations as in RICHTER (1968). The headwave coefficients are calculated from the equation relating H to ΔR (BERRY and WEST 1966).

DISCUSSION.

The integral equations have been evaluated asymptotically for wave-lengths that are short compared with the dimensions of the model. Using this method the displacement potential at the point of observation is predominantly due to contributions from plane waves following the geometric ray paths from source to receiver. The reflection and transmission coefficients have thus been calculated assuming geometric ray theory. However, since the integrand in equation A11 is evaluated for a range of values of p about p_0 , the saddle point, the R-T coefficients will also vary over that range as they are functions of p . In order to overcome this problem, the R-T coefficients are treated as slowly varying functions of p .

As the point of observation approaches the point at which the front of the headwave merges with the front of the reflected wave, the angle between the reflected ray and the normal to the boundary is close to the angle of total internal reflection. At this point

$$Z_{\text{HEAD}} \rightarrow \infty$$

since $L \rightarrow 0$ in equation (A20).

The formulae thus become inapplicable as the angle of reflection tends to the critical angle. This is because the reflection coefficient is not a slowly varying function of p in this region. On the contrary

$$\frac{dV(p)}{dp} \rightarrow \infty \quad (\text{BFEKOVSKIKH 1960})$$

CERVENY (1966) has shown that the amplitude of the reflected wave does not reach its maximum value directly at the critical point (as follows from geometrical ray theory) but beyond it. In this analysis the reflection and transmission coefficients have been considered independent of the frequency of the incident wave. This is not so.

CERVENY (1966) has shown that the maximum amplitude of the reflected waves occurs at increasing distances from the source for decreasing frequencies. The maximum value also decreases with a decrease in frequency.

However, for incident rays with angles below the angle of total internal reflection, geometric ray theory gives relatively exact results, for all frequencies.

No account has been taken of the attenuation of the medium. This will be due to absorption, and loss of energy on diffraction and dispersion from inhomogeneities. Assuming a homogeneous layered medium, the amplitude of the seismic wave will be decreased as

$$A = A_0 E^{-\alpha r}$$

where α is the absorption coefficient and r the distance travelled by the wave. However, for local and regional seismic work α is of the order of 10^{-6} through igneous, metamorphic and dense sedimentary rocks, and hence may be neglected. However, the reflection and transmission coefficients will also be affected by the presence of an absorbing layer. They can be shown to be oscillatory functions of that layer's thickness, d . As d increases the amplitude of the oscillations of the reflection coefficient decreases, until with d sufficiently large, R becomes constant. It is then equal to the reflection coefficient at the upper surface of the layer. In this case no wave is transmitted. (BĚKOVSKIKH 1960). However, as stated, absorption is not considered in this analysis.

The integrals have been evaluated assuming a point source, the source potential being converted from that of a spherical wavefront to that of a plane wavefront, with arbitrary time dependence.

The amplitude at the point of observation has been calculated in terms of the initial displacement. However, on a real seismic record, the waveform is related to the displacement of the seismometer mass. This will not be identical with the ground displacement, since it will be affected by the seismometer characteristics. However, since the initial disturbance is likely to be highly complex, being associated with an earthquake mechanism, it was considered unnecessary to include the seismometer characteristics in the final amplitude formulae. The errors thus involved, will be negligible compared with the error incorporated in assuming an initial point source.

In the analysis, only a compressional point source is considered. The solutions are not applicable to a shear wave source which will generate SH and SV waves. A compressional source will only generate SV waves on interaction of the wavefront with an interface. However, in the programme, an 'S wave source' has been included by considering a compressional point source generating spherical waves with vectors corresponding to S waves. This facet was included in order primarily to determine the travel time and apparent velocity of the S arrivals.

No account has been taken of the curvature of the earth, or of models other than a homogeneous, horizontally layered system. Thus the final amplitude formulae correspond to an idealized situation. Even with this situation due to the discrepancies involved in using geometric ray theory, the final synthetic seismogram is unlikely to correspond to a real seismogram from the same crustal model. Thus the results should not be equated exactly with records of a real seismogram which is likely to have a highly complex structure, due to inhomogeneities in the crust, small scale velocity fluctuations with depth, attenuation and near surface effects. However, the results will give an estimate of the relative amplitudes (and a direct indication of onset times, and apparent velocities) of the various major arrivals. This will assist identification of the large amplitude arrivals on the real seismic records, which in turn will aid interpretation of those records in terms of crustal thickness, structure and focal depths.

APPENDIX 2

REFLECTION, TRANSMISSION, HEADWAVE and KNOPOFF
COEFFICIENTS.

A.2.1. REFLECTION and TRANSMISSION COEFFICIENTS.

Consider plane waves in the vicinity of a plane interface between two homogeneous media, differing both in elastic constants and density.

Consider the 6 waves, corresponding to rays at different angles with the normal to the interface.

	VELOCITY	AMPLITUDE	ANGLE WITH NORMAL
INCIDENT P	U	A	a
INCIDENT S	V	B	b
REFLECTED P	U	C	c
REFLECTED S	V	D	d
REFRACTED P	Y	E	e
REFRACTED S	Z	F	f

The ratio of the density of the second medium to that of the first is K. All angles and velocities conform to Snell's Law.

The theory assumes that all 6 wavefronts represent pure sine waves of the same frequency ω .

By applying the two boundary conditions at the interface

- 1) the vector sum of the displacements due to all the waves along the boundary in one medium must equal the corresponding sum in the second medium,
- and
- 2) the corresponding components of stress must be equal on the two sides of the interface.

we may formulate four equations, the Zoeppritz equations, for an incident P wave and an incident S wave, from which the values of A, B, C, D, E and F may be determined (see RICHTER, 1958).

Now, since the angles of incidence and refraction are related by Snell's Law, when the angle of incidence becomes greater than critical angle, the sine of angle c, d, e or f will become greater than unity. Thus the corresponding cosine becomes imaginary. It is necessary, therefore, that the amplitudes are composed of real and imaginary parts. We may solve the Zoeppritz equations incorporating four real and four imaginary amplitude coefficients by matrix inversion.

We have that:-

$$\begin{bmatrix}
 + \sin a & - \cos b & + \sin e & - \cos f & 0 & 0 & 0 & 0 \\
 - \cos a & \sin b & 0 & - \sin f & 0 & 0 & \sqrt{(\sin^2 e - 1)} & 0 \\
 \sin 2a & \frac{U}{V} \cos 2b & 0 & K\left(\frac{Z}{V}\right)^2 \frac{U}{Z} \cos 2f & 0 & 0 & -K\left(\frac{Z}{V}\right)^2 \frac{U}{Y} 2 \sin e \sqrt{\sin^2 e - 1} & 0 \\
 - \cos 2b & -\frac{V}{U} \sin 2b & -K\frac{Y}{U} \cos 2f & -K\frac{Z}{U} \sin 2f & 0 & 0 & 0 & 0 \\
 0 & 0 & 0 & 0 & + \sin a & - \cos b & + \sin e & - \cos f \\
 0 & 0 & -\sqrt{(\sin^2 e - 1)} & 0 & - \cos a & \sin b & 0 & - \sin f \\
 0 & 0 & K\left(\frac{Z}{V}\right)^2 \frac{U}{Y} 2 \sin e \sqrt{\sin^2 e - 1} & 0 & \sin 2a & \frac{U}{V} \cos 2b & 0 & K\left(\frac{Z}{V}\right)^2 \frac{U}{Z} \cos 2f \\
 0 & 0 & 0 & 0 & - \cos 2b & -\frac{V}{U} \sin 2b & -K\frac{Y}{U} \cos 2f & -K\frac{Z}{U} \sin 2f
 \end{bmatrix}
 \begin{bmatrix}
 C_R \\
 D_R \\
 E_R \\
 F_R \\
 C_I \\
 D_I \\
 E_I \\
 F_I
 \end{bmatrix}
 =
 \begin{bmatrix}
 + \sin a \\
 + \cos a \\
 - \sin 2a \\
 - \cos 2b \\
 0 \\
 0 \\
 0 \\
 0
 \end{bmatrix}$$

where the incident wave is of unit amplitude and the complex coefficients

$$H = H_R + i H_I$$

A similar matrix form holds for an incident S-wave.

The resultant amplitudes are

$$H = \sqrt{(H_R^2 + H_I^2)}$$

with an associated phase

$$\delta = \arctan H_I/H_R$$

In the present analysis the S velocities have been related to P velocities as

$$v = c/1.74 \quad (\text{ANDERSON 1965})$$

and the P velocities related to the density of the medium, with a three component linear approximation to the Nafe-Drake Curve (NAFE and DRAKE 1959).

$$\text{For } \rho \leq 2.19 \text{ gm/cc}$$

$$v = \frac{1}{0.775} (\rho - 0.42)$$

$$\text{For } 2.19 < \rho \leq 2.81 \text{ gm/cc}$$

$$v = \frac{1}{0.155} (\rho - 1.84)$$

$$\text{For } \rho > 2.81 \text{ gm/cc}$$

$$v = \frac{1}{0.335} (\rho - 0.71).$$

For waves incident on the free surface, only two resultant reflected waves are produced. The equations for the amplitudes of the resultant P and S waves are as:-

$$\begin{aligned} \text{P:} \quad & 2C \cos c \sin d + D \cos 2d = 2 \cos a \sin d \\ & -C \cos 2d \sin c + D \sin d \sin 2d = \cos 2d \sin a \end{aligned}$$

and

$$\begin{aligned} \text{S:} \quad & -C \sin 2d \sin d + D \sin c \cos 2d = \sin 2b \sin b \\ & C \cos 2d + 2D \sin d \cos c = \cos 2b \end{aligned}$$

(KOLSKY 1963)

For an incident S wave, $\cos c$ becomes imaginary when b becomes greater than $\sin^{-1} \frac{U}{V}$. In this case all the energy will be reflected in the S wave with a resultant phase shift in D , where the phase shift

$$\delta = \arctan \left(\frac{4 \sqrt{1 - \frac{1}{\sin^2 a}} \sqrt{\frac{1}{\sin^2 b} - 1}}{\left(2 - \frac{1}{\sin^2 b}\right)^2} \right)$$

(EWING et al 1957)

Graphs have been drawn of the amplitudes and associated phases of the resultant waves from a P and an S wave, incident on the boundary between two elastic media, for all angles of incidence between 0 and 90 degrees. (Fig. 55 - 58) The graphs incorporate both reflection and transmission from a high-low and low-high density interface. It can be seen that the variations of T and R , the reflection and transmission coefficients, are highly complex. The variation in general is sharpest in the vicinity of the critical point, with resultant inaccuracies arising as stated in the evaluation of the integrals in Appendix A.1.

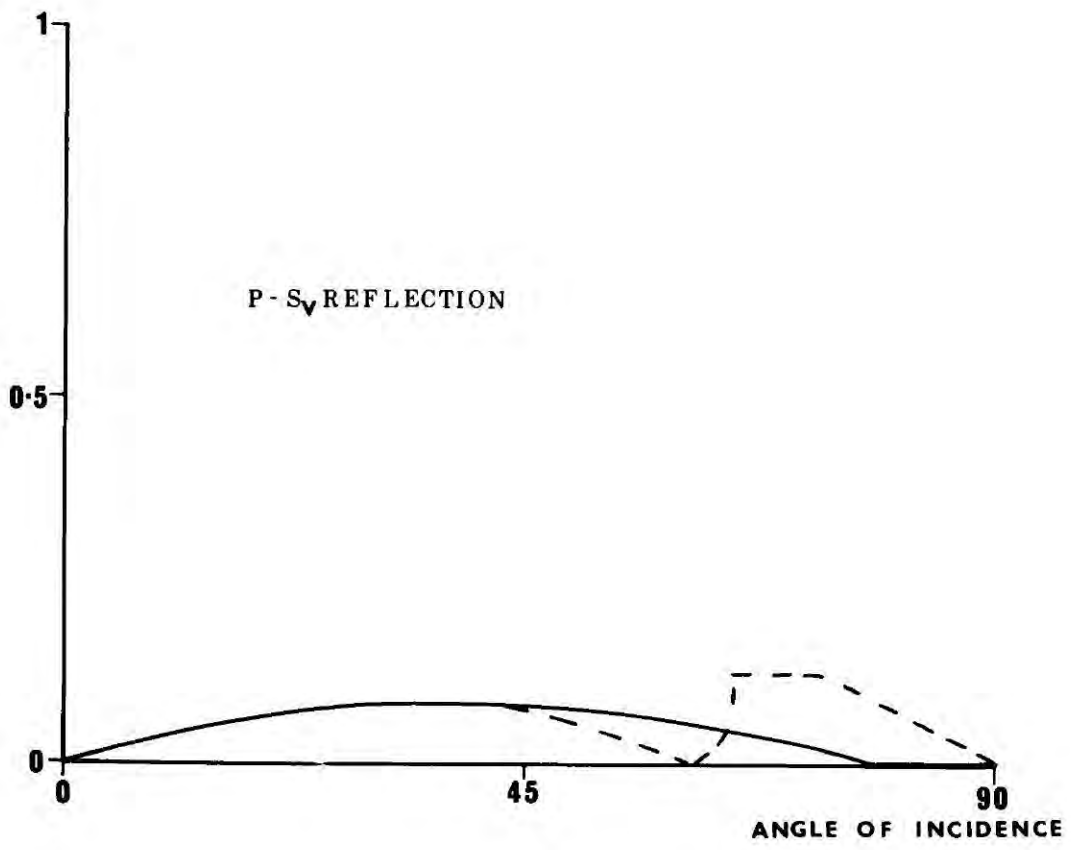
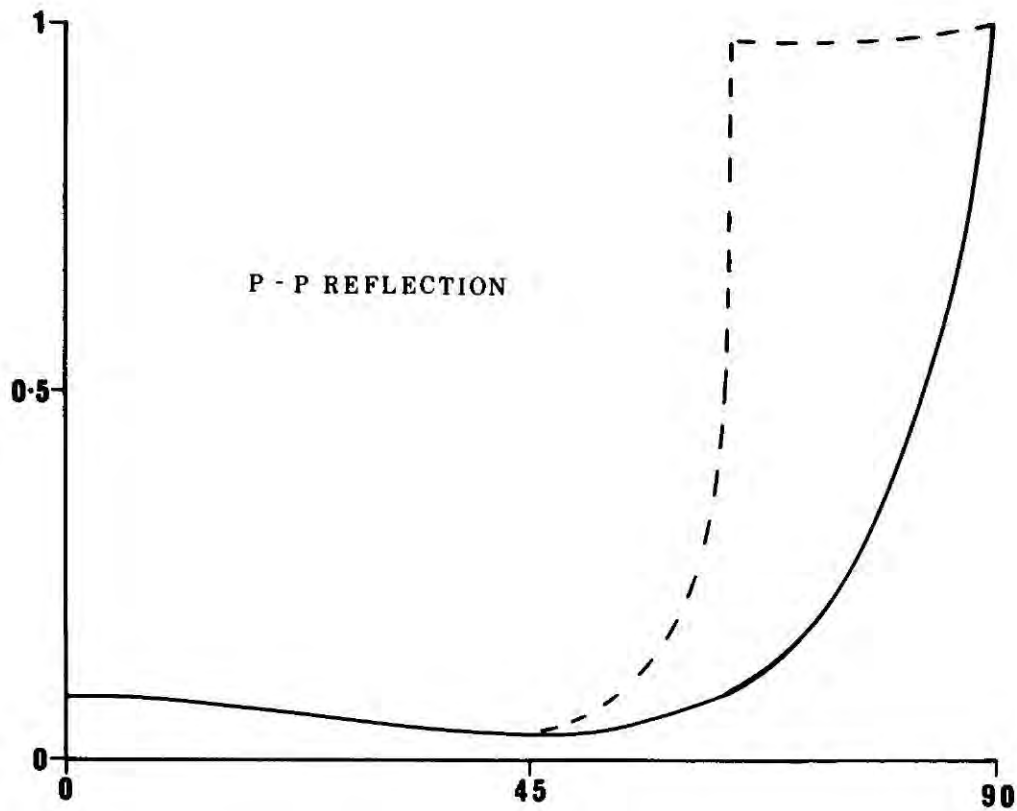
Graphs have also been drawn of the amplitudes of the resultant waves from a P and S wave incident on the free surface (Fig. 59).

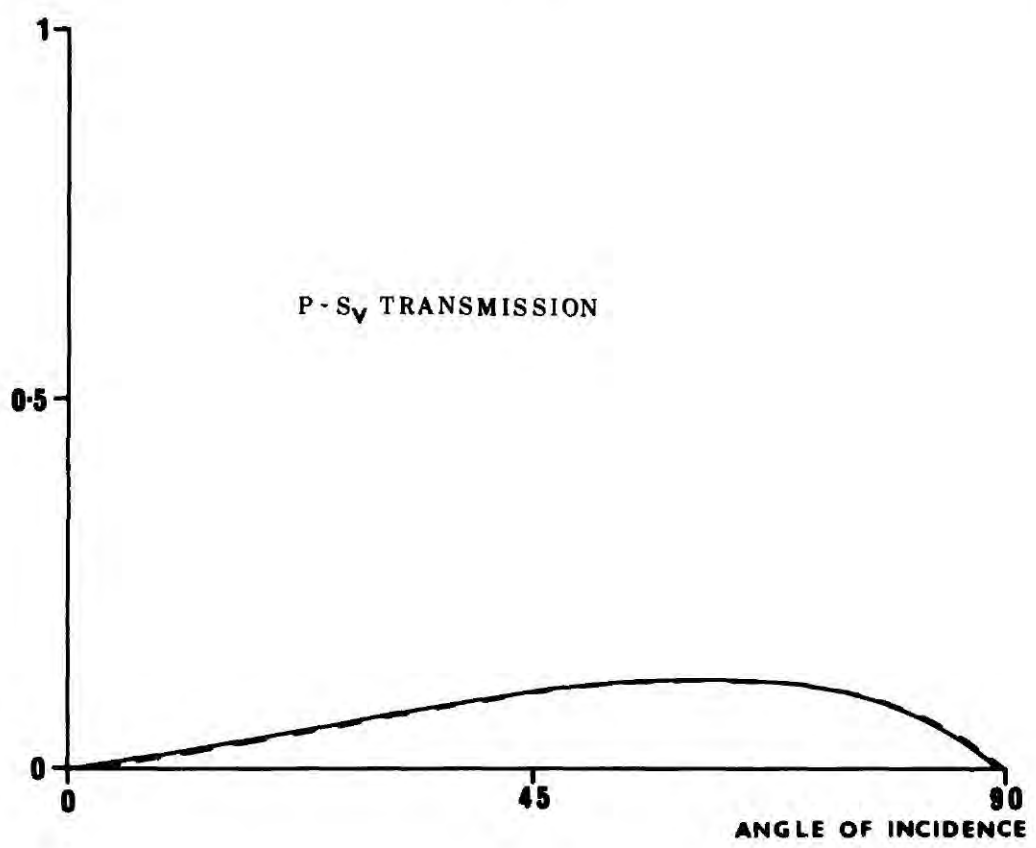
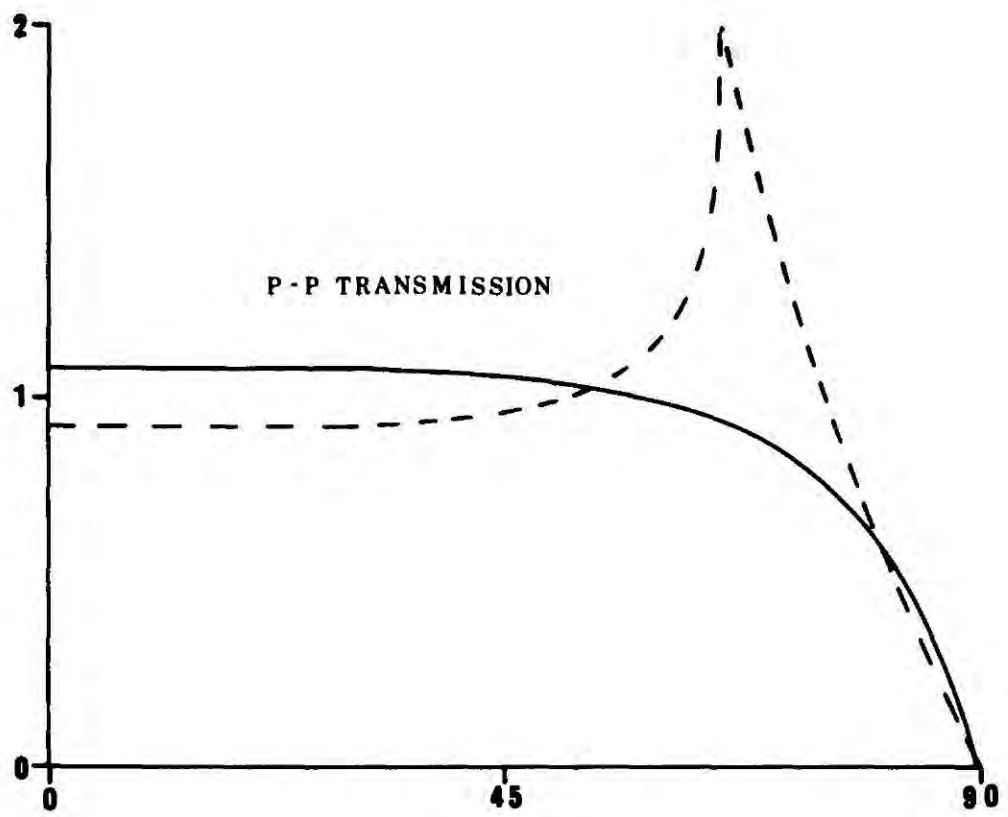
Fig. 55 Reflection and Transmission coefficients for
to P and Sv waves calculated from Zoeppritz
Fig. 58 equations.

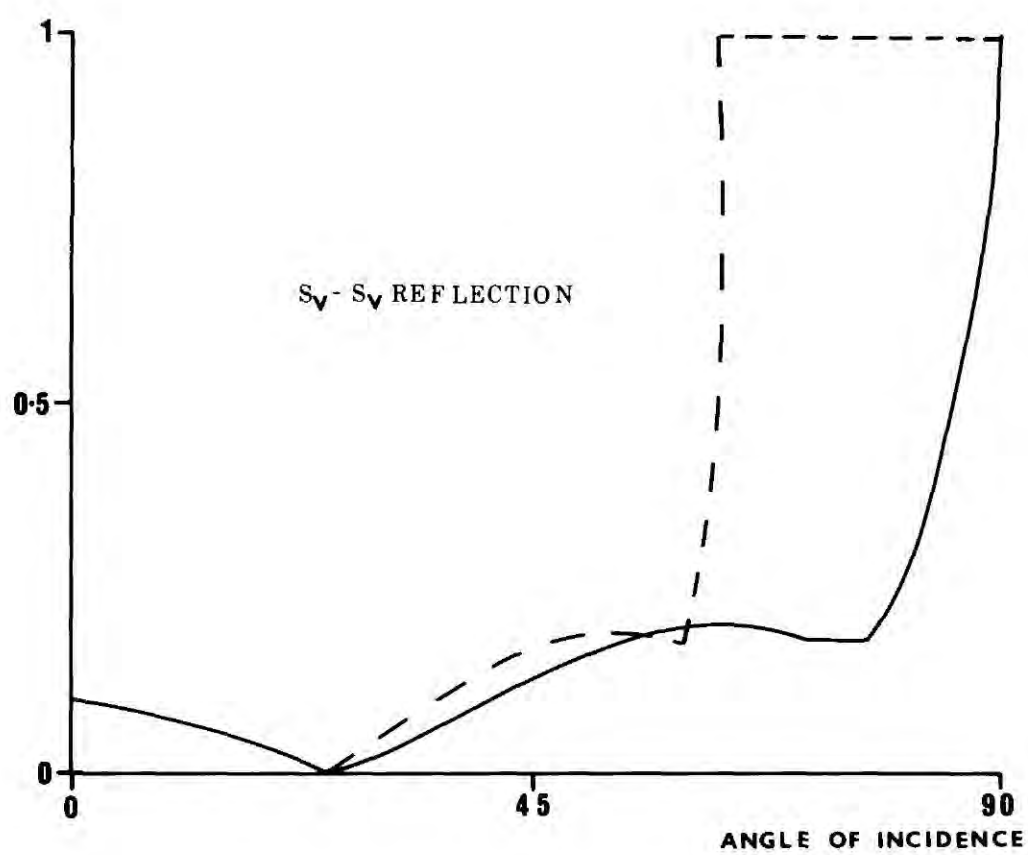
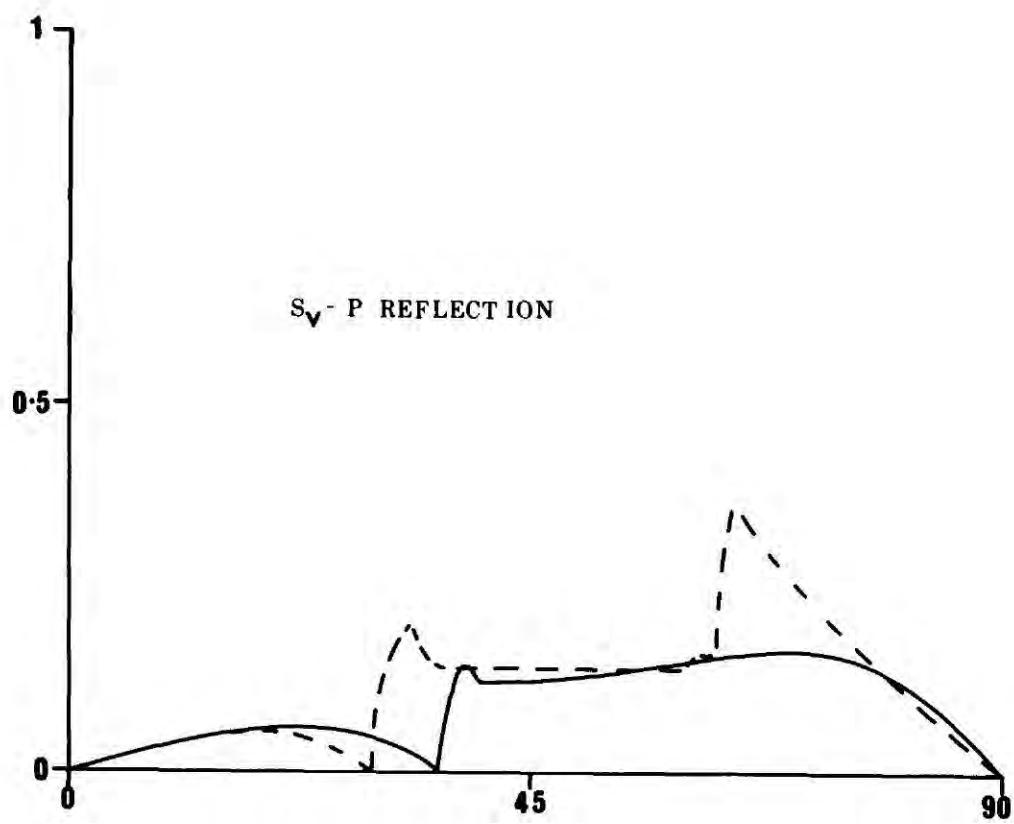
----- represents coefficients with
incident wave in lower
velocity medium
————— represents coefficients with
incident wave in higher
velocity medium.

Wave velocities in two media (assumed).

	Vp(km/s)	Vs(km/s)
a)	6.4	3.6
b)	5.8	3.2







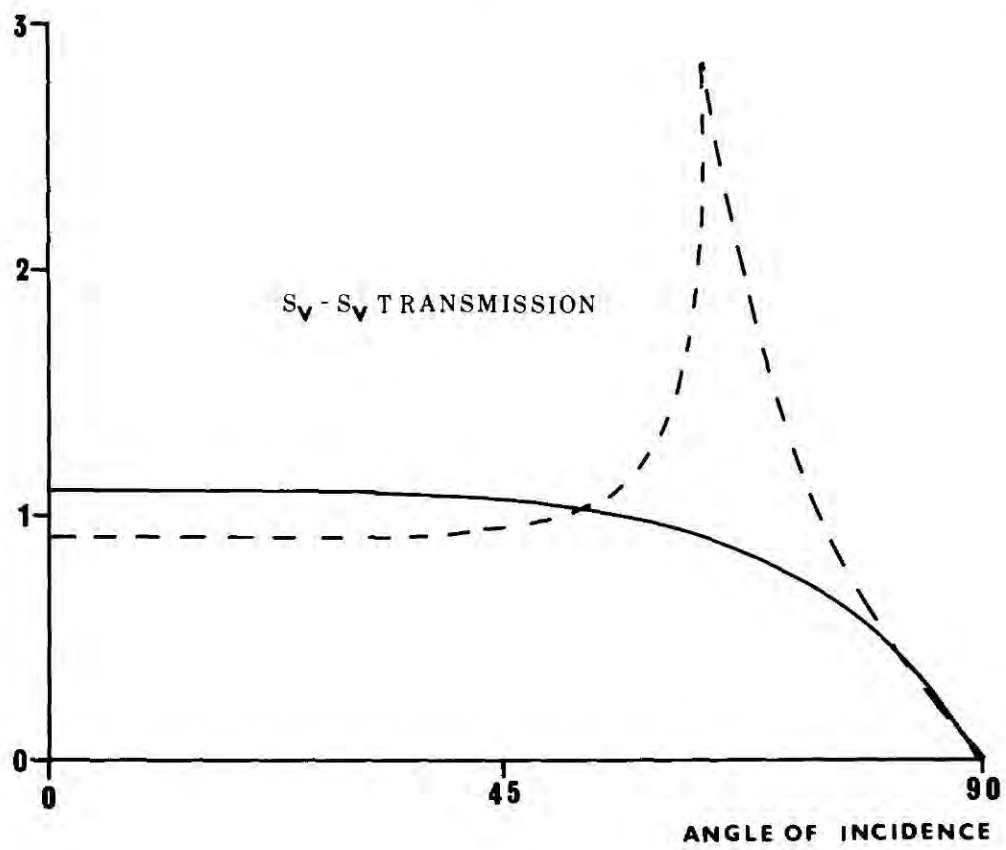
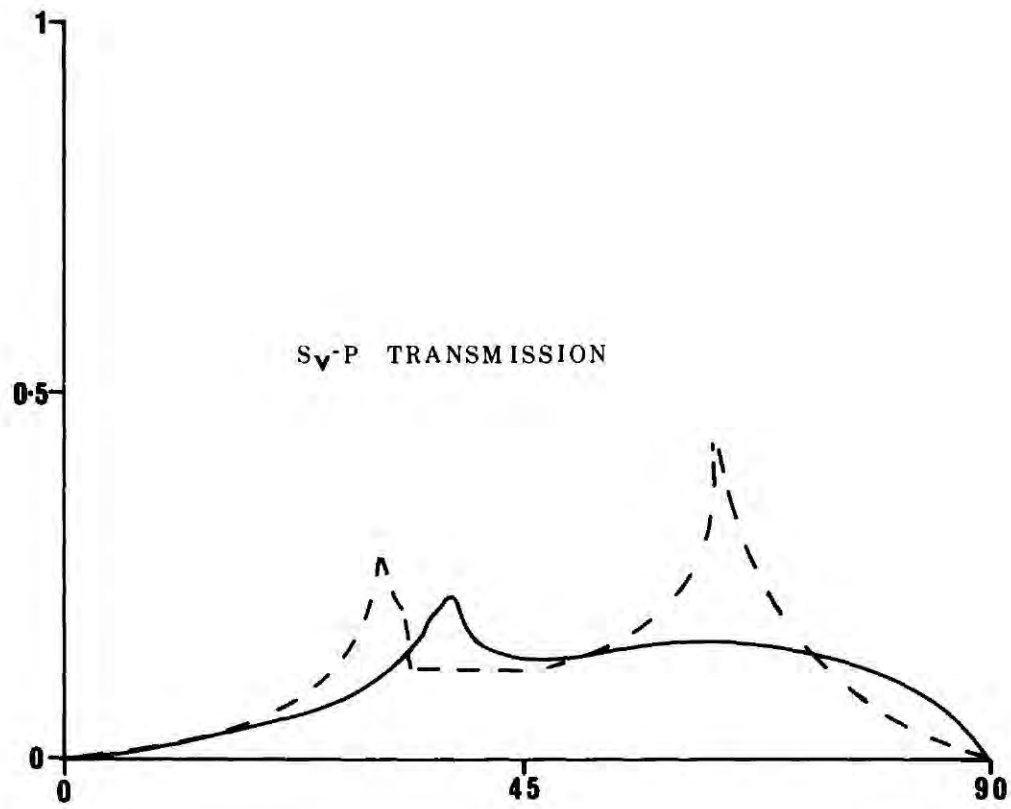
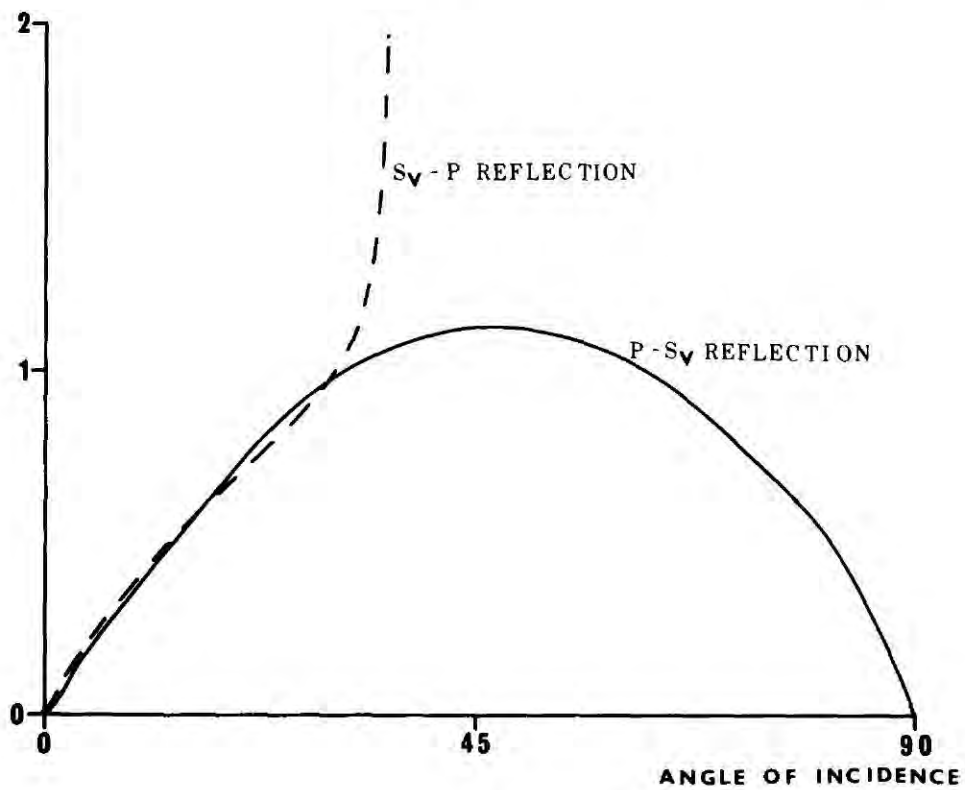
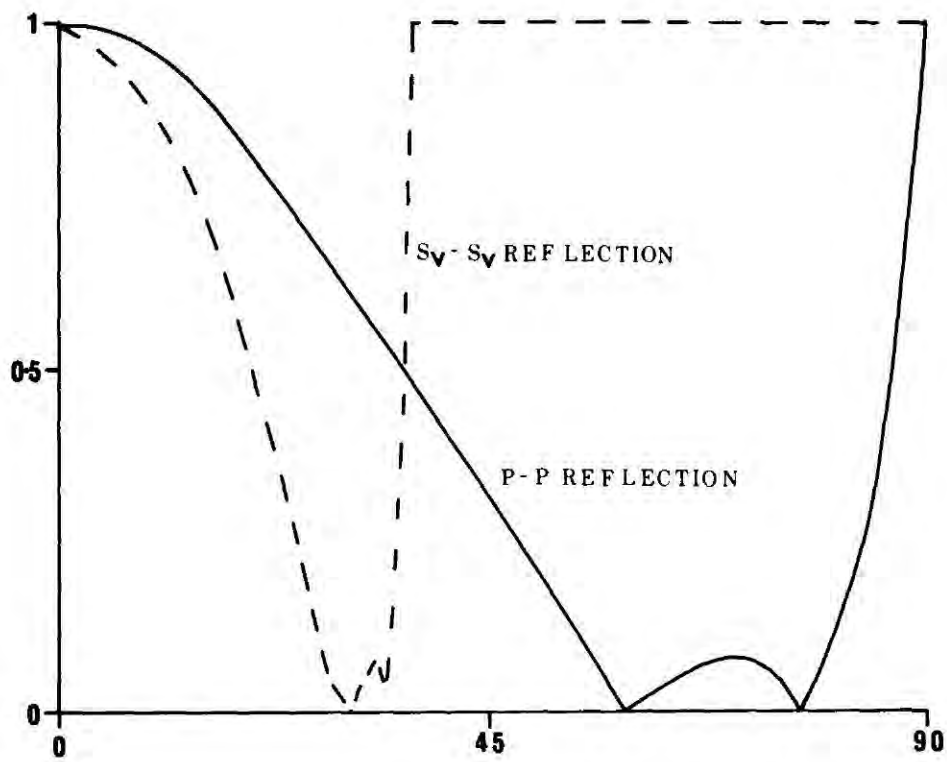


Fig. 59. Reflection coefficients for P and Sv waves incident on the free surface from within a medium with wave velocities (calculated from $V_p = 1.74 V_s$)

$V_p(\text{km/s})$	$V_s(\text{km/s})$
6.35	3.67



A.2.2. HEADWAVE COEFFICIENTS.

The headwave coefficients are calculated from the equation relating H to ΔR , where F_{OUT} and F_{IN} differ by the sign in the radical $(1 - p^2 V_{n+1}^2)^{\frac{1}{2}}$.

If α_1, ρ_1, ℓ_1 are the parameters of the upper layer and α_2, ρ_2 and ℓ_2 the parameters of the lower layer it is found that

$$\text{with } \ell = \ell_2 / \ell_1$$

$$H_{PSP} = -(\ell K_{12}^2) / (2 (\alpha_1 / \beta_2))$$

$$H_{PSS} = \ell K_{12} K_{22} / 2 (\alpha_1 / \beta_2)$$

$$H_{SSP} = (\ell K_{22} K_{12} / 2 (\alpha_1 / \beta_2) (\alpha_1 / \beta_1)^2)$$

$$H_{SSS} = -(\ell K_{22}^2 / 2 (\alpha_1 / \beta_2) (\alpha_1 / \beta_1)^2)$$

$$H_{PPP} = \ell K_{11}^2 / 2 (\alpha_1 / \alpha_2)$$

$$H_{PPS} = \ell K_{11} K_{21} / 2 (\alpha_1 / \alpha_2)$$

$$H_{SPP} = \ell K_{21} K_{11} / 2 (\alpha_1 / \alpha_2) (\alpha_1 / \beta_1)^2$$

$$H_{SPS} = \ell K_{21}^2 / 2 (\alpha_1 / \alpha_2) (\alpha_1 / \beta_1)^2$$

where H_{XYZ} corresponds to

a downgoing X wave

a lateral Y headwave

and an upgoing Z wave from the interface.

$$\text{If } A_{11} = (1 - (\alpha_1/\alpha_2)^2)^{\frac{1}{2}}$$

$$B_{11} = (1 - (\epsilon_1/\alpha_2)^2)^{\frac{1}{2}}$$

$$\text{and } B_{21} = (1 - (\beta_2/\alpha_2)^2)^{\frac{1}{2}}$$

$$B_{12} = (1 - (\alpha_1/\beta_2)^2)^{\frac{1}{2}}$$

$$A_{12} = (1 - (\alpha_1/\rho_2)^2)^{\frac{1}{2}}$$

$$A_{22} = (1 - (\alpha_2/\rho_2)^2)^{\frac{1}{2}}$$

$$K_{11} = [(\{M_1 - \frac{1}{2}\} B_{21}) / (\alpha_1/\epsilon_1) - (\{M_1 + \rho/2\} B_{11}) / (\alpha_1/\rho_2)] / D_1$$

$$K_{21} = [(\{M_1 \cdot A_{11} \cdot B_{21}\} / (\alpha_1/\alpha_2)) + (\{M_1 + (\rho - 1)/2\} / (\alpha_2/\beta_2))] / D_1$$

$$K_{12} = [(\{M_2 \cdot A_{22} \cdot B_{12}\} / (\alpha_1/\rho_2)) + (\{(\alpha_2/\rho_2)(M_2 + (\rho - 1)/2)\} / (\alpha_1/\epsilon_2))] / D_2$$

$$K_{22} = [(\{M_2 - \frac{1}{2}\} A_{22}) - (\{M_2 + \rho/2\} A_{12}) / (\alpha_1/\alpha_2)] / D_2$$

where

$$\text{if } D_{11} = (M_1 + (\rho - 1)/2)^2 / ((\alpha_1/\rho_1)(\alpha_2/\beta_2))$$

$$D_{12} = (\rho A_{11} B_{21}) / 4((\alpha_1/\rho_1)(\alpha_1/\alpha_2))$$

$$D_{13} = [(M_1 + \rho/2)^2 A_{11} B_{11}] / ((\alpha_1/\alpha_2)(\alpha_1/\rho_2))$$

$$\text{then } D_1 = -(D_{11} + D_{12} + D_{13})^2$$

and if

$$D_{21} = [(\alpha_2/\beta_2)(M_2 + (\rho - 1)/2)^2]/(\alpha_1/\beta_1)$$

$$D_{22} = (\rho A_{22} B_{12})/4(\alpha_1/\alpha_2)$$

$$D_{23} = [(M_2 + \rho/2)^2 A_{12} B_{12}]/(\alpha_1/\alpha_2 \cdot \alpha_1/\alpha_2)$$

$$\text{then } D_2 = -(D_{21} + D_{22} + D_{23})^2$$

where

$$M_1 = (\beta_1/\alpha_2)^2 - \rho(\alpha_2/\alpha_2)^2$$

$$M_2 = (\beta_1/\beta_2)^2 - \rho$$

from BERRY and WEST (1966)

It can be seen from the values of B_{21} , A_{12} and A_{22} that complex coefficients will occur, in which case H_{XYZ} must be divided into its real and imaginary parts.

$$H = H_r + iH_i$$

with resultant amplitude

$$H = |H|$$

and phase shift

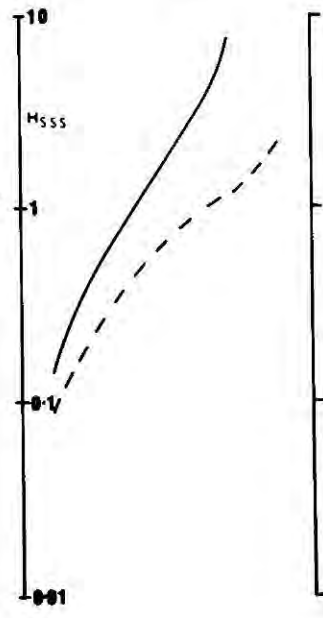
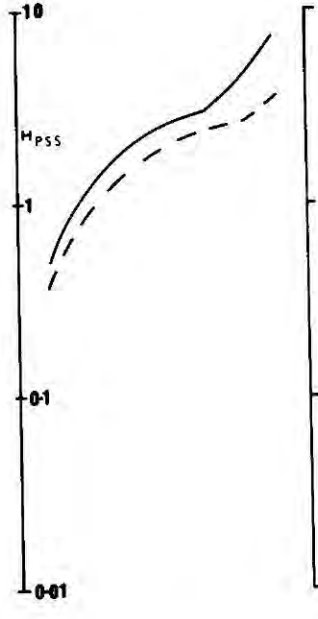
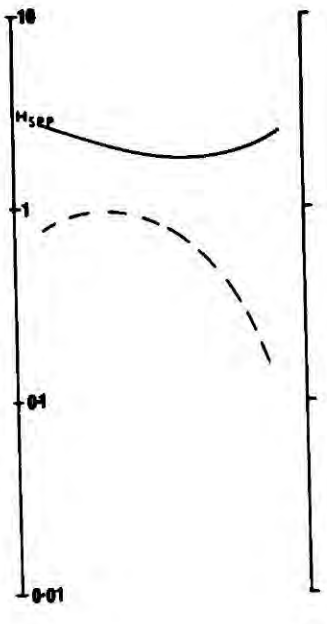
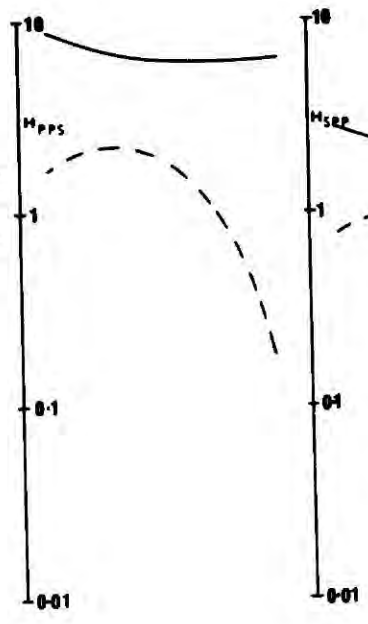
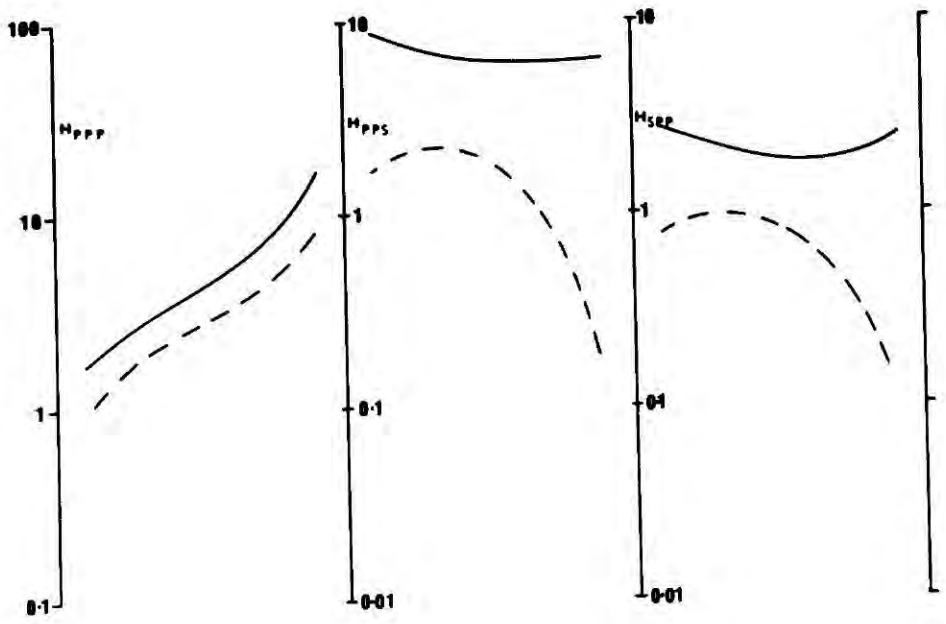
$$\delta = \tan^{-1} \frac{H_i}{H_r}$$

Graphs of H_{XYZ} have been drawn for various values of Poisson's ratio for the two media above and below the interface, for a range of values of the P-velocity ratio.

H_{PSP} , H_{PPS} , H_{SSP} and H_{SSS} are all complex (Fig. 60)

Fig. 60. Headwave coefficients for a range of values of the P wave velocity ratio (abscissa from 0 to 1), and for two values of the Poisson ratio ratio between the two media on either side of the refracting interface.

----- represents $\sigma_1:\sigma_2 = 0.15 : 0.35$
————— represents $\sigma_1:\sigma_2 = 0.35 : 0.15$



A.2.3. KNOPOFF COEFFICIENTS.

Consider plane waves incident upon a free surface at any angle, θ , from within an elastic homogeneous half-space. The boundary conditions require that the normal and shear stress vanish at the surface.

For an incident P-wave the vertical component of displacement

$$S_{zp} = \frac{2 \sin \theta}{\cos 2\theta \tan \theta + 2 \sin^2 \theta \tan \theta}$$

where $\frac{\sin \theta}{\sin \theta} = \alpha/\beta$

For an incident S-wave

$$S_{zs} = \frac{2 \sin \theta \tan 2\theta}{\cos 2\theta \tan \theta + 2 \sin^2 \theta \tan \theta}$$

In the latter case, when θ is greater than the critical angle, the incident S wave is totally internally reflected and undergoes a phase shift.

If we allow θ to become imaginary at angles above the critical angle

$$\text{i.e. } \tan \theta \rightarrow i \tanh \theta'$$

we have

$$\left| S_{zs} \right| = \frac{2 \sin \theta \tan 2\theta}{(\cos^2 \theta \tanh^2 \theta' + 4 \sin^4 \tan^2 2\theta)^{\frac{1}{2}}}$$

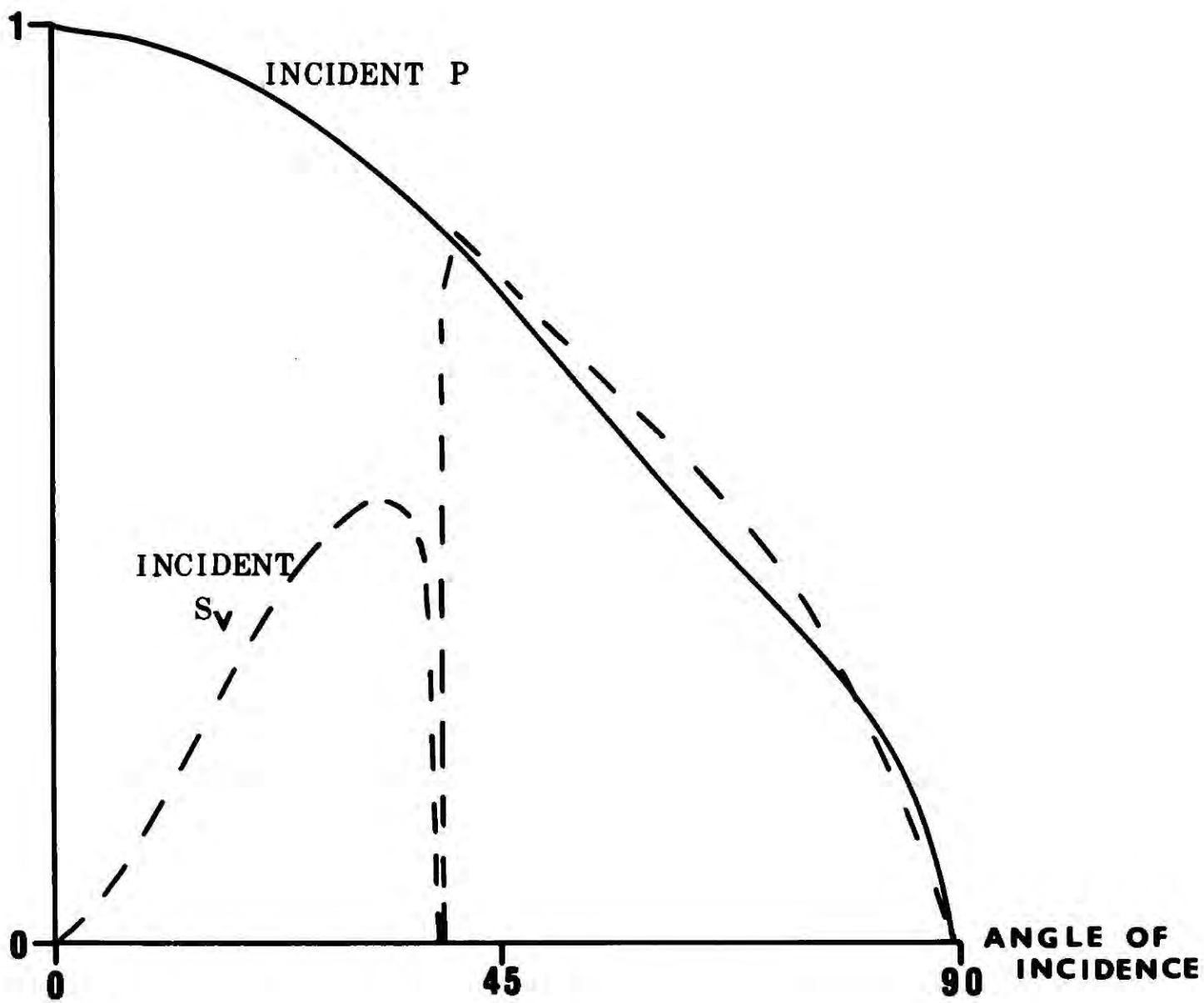
with an associated phase shift

$$\hat{\phi} = \arctan \frac{\tanh \theta' \cos 2\theta}{2 \sin^2 \theta \tan 2\theta}$$

Graphs have been drawn for the vertical component of ground motion for both P and S waves, after normalizing the peak amplitude to unity for vertical incidence, (Fig. 61). The medium is characterized by a Poisson's ratio of 0.25.

Fig. 61. Vertical component of ground motion,
normalized to unity for vertical incidence,
(KNOPPOFF Coefficients (1957)) for incident

————— P waves.
- - - - - S waves.



APPENDIX 3
THE PROGRAMME

The programme is written in FORTRAN IV language. It can be run on a 360 IBM computer. One subroutine from the IBM scientific subroutine package is used, SIMQ, for solving a matrix equation.

The programme is divided into two parts

- 1) to compute the amplitude of all required arrivals
- and 2) to convert these numerical results into a synthetic seismogram.

PART 1 requires 1 data block and output is from the line printer

PART 2 requires 1 data block plus the output from PART 1, and output is on the IBM 360 plotter.

A.3.1. PART 1.

The problem to be solved is as follows.

- Given
- 1) the position of a source, S, in an n-layered model
 - 2) the point of observation, O, on the free surface
 - 3) the time length of record required

calculate the vertical component of ground motion at O, due to every possible ray emerging from S which reaches O within the specified time limit. A further restriction is imposed in discarding those arrivals whose amplitude falls below a specified value

'Every possible ray' includes

- 1) multiply reflected ray paths
- 2) headwaves
- 3) degenerate arrivals i. e. rays that travel from S to O in the same time, but along different ray paths.
- and 4) all possible P-S conversions along the ray path.

No restrictions will be imposed on the position of the source, and the programme will accept a model of up to 20 layers.

(Restrictions arising from the theory in Appendix A1, have to be imposed by the user.)

The programme consists of 1 main and 10 subroutines.

MAIN

Consider an n-layered model with an event originating at focal depth FD.

The layers are numbered from the immediate subsurface, Layer 1, to the lowest layer, Layer NOL.

The layer of focus is calculated layer FL. If the focus lies on a boundary, it is programmed as existing in layer FL, where FL corresponds to the layer number above the boundary. If it exists on the surface $FL = 1$.

MAIN then generates and calculates the number of ray segments within each layer, for all possible ray paths from the source to receiver.

Since there are an infinite number of arrivals for any model with more than one layer, the ray generation process must be limited in order to be able to use the computer. This is done by calling subroutines which impose the conditions laid down in the formulation of the problem.

Consider a focus in layer FL.

Initially CODE (I), $I = 1$, FL is set to 1

while CODE (I), $I = FL + 1$, NOL is set to 0

i. e. the direct wave has been generated, since CODE (I) corresponds to the number of ray segments in the I^{th} layer.

PROCESS A.

By calling the subroutines, the amplitude, phase, apparent ground velocity, and travel time for all possible P, S and P-S conversion rays are calculated.

PROCESS B.

If $1 < FL$, $CODE(1) = CODE(1) + 2$

i. e. one reflection from the free surface and the first boundary before the ray arrives at the observation point.

PROCESS A is repeated.

PROCESS B is repeated until the travel time of the multiply reflected ray becomes greater than $T_0 + T$.

where T_0 is the travel time of the direct P wave
and T the time limit imposed in the data.

PROCESS C.

If $2 < FL$, $CODE(1)$ is set to 1
and $CODE(2) = CODE(2) + 2$

PROCESS A is repeated.

PROCESS B is repeated until again $T > T_0 + T$.

PROCESS C is repeated until the maximum number of reflections in layer 2 is reached.

Again $CODE(1)$ is set to 1
 $CODE(2)$ is set to 1
while $CODE(3)$ is increased

and the whole process repeated.

In this way, all possible ray paths of multiply reflected rays in

the model are generated.

When the moment comes to generate the next reflection in the layer of focus

$$\text{CODE (FL)} = \text{CODE (FL)} + 1$$

Since both upward and downward travelling initial rays are allowable.

For reflections in any layer beneath the focal layer

$$\text{CODE (I)} \geq 2$$

No reflections are allowed in the lowest layer since the medium below that layer is not defined.

If the focus originates on the free surface, for the first reflection

$$\text{CODE (FL)} = \text{CODE (FL)} + 1$$

while for any subsequent reflection

$$\text{CODE (FL)} = \text{CODE (FL)} + 2$$

The last equation is applied for any increase in the number of reflections in the layer of focus, when the focus is on an intermediate boundary.

Thus on running the main programme all multiply reflected rays are generated with all the required parameters calculated as in process A.

MAIN is then rerun to generate all possible headwaves and their multiple reflections.

A headwave can only exist in any layer beneath the focus. An exactly similar procedure is carried out, as for the multiple reflections with $\text{CODE (HEADWAVE LAYER)} = 1$.

This time PROCESS A also contains the limitation that the distance travelled in the headwave layer must be greater than a certain value

X where $X > 0$. $X > 0$ is applied since $\text{Amp}_{\text{HEAD}} \rightarrow \infty$ as $X \rightarrow 0$.

On running through MAIN this second time, all possible headwaves, together with their multiple reflections are generated, with all the required parameters again calculated as in PROCESS A.

The programme then stops.

SUBROUTINE SUMRAY.

This is for computational use only and calculates the total number of ray segments for each ray path for the reflected arrivals.

It also converts $\text{CODE}(I)$, $I = 1, \text{NOL}$ into RC. For example, if

$$\text{CODE}(1) = 3$$

$$(2) = 3$$

$$(3) = 2$$

$$(4) = 0$$

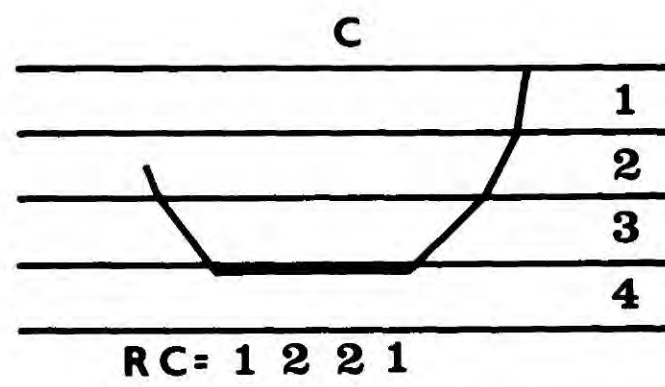
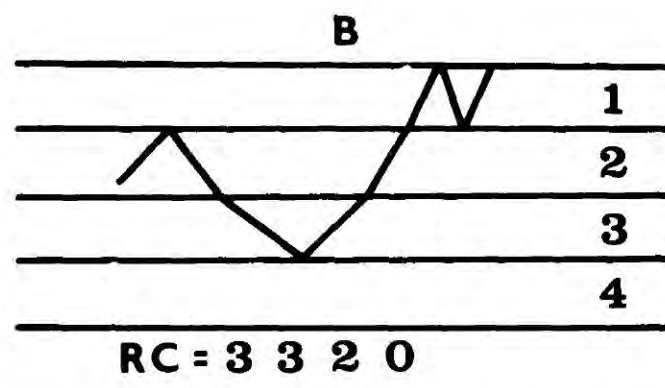
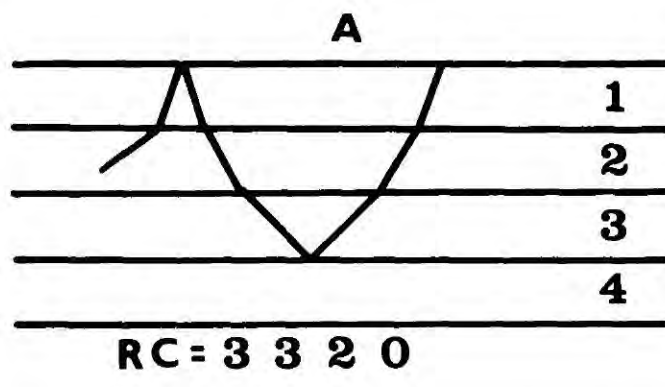
$$\text{RC} = 3320 \quad (\text{Fig. 62 a, b})$$

SUBROUTINE T.D.L.

For a single multiply reflected ray path between the source and observation point (i.e. excluding headwaves), this subroutine computes

- 1) the type of interaction at each boundary along the ray path T.
 - 2) the direction of each ray segment D.
- and
- 3) the layer numbers of the two layers, involved at each reflection or transmission L1, L2.

- Fig. 62. a) Ray path corresponding to $RC = 3320$
b) Degenerate ray path for $RC = 3320$
c) Ray path corresponding to $RC = 1221$.



$T = \begin{matrix} 0 \\ 1 \\ 2 \end{matrix} \}$ corresponds to $\left\{ \begin{array}{l} \text{reflection at free surface} \\ \text{transmission} \\ \text{reflection} \end{array} \right.$

$D = \begin{matrix} 1 \\ 2 \end{matrix} \}$ corresponds to $\left\{ \begin{array}{l} \text{an upward travelling ray} \\ \text{a downward travelling ray} \end{array} \right.$

A single example will be analysed in full. The subroutine in fact can handle any complete ray path, for any focal depth within the model.

Consider the ray path as in Fig. 62a

where the initial data is that

$$RC = 3320 \quad \text{and} \quad FL = 2.$$

There are 8 ray segments, therefore there will be 8 values of T, D, L1 and L2.

T (1) must always be set equal to 2.

and L1(2) must always be set equal to FL.

If CODE (FL) is even then the first ray segment must travel downwards.

$$\text{i.e. } D(1) = 2.$$

If it is odd, then as long as the source is not situated on an interface (which, in fact, has been accounted for in the programme)

$$D(1) = 1$$

Every time the values of T, D, L1 and L2 for a ray segment are determined, the code for the layer L1 is diminished by 1.

Priority is always given to transmission.

In the example we thus have

$$T(1) = 2, \quad D(1) = 1, \quad L1(1) = 2, \quad L2(1) = * \\ \text{and } RC^1 = 3220.$$

(L2(1) is not required in the computation). Since CODE (1) is greater than 1, we can immediately let T (2) = 1 (transmission) and thus

D (2) = 1. L1 (2) and L2 (2) are set equal to 2 and 1 respectively. Thus we have determined the type of interaction at the first boundary encountered by the ray, and the medium of the incident and resultant rays.

$$\text{Now } RC^1 = 2220.$$

The values of all the subsequent T, D, L1 and L2s can thus be determined by an iterative method, imposing the condition that when all the values for T, D, L1 and L2 have been determined,

$$\text{CODE (I) = 0 for I = 1, NOL.}$$

or $RC^1 = 0000$ for the case in question.

In the example:-

	T	D	L1(incident layer)	L2(resultant layer)
1	2	1	2	*
2	1	1	2	1
3	0	2	1	0
4	1	2	1	2
5	1	2	2	3
6	2	1	3	4
7	1	1	3	2
8	1	1	2	1

(when L2 = 0, the ray is reflected from the free surface).

SUBROUTINE DEG.

Some multiply reflected ray paths between source and receiver will be degenerate. For example, a ray with

$$RC = 3320$$

can travel by two paths from S to O, (Fig. 62a, b) each path having the same travel time, but different resultant amplitudes due to the different

number of reflections of transmissions in each case.

Initially SUBROUTINE TDL defines the path as in Fig. 62 a with the priority on transmission at each interface.

SUBROUTINE DEG starts with the initial values of T, D, L1 and L2 as calculated in SUBROUTINE TDL and then alters each successive type code T = 1 (i. e. transmission) to T = 2 (i. e. reflection), from T(max) to T (1). At each stage the condition is imposed that when the values of T, D, L1 and L2 have been redetermined,

CODE (I), I = 1, NOL must be zero
 or $RC^1 = 0000$ for the case in question.
 (see SUBROUTINE TDL).

In the example given this is only true when T (2) is changed from a transmission to a reflection.

After such an alteration, the cycle is repeated again, starting with T(max) through to T(change) in this case, T (2). In the example there are no other degenerate arrivals up to this point. T(change - 1) through to T (1), when equal to 1, are then successively altered from T = 1 to T = 2, subject to the restricting condition. Again, after each successful alteration the cycle is repeated starting with T(max) through to T(change). Thus all degenerate arrivals are determined and analysed.

Analysis of reflected refractions is limited to degeneracy 1, (unless the reflections are degenerate), since the output from one or more refractions from the same layer is identical. No allowance has been made for the change in amplitude due to degenerate reflected refractions.

SUBROUTINE HEA.

When a ray path has been critically refracted, an extra value of T, D, L1 and L2 has to be included corresponding to the value of each of those parameters for the critically refracted wave. In this case

$$D(\text{HEADWAVE}) = 0.$$

Thus for a ray path as

$$RC = 1, 2, 2, 1$$

with FL = 2 (the layer of focus) (Fig. 62c)

	T	D	L1	L2
1	2	2	2	*
2	1	2	2	3
3	1	0	3	4
4	1	1	4	3
5	1	1	3	2
6	1	1	2	1

Having calculated the required parameters of this arrival by calling other subroutines, the values of T, D, L1 and L2 are restored to those values for the equivalent reflected wave; in this case

$$RC = 1, 2, 2, 0$$

where	T	D	L1	L2
1	2	2	2	*
2	1	2	2	3
3	2	1	3	4
4	1	1	3	2
5	1	1	2	1

SUBROUTINE PS.

This subroutine calculates all the possible P-S conversions for a specified ray path. Initially the complete ray path is composed of P rays (coding 1). The first ray segment is then converted to an S wave (coding 2), with successive alterations as (for a ray path containing three segments)

111
211
121
221
112
212
122
222

At each stage, the required parameters of the complete ray path are calculated by calling other subroutines.

This subroutine also contains the output commands (SEE COMPUTATIONAL PROCEDURE).

SUBROUTINE ZVANGT.

This subroutine computes for multiply reflected arrivals only,

- 1) the velocity and layer thickness for each part of the ray path.
 - 2) the angle of incidence at each interface
 - 3) the apparent ground velocity of the arrival
- and 4) the total travel time of that arrival.

It is not possible to calculate the exact ray path between source and receiver directly. However, since

- 1) the direction of each segment of the ray path is known

2) every interaction at each interface (whether transmission or reflection) is known
 and 3) the P or S type of each segment of the ray path is known
 it is possible by varying the angle of descent or ascent of the initial ray segment from the source to vary the epicentral distance of that complete ray path until it lies within specified limits on either side of the observation point. Once the ray path has been determined, the travel time may be computed.

SUBROUTINE ZVA.

This subroutine performs the same function as ZVANGT, for critically refracted headwaves. In this case, the initial angle of descent is fixed by the critical angle for the headwave. If the observation distance from the source is less than the critical distance for a headwave arrival, the action will be returned to the part of the programme which called this subroutine.

SUBROUTINE AMPHA.

This subroutine calculates the final amplitude and associated phase (arising from reflection and transmission) of the ground motion for a complete ray path.

For each ray incident upon an interface, the following parameters are known and recorded

- 1) the type of incident ray, whether a P or an S wave
- 2) the type of interaction with the interface whether
 - a) reflection
 - b) transmission
 or c) headwave refraction

- 3) the velocity of the incident ray medium, and the medium on the opposite side of the interface
- 4) the angle of incidence of the incident ray
- 5) in the case of headwaves, the type of the emanating ray, whether P or S.

thus it is possible to compute (in this case by calling either subroutine ZO or HEAD), the amplitude and phase of the resultant wave at each of the interfaces. The Knoppoff coefficient for the surface displacement is also calculated for the particular angle of incidence and type of the final ray segment.

The final amplitudes are then calculated as in equation A22. The associated phase

$$\delta = \sum \delta_i,$$

where δ_i is the phase change associated with the i^{th} interaction at an interface.

(in fact, if equation A22 is written as

$$Z_R = A * (\text{COEFFICIENTS OF INTERACTION})$$

$$Z_C = B * (\text{COEFFICIENTS OF INTERACTION})$$

Both A and B are 'carried over' to SUBROUTINE AMP from ZVANGT and ZVA respectively.

SUBROUTINE ZO.

This subroutine calculates the reflection and transmission coefficients for a specific ray incident on a boundary, returning the amplitude and phase of the specified resultant ray to AMP. The method used is as described in APPENDIX A. 2. 1.

SUBROUTINE HEAD.

This is equivalent to ZO, but calculates the required headwave coefficients (see Appendix A. 2. 2.).

A. 3. 2. COMPUTATIONAL PROCEDURE.

Fig. 63 represents the main procedure followed. Data is input into the main programme. The number of ray segments in each layer is generated in MAIN.

1) REFLECTIONS AND TRANSMISSIONS.

Consider the point in MAIN where

3 segments have been generated in layer 1.

3 segments in layer 2.

2 segments in layer 3.

0 segments in layer 4.

for a four layered model, with the focus in layer 2.

CALL SUMRAY to calculate $RC = 3320$

and the total number of ray segments $SC = 8$.

RETURN TO MAIN.

CALL TDL to calculate T, D, L1 and L2 for all the ray segments.

RETURN TO MAIN.

CALL PS

(POINT 1) All segments are initially P rays

(POINT 2) CALL ZVANGT.

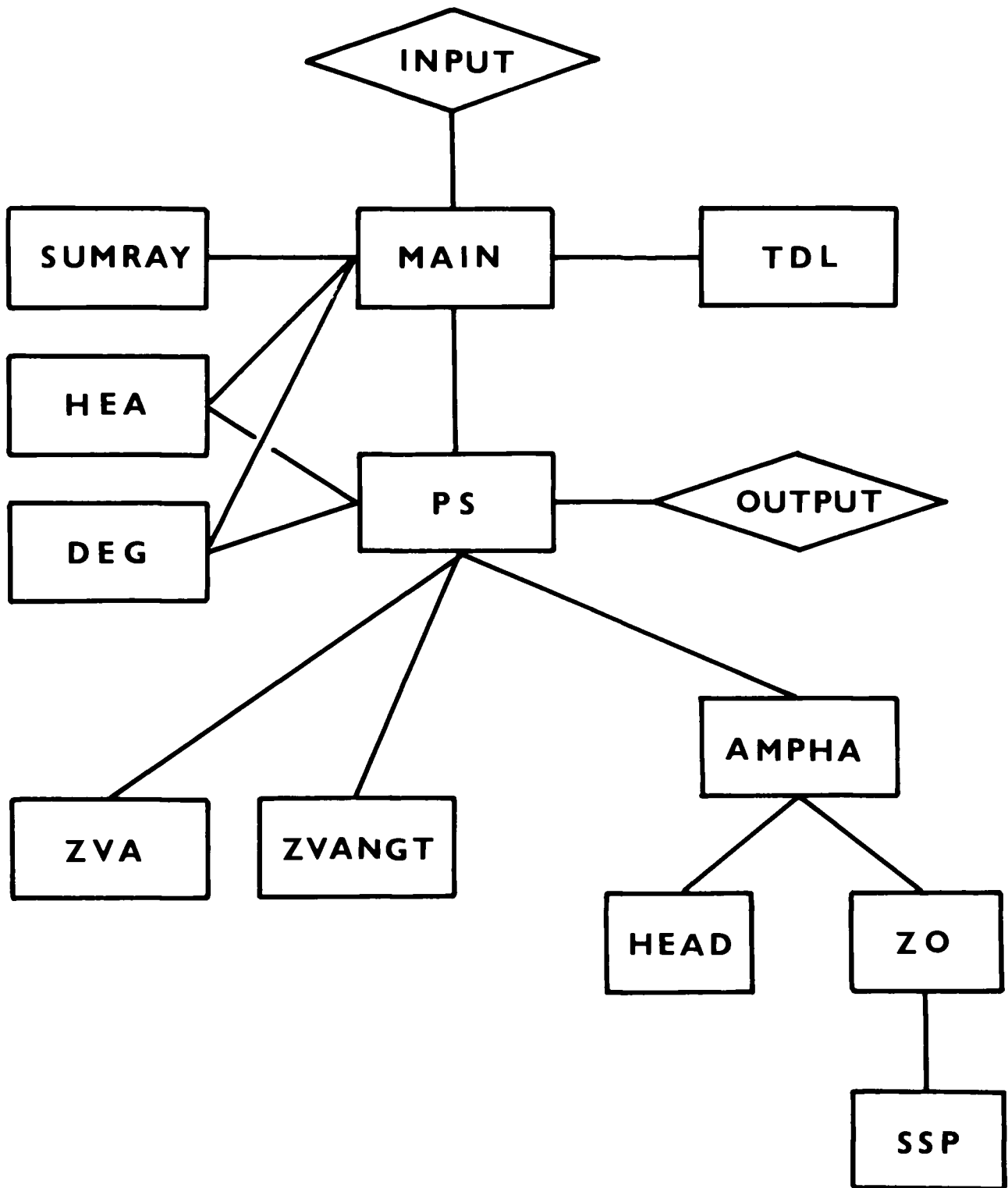
Calculate 1) Velocity

2) Layer thickness

and 3) angle of incidence of each

ray segment such that epicentral distance lies within required limits. Calculate travel time T.

Fig. 63. Computational Procedure for Synthetic Seismogram Programme.



RETURN TO PS.

CALL AMP

Calculate final amplitude and associated phase by calling ZO.

RETURN TO PS

OUTPUT

Change P segments to S segments returning to POINT 2 for each P-S conversion (POINT 3).

RETURN TO MAIN.

CALL DEG

Calculate degenerate ray path T, D, L1 and L2

CALL PS (repeat section from POINT 1 - POINT 3)

RETURN TO DEG

If there are no other degenerate arrivals

RETURN TO MAIN

Generate the next ray path.

2) When all reflections have been analysed, the programme is repeated for headwaves

ZVANGT being replaced by ZVA

ZO being replaced by HEAD

and HEA included to calculate the extra values of T, D, L1 and L2 corresponding to the headwave segment.

INPUT.

The following parameters are required as data.

1) NOL, the number of layers in the model.

2) PTS = 0 if all P and S conversions are to be considered.

= 1 if only P waves are to be considered.

3) MARK = 1 if critical distance of headwaves is to be output.

- = 0 if it is not.
- 4) IWR = 0 if output is to include information about the model.
 = 1 if output is only to include parameters of the various arrivals.
- 5) ROH = 0 if both multiply reflected waves and headwaves are to be considered.
 = 1 if only headwaves are to be considered.
 = -1 if only multiply reflected waves are to be considered.
- 6) Z(I), V(I), I = 1 → NOL.
 The layer thicknesses and associated compressional wave velocities of the model.
- 7) FD the focal depth of event.
- 8) AML the amplitude cut off.
- 9) UD the normalizing distance, h
- 10) XO observation distance.
- 11) DELX limits imposed on XO.
- 12) DELT the length of record required in seconds after the onset of the direct P wave arrival.

OUTPUT.

The initial output contains information about the model, which has been read in as input.

If the focal depth is greater than the sum of the layer thickness 'FOCUS BELOW STRUCTURE' is printed and the programme terminates.

The required parameters are printed as

```

RAY NUMBER  RAY  TIME  DISTANCE  VELOCITY
AMPLITUDE  PHASE  DIS. IN. REF.  DIRECTION
P-S CODE.
```

Where

RAY NUMBER	:	is an integer counting the number of output ray paths.
RAY	:	RC giving number of ray segments in each layer.
TIME	:	Travel time of RAY.
DISTANCE	:	Epicentral distance (lying within $XO \pm DELX$).
VELOCITY	:	Apparent ground velocity of arrival.
AMPLITUDE	:	Calculated amplitude of arrival.
PHASE	:	Associated phase of arrival (in degrees).
DIS. IN. REF.	:	Distance travelled in refracting layer for headwave arrival.
DIRECTION	:	coded direction path $D(I)$, $I = 1, SC$ (where $SC =$ total number of ray segments).
P-S CODE	:	coded P-S type of ray segments in ray path.

For headwave arrivals, if the distance travelled in the headwave layer is less than a certain distance X , (set equal to 10 units in AMPHA)

'NO HEADWAVE AT CRITICAL DISTANCE'

is printed.

If the observation distance from the source is less than the critical distance from source to receiver, the programme merely proceeds to the next ray path without any output being printed.

If the total path length is less than the normalizing distance

'RAY PATH LESS THAN UNIT DISTANCE'

is printed.

This part of the programme has been completely debugged, and has been shown to work for any horizontally n-layered model (where $n \leq 20$) and any focal depth, subject to the limitations discussed in APPENDIX 1.

A.3.3. PART 2.

The resultant output from PART 1 is a spike function in the time domain, each spike with its associated phase. This function cannot be immediately interpreted in terms of a synthetic seismogram. In order to produce such a result an input function must be altered by a factor depending on the amplitude and phase of each of the resultant 'spikes'.

An exactly similar source function satisfying the radiation condition that

1) the disturbance vanishes at infinity
and 2) no energy is radiated from infinity into the source region, has been assumed for both P and S sources. This has been taken since the wave equation is exactly equivalent to

$$\nabla^2 \bar{\Psi} = -K_s^2 \bar{\Psi}$$

where $\bar{\Psi}$ is the shear wave potential.

The resultant solutions are identical, except that K_p is replaced by K_s , (BERRY and WEST 1966).

However the source function for S-waves is highly unlikely to be equivalent to that for P waves, and the resultant arrivals should only be taken as indicative of the relation between P-wave and S-wave amplitudes.

The interaction coefficients in this analysis are independent of frequency. It can thus be seen that the multiple reflection 'amplitude' is also independent of frequency (Equation A22). The headwave 'amplitudes'

depend on $1/w$ and have been evaluated in PART 1 assuming unit frequency.

Thus interaction between the spike function and the source function, will depend on the frequency content of the source function since

$$\bar{Z}_{\text{HEAD}} = \frac{Z_{\text{HEAD}}}{w}$$

where Z_{HEAD} is the calculated headwave amplitude from PART 1.

INPUT FUNCTION.

Consider the function.

$$F(t) = \frac{1}{\delta} \left[1 - \cos \delta t + \frac{1}{m^2} (\cos m \delta t - 1) \right]$$

$$\text{for } 0 \leq t \leq T.$$

where $F(t) = 0$ for $t < 0$

and $F(t) = F(T)$ for $t > T$

(MUELLER 1967).

$$m = \frac{N+2}{N}$$

$$\text{and } \delta = \frac{N\pi}{3}$$

for $N = 1, 2, 3, 4$ etc.

$$F^1(t) = \sin \delta t - \frac{1}{m} \sin m \delta t$$

may be said to correspond to an 'input' function of order 1, 2, 3, 4 etc. This function has been plotted as in Fig. 64. In order to obtain a synthetic seismogram, the input function was transformed to obtain the complex Fourier spectrum

with amplitude spectrum $A(w)$

and phase spectrum $\phi(w)$

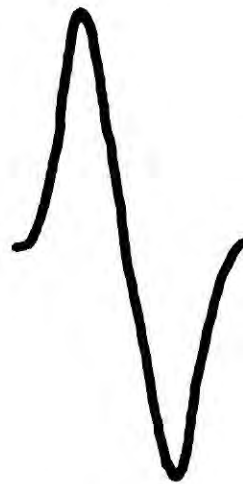
These two spectra were then altered for each individual spike as

Fig. 64. Input Function for $N = 1, 2, 3, 4$.

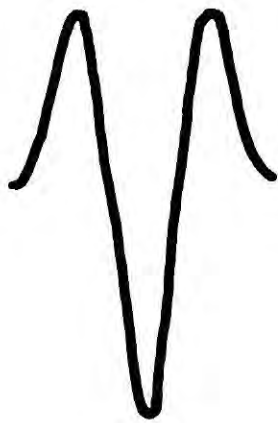
N=1



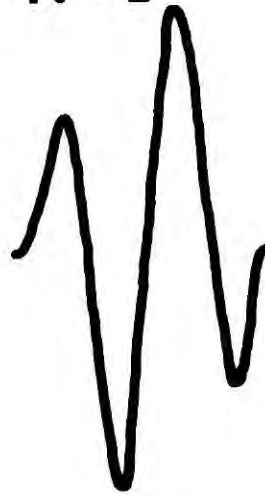
N=2



N=3



N=4



$$A^1(\omega) = A(\omega) * Z(\omega)$$

$$\text{and } \phi^1(\omega) = \phi(\omega) + \delta(\omega)$$

where $Z(\omega)$ is the amplitude of the spike

and $\delta(\omega)$ its associated phase.

As stated, in this analysis only Z_{HEAD} is a function of frequency.

The resultant amplitude and phase spectra were then transformed back into the time domain, to obtain the output waveform for each individual arrival.

The resultant wavelets were summed in the time domain to obtain the final seismogram. The transform method used was the Fast Fourier Transform of COOLEY and TUKEY (1965). This requires that the data consists of 2^N values where N is some positive integer.

The initial wavelet as in Fig. 64, was thus sampled at 32 equally spaced points (i. e. $N = 5$). A 'time unit' thus corresponded to 0.01 seconds.

This time function was transformed into its Fourier spectrum using the SUBROUTINE NLOGN (ROBINSON 1967). Thus, the frequency spectrum was obtained sampled at frequencies $f = j/q$ cycles per time unit, where $q = 32$

$$\text{and } j = 0, 1, 2, \dots, q-1.$$

The associated amplitude and phase spectra were altered for each individual spike and the resultant frequency spectrum transformed into the time domain, again using subroutine NLOGN. The resulting wavelets were summed in the time domain, with a sampling interval equal to the time unit, 0.01 seconds. The amplitude at time $T_{\text{MIN}} + T$ was then output on the IBM 360 plotter.

T_{min} is the onset time of the first arrival at the observation point.

t increases from 0 to $T_{\max} + 0.32$ secs. where T_{\max} is the onset time of the last calculated arrival.

This procedure was computed as Programme FIS.

INPUT.

N	:	Number of output arrivals from Part 1.
TIM (I)		Onset time
AMP (I)		Amplitude
PHA (I)		Phase
XH (I)	I = 1, N.	Distance travelled in refracted layer of the N arrivals determined from Part 1.
FIX	:	If equal to YES Amplitude scales on graph are input in CMIN and CMAX.
	:	If equal to NO New scales are computed.
X (I),	I = 1, 32.	The input time function data.
CMIN		Maximum and Minimum values of
CMAX		Amplitude Scale.

The final amplitudes have been increased by a factor of 10^2 for ease of computation. The programme was run on the IBM 360 NUMAC computer and considerable use was made of scratch files. The commands for running the complete programme are noted after the printout of the programmes.

XC denotes the compiled version of file X

DAT 1 contains the data for PART 2

D contains FIX and X (I), I = 1, 32 for part 2.

The programme uses an increasing amount of CPU time

with 1) increasing epicentral distance

and 2) increasing length of record required.

However, 10 second records for an event originating 50 km from the observation point can be computed in approximately 100 seconds. For epicentral distances beyond 200 km, it is necessary to divide the analysis into component parts making use of PTS and ROH in the input.

COMPUTER PROGRAMME

C
C
C
PART 1 SYNTHETIC SEISMOGRAMS P. MAGUIRE

COMMON/A1/NDL
COMMON/A2/SC
COMMON/A3/FL,ZL,FD
COMMON/A4/CODE(20)
COMMON/A5/Z(20),V(20)
COMMON/A6/AN
COMMON/A7/RC
COMMON/A8/T(100),D(100),LI(100),L2(100)
COMMON/A9/ZINF
COMMON/A10/X0,DELX
COMMON/A11/TIM
COMMON/A12/TC
COMMON/A13/DELT,PTS
COMMON/A18/IND
COMMON/A19/TIM1,H
COMMON/A20/IDEG
COMMON/A24/LK
COMMON/A25/AH
COMMON/A27/AML,MARK
COMMON/A29/XG,XF,GF
COMMON/A30/LD
COMMON/A32/NUM

INTEGER SC,RC,FL,CODE,T,L,PTS,PTSE,H,ROH,AH

C
C
C
READ LAYER THICKNESS AND VELOCITY. COMPUTE FOCAL LAYER AND DEPTH

READ (5,1) NCL,PTS,MARK,IWR,RCF

1 FORMAT(5I5)

READ (5,10) (Z(I),V(I),I=1,NCL)

10 FORMAT(2F10.0)

READ (5,101) FD,AML,UD

```

101 FORMAT(3F10.0)
ZL=C.0
XH=C.0
DC 102 I=1,NOL
ZL=ZL+Z(I)
FL=I
IF (FC-ZL) 2,2,102
102 CONTINUE
WRITE (6,103)
103 FORMAT(1H1,'FOCUS BELOW STRUCTURE')
GO TO 58
2 ZINF=FC-ZL+Z(FL)
IF (IWR-1) 200,2022,200
200 WRITE (6,20)
20 FORMAT(1H ,//'LAYER THICKNESS VELOCITY')
WRITE (6,201) (I,Z(I),V(I),I=1,NOL)
201 FORMAT(1H ,//(I3,2F14.2))
WRITE (6,202) FD,FL
202 FORMAT(1H ,//,'FOCAL DEPTH = 'F6.2,' IN LAYER ',I4)
WRITE(6,2021) AML,UD
2021 FORMAT(1H ,//,'AMPL CUTOFF : ',F10.8,' NORMALISING DISTANCE : ',F
110.2)
C
C READ OBSERVATION DISTANCE WITH LIMITS AND TIME LIMIT ON RECORD
C
2022 READ (5,203) XC,DELX,DELT
203 FORMAT(3F10.0)
IF (IWR-1) 2030,2050,2030
2030 WRITE(6,204) XC,DELX,DELT
204 FORMAT(1H ,//'OBSERVATION DISTANCE = 'F6.1,' + CR - ',F4.1,
1//,'LENGTH OF RECORD FROM DIRECT WAVE CNSET = ',F6.2)
WRITE(6,205)
205 FORMAT(1H ,//(7X,'PAY',10X,'TIME',4X,'DISTANCE',4X,'VELOCITY',4X,
1,'AMPLITUDE',2X,'PHASE',4X,'DIS IN REF',4X,'DIRECTION',10X,'P-S CCE

```

```

2E*)
C
C START RAY GENERATION : DIRECT WAVE
C
2050 AH=0
IF (ROH) 2051,2052,2052
2051 H=0
GO TO 2053
2052 H=1
2053 NUM=0
2054 LK=0
M=1
IDEG=0
DO 3 I=1,FL
3 CODE(I)=1
J=FL+1
IF (J-NOL) 4,4,6
4 DO 5 I=J,NOL
5 CODE(I)=0
6 AN=45.C
60 CALL SUMRAY
IND=1
IF (FD) 602,601,602
601 TO=XD/V(1)
GO TO 603
602 CALL TDL
IF (H-1) 6021,6020,6021
6020 PTSE=PTS
PTS=1
AH=H
H=0
6021 CALL PS
H=AH
AH=0

```

```
IF (H-I) 603,6022,603
6022 PTS=PTSE
603 IF (TO) 11,8,11
8 IF (FL-1) 80,9,80
80 CODE(1)=CODE(1)+2
GO TO 60
9 CODE(1)=CCODE(1)+1
GO TO 60
```

```
C
C
C
```

```
REFLECTIONS IN LAYERS ABOVE FOCUS
```

```
11 IF (H-I) 1102,110,1102
110 IF (FD-ZL) 23,1101,23
1101 LK=1
```

```
CALL HEA
```

```
1102 IF (M-FL) 12,23,23
```

```
12 CODE(M)=CODE(M)+2
```

```
CALL SUMRAY
```

```
CALL TDL
```

```
IF (H-I) 1202,1201,1202
```

```
1201 CALL HEA
```

```
GO TO 1203
```

```
1202 CALL PS
```

```
1203 IF (TIM1-(TO+DELT)) 13,13,21
```

```
13 CALL DEG
```

```
CODE(1)=CCODE(1)+2
```

```
CALL SUMRAY
```

```
CALL TDL
```

```
IF (H-I) 1302,1301,1302
```

```
1301 CALL HEA
```

```
GO TO 1303
```

```
1302 CALL PS
```

```
1303 IF (TIM1-(TO+DELT)) 13,13,16
```

```
16 J=1
```

```

160 DO 17 I=1,J
17 CODE(I)=1
   IF (J-M) 18,22,18
18 CODE(J+1)=CCDE(J+1)+2
   CALL SUMRAY
   CALL TDL
   IF (H-I) 1802,1801,1802
1801 CALL HEA
   GO TO 1803
1802 CALL PS
1803 IF (TIM1-(TO+DELT)) 13,13,19
19 J=J+1
   IF (J-M) 160,21,160
21 CODE(M)=1
22 M=M+1
   GO TO 1102

C
C REFLECTICNS IN LAYER OF FOCUS
C
23 LK=G
   IF (H-I) 231,2300,231
2300 M=FL
231 IF (FL-NOL) 230,5601,230
230 IF (FD-ZL) 24,2301,24
2301 CODE(M)=CCDE(M)+2
   CALL SUMRAY
   CALL TDL
   IF (H-I) 2303,2302,2303
2302 CALL HEA
   GO TO 2304
2303 CALL PS
2304 IF (TIM1-(TO+DELT)) 25,25,350
24 CODE(M)=CCDE(M)+1
240 CALL SUMRAY

```

```

CALL TDL
IF (H-1) 2402,2401,2402
2401 CALL HEA
GO TO 2403
2402 CALL PS
2403 IF(TIM1-(TO+DELT)) 25,25,36
25 IF (FL-1) 27,26,27
26 IF (FD) 230,260,230
260 CODE(M)=CCODE(M)+2
GO TO 240
27 CALL DEG
CODE(1)=CCODE(1)+2
CALL SUMRAY
CALL TDL
IF (H-1) 2702,2701,2702
2701 CALL HEA
GO TO 2703
2702 CALL PS
2703 IF (TIM1-(TO+DELT)) 27,27,31
31 J=1
310 DO 32 I=1,J
32 CODE(I)=1
IF (J-(M-1)) 33,230,33
33 CODE(J+1)=CODE(J+1)+2
CALL SUMRAY
CALL TDL
IF (H-1) 3302,3301,3302
3301 CALL HEA
GO TO 3303
3302 CALL PS
3303 IF (TIM1-(TO+DELT)) 27,27,34
34 J=J+1
IF (J-(M-1)) 310,35,310
35 CODE(J)=1

```

```

C
C
C
GO TO 23C
REFLECTIONS IN LAYER RELCW FCCUS
350 CCDE(M)=1
GO TO 36C
36 CODE(M)=2
360 M=M+1
37 IF (M-NCL) 37,5601,37
CODE(M)=CCDE(M)+2
CALL SUMRAY
CALL TDL
IF (H-1) 3702,3701,3702
3701 CALL HEA
GO TO 3703
3702 CALL PS
3703 IF (TIM1-(TC+DELT)) 38,38,36
38 CALL DEG
IF (FL-1) 43,410,43
410 IF (FD) 4101,43,4101
4101 IF (FL-ZL) 42,43,42
42 CODE(1)=CCDE(1)+1
GO TO 430
43 CODE(1)=CCDE(1)+2
430 CALL SUMRAY
CALL TCL
IF (H-1) 4302,4301,4302
4301 CALL HEA
GO TO 4303
4302 CALL PS
4303 IF (TIM1-(TC+DELT)) 38,38,44
44 J=1
440 IF (J-(FL-1)) 45,45,52
45 DO 46 I=1,J

```

```
46 CODE(I)=1
   IF (J-(FL-1)) 47,460,47
460 IF (FD-ZL) 48,47,48
47 CODE(J+1)=CODE(J+1)+2
   GO TO 49
48 CODE(J+1)=CCODE(J+1)+1
49 CALL SUMRAY
   CALL TDL
   IF (H-1) 4902,4901,4902
4901 CALL HEA
   GO TO 4903
4902 CALL PS
4903 IF (TIM1-(TO+DELT)) 38,38,51
51 J=J+1
   GO TO 440
52 IF (FL-1) 520,5205,520
520 IF (FD-ZL) 53,5201,53
5201 DO 5202 IJ=1,FL
5202 CODE(IJ)=1
   IF (J-FL) 550,550,5203
5203 JFL=FL+1
   DO 5204 IK=JFL,J
5204 CODE(IK)=2
   GO TO 550
5205 IF (FD-ZL) 540,5206,540
5206 CODE(FL)=1
   IF (J-1) 5203,550,5203
53 IFL=FL-1
   DO 54 I=1,IFL
54 CODE(I)=1
540 DO 55 I=FL,J
55 CODE(I)=2
550 CODE(J+1)=CODE(J+1)+2
   CALL SUMRAY
```

```
CALL TDL
IF (H-I) 5502,5501,5502
5501 CALL HEA
GO TO 5503
5502 CALL PS
5503 IF (TIM1-(TC+DELT)) 38,38,56
56 J=J+1
IF (J-M) 52,36,52
5601 H=H-1
IF (ROH) 58,57,58
57 ROH=-1
GO TO 2054
58 WRITE(4,59) NUM
59 FORMAT(I5)
STOP
ENC
```

```
C
C
C
SUBROUTINE SUMRAY
  COMPUTE SUMCODE AND RAYCCDE
  COMMON/A1/NCL
  COMMON/A2/SC
  COMMON/A4/CODE(20)
  COMMON/A7/RC
  INTEGER SC,RC,CODE
  SC=0
  RC=0
  DO 101 IJ=1,NCL
    SC=SC+CODE(IJ)
    KL=NCL-IJ
    IF (KL) GO,1,1C
  1 RC=RC+CODE(IJ)
    GO TO 101
  10 RC=RC+(CODE(IJ))*(1C**KL)
  101 CONTINUE
  RETURN
  END
```

SUBROUTINE TCL

C
C

```
COMMON/A1/NOL
COMMON/A2/SC
COMMON/A3/FL,ZL,FC
COMMON/A4/CODE(20)
COMMON/A8/T(100),D(100),L1(100),L2(100)
COMMON/A20/IDEG
COMMON/A21/CDC(20)
COMMON/A22/ST,L
INTEGER FL,CODE,T,D,CCD,SC,ST
```

C
C
C

```
COMPUTE T(1) AND D(1)
```

```
IF (IDEG) 40,99,40
99 I=(CODE(FL)-1)/2
ST=0
T(1)=2
L1(1)=FL
IF(CODE(FL)-((2*I)+1)) 2,1,2
1 IF (FD-ZL) 103,10,103
10 IF (CODE(FL)-1) 103,101,103
101 IF (FL-NCL) 102,103,102
102 IF (CODE(FL+1)) 104,103,104
103 D(1)=1
GO TO 3
104 L1(1)=FL+1
2 D(1)=2
3 CONTINUE
```

C
C
C

```
COMPUTE T,D,L1,L2(1 - SC)
```

```
DO 4 I=1,NCL
```

```

4  COD(I)=CCODE(I)
   COD(L1(I))=COD(L1(I))-1
   ST=ST+1
   L=1
40 IF (D(L)-1) 5,15,5
5  IF (T(L)-1) 6,7,6
6  L1(L+1)=L1(L)
   L2(L+1)=L1(L)+1
   GO TO 8
7  L1(L+1)=L2(L)
   L2(L+1)=L2(L)+1
8  IF (L2(L+1)-NCL) 9,12,9
9  IF (COD(L2(L+1))) 11,12,11
11 D(L+1)=2
   T(L+1)=1
   GO TO 13
12 D(L+1)=1
   T(L+1)=2
120 COD(L1(L+1))=COD(L1(L+1))-1
   ST=ST+1
   GO TO 14
13 COD(L2(L+1))=COD(L2(L+1))-1
   ST=ST+1
14 L=L+1
   GO TO 40
15 IF (T(L)-1) 16,17,16
16 L1(L+1)=L1(L)
   L2(L+1)=L1(L)-1
   GO TO 18
17 L1(L+1)=L2(L)
   L2(L+1)=L2(L)-1
18 IF (L2(L+1)) 22,15,22
19 IF (CCC(L1(L+1))) 21,26,21
21 D(L+1)=2

```

```
T(L+1)=0
GO TO 120
22 IF (CCD(L2(L+1))-1) 24,23,24
23 IF (CCD(L1(L+1))) 25,24,25
24 C(L+1)=1
   T(L+1)=1
   GO TO 13
25 D(L+1)=2
   T(L+1)=2
   GO TO 120
25 RETURN
   END
```

SUBROUTINE DEG

C
C
C
C

CCOMPUTE ALL POSSIBLE DEGENERATE RAYS

```
COMMON/A1/NCL
COMMON/A2/SC
COMMON/A3/FL,ZL,FD
COMMON/A4/CODE(20)
COMMON/A6/AN
COMMON/A7/RC
COMMON/A8/T(100),D(100),L1(100),L2(100)
COMMON/A9/ZINF
COMMON/A10/X0,DELX
COMMON/A11/TIM
COMMON/A12/T0
COMMON/A13/DELT,PTS
COMMON/A14/INC(100)
COMMON/A15/RES(100)
COMMON/A18/INC
COMMON/A19/TIM1,H
COMMON/A20/IDEG
COMMON/A21/CDE(20)
COMMON/A22/ST,L
COMMON/A24/LK
COMMON/A27/AML,MARK
DIMENSION T1(100),D1(100),L11(100),L21(100)
INTEGER T,D,SC,FL,T1,D1,ST,CODE,COD,RES,PTS,H
```

C
C

```
IDEG=1
IF (SC-5) 24,24,30
30 DO 4 K=1,NOL
4 COD(K)=CCDE(K)
```

```

DO 5 J=1,SC
  T1(J)=T(J)
  D1(J)=D(J)
  L1(J)=L1(J)
5  L21(J)=L2(J)
  I=SC-1
  ST=SC
51 IF (T(I)-1) 6,7,6
6  I=I-1
  IF (I-1) 51,16,51
7  T(I)=2
71 II=I+1
  DO 8 K=II,SC
  COD(L1(K))=COD(L1(K))-1
8  ST=ST-1
  COD(L1)=CCC(L1)-1
  ST=ST-1
  IF (I-1) 9,18,9
9  IF (D(I)-1) 11,12,11
11 D(I)=1
  GO TO 13
12 D(I)=2
13 COD(L1(I))=COD(L1(I))+1
  ST=ST+1
  IF (COD(L1(I))-CODE(L1(I))) 21,14,14
14 DO 15 K=I,SC
  T(K)=T1(K)
15 D(K)=D1(K)
  DO 151 K=1,NCL
151 COD(K)=CODE(K)
  ST=SC
  GO TO 6
16 IF (FD-ZL) 24,17,24
17 IF (FL-(NCL-1)) 71,24,71

```

```
18 IF (D(I)-1) 24,19,24
19 D(I)=2
   LI(I)=LI(I)+1
   COD(LI(I))=CCC(LI(I))+1
   ST=ST+1
   IF (COD(LI(I))-CODE(LI(I))) 21,24,24
21 L=I
   DO 22 N=1,NUL
   22 COD(N)=CCLE(N)-COD(N)
      CALL TDL
      IF (ST-SC) 14,23,14
23 IF (H-1) 2302,2301,2302
2301 CALL HEA
      GO TO 30
2302 CALL PS
      GO TO 30
24 IDEG=0
      RETURN
      END
```

```

C
C
C
SUBROUTINE HEA
CCOMPUTE TRANSMISSION CODE FOR HEADWAVES

COMMON/A1/NOL
COMMON/A2/SC
COMMON/A3/FL,ZL,FD
COMMON/A4/CCDE(20)
COMMON/A5/Z(20),V(20)
COMMON/A6/AN
COMMON/A7/RC
COMMON/A8/T(100),D(100),L1(100),L2(100)
COMMON/A9/ZINF
COMMON/A10/XC,DELX
COMMON/A11/TIM
COMMON/A12/T0
COMMON/A13/DELT,PTS
COMMON/A14/INC(100)
COMMON/A15/RES(100)
COMMON/A16/ANG(100)
COMMON/A18/IND
COMMON/A19/TIM1,H
COMMON/A20/IDEG
COMMON/A23/ILL
COMMON/A24/LK
COMMON/A27/AML
DIMENSION TR(100),DR(100),LIR(100),L2R(100)
INTEGER SC,CCDE,PC,FL,T,C,TR,DR,RES,PTS,H
I=0
LMA=J
DC 1 K=1,SC
TR(K)=T(K)
DR(K)=D(K)
LIR(K)=L1(K)

```

```

1 L2R(K)=L2(K)
  IF (LK-1) 2,40,2
2 IF (SC-1) 3,65,3
3 IS=SC-1
  DO 4 J=1,IS
    IF (J-1) 301,30,301
30 IF (L1(J)-L2(J+1)) 3,2,302,4
301 IF (L2(J)-L2(J+1)) 302,302,4
302 LM=L2(J+1)
    IF (LMA-LM) 303,4,4
303 I=J+1
    LMA=LM
4 CONTINUE
  IF (I) 5,65,5
40 I=LK
5 DO 6 K=I,SC
  J=(SC+1)-K
  T(J+1)=T(J)
  D(J+1)=D(J)
  L1(J+1)=L1(J)
6 L2(J+1)=L2(J)
  T(I)=1
  D(I)=0
  T(I+1)=1
  IF (I-1) 62,61,62
61 L1(I+1)=L1(I)+1
  L2(I)=L1(I+1)
  GO TO 63
62 L1(I+1)=L2(I)
63 L2(I+1)=L1(I)
  CODE(L2(I))=1
  ILL=I
  CALL SUMRAY
  CALL PS

```

```
CODE(L2(I))=0
SC=SC-1
DO 64 K=1,SC
T(K)=TR(K)
D(K)=DR(K)
L1(K)=L1R(K)
64 L2(K)=L2R(K)
65 RETURN
END
```

```

C
C
C
SUBROUTINE PS
COMPUTE ALL P TC S CCNVERSICNS
COMMON/A2/SC
COMMON/A3/FL,ZL,FC
COMMON/A5/Z(20),V(20)
COMMON/A6/AN
COMMON/A7/RC
COMMON/A8/T(100),D(100),L1(100),L2(100)
COMMON/A9/ZINF
COMMON/A10/X0,DELX
COMMON/A11/TIM
COMMON/A12/TC
COMMON/A13/DELT,PTS
COMMON/A14/INC(100)
COMMON/A15/RES(100)
COMMON/A16/ANG(100)
COMMON/A18/INC
COMMON/A19/TIM1,H
COMMON/A20/IDEG
COMMON/A23/ILL
COMMON/A25/AH
COMMON/A26/AMPL,PHASE
COMMON/A27/AML,MARK
COMMON/A28/XT,VAR
COMMON/A29/XG,XH,GF
COMMON/A32/NUM
DIMENSION VF(100),ZR(100)
LOGICAL *IFMT(60),QS(10)
DATA FMT/,'(IH ,I3,I7,F14.2,2F10.2,F15.9,F8.2,4X,F6.1,8X, I2, X,
1 I2)',/,QS/,'1234567890' /
INTEGER SC,FL,T,D,RES,PTS,RC,H,AH,RAY
LIS=SC/10

```

```

L2S=SC-L1S*10
IF (L1S) 15,14,15
14 L1S=10
15 IF (L2S) 17,16,17
16 L2S=10
17 FMT(47)=QS(L1S)
FMT(48)=QS(L2S)
FMT(56)=QS(L1S)
FMT(57)=QS(L2S)
ISC=20-2*SC
LS1=ISC/10
LS2=ISC-LS1*10
IF (LS1) 19,18,19
18 LS1=10
19 IF(LS2) 22,21,22
21 LS2=10
22 FMT(52)=QS(LS1)
FMT(53)=QS(LS2)
DO 1 I=1,SC
INC(I)=1
1 RES(I)=1
IF (H-1) 102,101,102
101 CALL ZVA
GC TO 103
102 CALL ZVANGT
XH=C.C
103 IF (IDEG) 1000,100,1000
100 TIMI=TIM
1500 IF (TG) 1001,12,1001
1001 IF (TIM-(TC+DELT)) 2,2,3
2 IF (TIM) 20,3,20
20 IF (AH-1) 201,3,201
201 CALL AMPHA
IF (AMPL-AML) 3,3,202

```

```

202 NUM=NUM+1
   WRITE(6,FMT)NUM,FC,TIM,XT,VAR,AMPL,PHASE,XT,(C(M),M=1,SC),(RES(M),
   IM=1,SC)
   WRITE(3,FMT)NUM,RC,TIM,XT,VAR,AMPL,PHASE,XT,(D(M),M=1,SC),(RES(M),
   IM=1,SC)
      3 IF(PTS) 12,31,12
      31 INC(I)=2
      RES(I)=2
      IF (H-1) 312,311,312
      311 CALL ZVA
      GO TO 313
      312 CALL ZVANGT
      313 IF (TIM1) 3132,3131,3132
      3131 TIM1=TIM
      3132 IF (TIM-(TO+DELT)) 4,4,5
      4 IF (TIM) 40,5,4C
      4C CALL AMPHA
      IF (AMPL-AML) 5,5,4C1
      401 NUM=NUM+1
      WRITE(6,FMT)NUM,RC,TIM,XT,VAR,AMPL,PHASE,XT,(C(M),M=1,SC),(RES(M),
      IM=1,SC)
      WRITE(3,FMT)NUM,RC,TIM,XT,VAR,AMPL,PHASE,XT,(D(M),M=1,SC),(RES(M),
      IM=1,SC)
      5 M=1
      6 INC(M)=1
      RES(M)=1
      IF (SC-1) 61,12,61
      61 IF (RES(M+1)-2) 7,10,7
      7 INC(M+1)=2
      RES(M+1)=2
      IF (H-1) 72,71,72
      71 CALL ZVA
      GO TO 73
      72 CALL ZVANGT

```

```
73 IF (TIM1) 732,731,732
731 TIM1=TIM
732 IF (TIM-(TO+DELT)) 8,8,9
8 IF (TIM) 8C,9,80
80 CALL AMPHA
IF (AMPL-AML) 9,9,801
801 NUM=NUM+1
WRITE(6,FMT)NUM,RC,TIM,XT,VAR,AMPL,PHASE,XH,(C(M),M=1,SC),(RES(M),
1M=1,SC)
WRITE(3,FMT)NUM,RC,TIM,XT,VAR,AMPL,PHASE,XH,(D(M),M=1,SC),(RES(M),
1M=1,SC)
9 GO TO 31
10 M=M+1
IF (M-SC) 11,12,11
11 GO TO 6
12 IF (H-1) 13,120,13
120 IF (TIM1) 13,121,13
121 TIM1=TO+2.0*DELT
13 RETURN
END
```

```

C
C
C
SUBROUTINE ZVANGT
      CCMPUTE VELOCITY, ANGLE, AND LAYER THICKNESS FOR EACH PART OF RAY
      COMMON/A2/SC
      COMMON/A3/FL,ZL,FD
      COMMON/A5/Z(20),V(20)
      COMMON/A6/AN
      COMMON/A8/T(100),D(100),L1(100),L2(100)
      COMMON/A9/ZINF
      COMMON/A10/XG,DELX
      COMMON/A11/TIM
      COMMON/A12/T0
      COMMON/A15/RES(100)
      COMMON/A16/ANG(100)
      COMMON/A18/INC
      COMMON/A28/XT,VAR
      COMMON/A27/AML,MARK
      COMMON/A29/XG,XH,GF
      COMMON/A30/UD
      DIMENSION VR(100),ZR(100)
      INTEGER SC,FL,T,D,RES
      PX(Y)=(1.-Y**2)/Y
      DR=(4.0*ATAN(1.0))/180.)
      DELA=5.0
      ANG(1)=AN
      IF (SC-1) 27,33,27
      IF (SC-2) 28,31,28
      27 DO 29 I=3,SC
      J=I-1
      29 ZR(J)=Z(L1(I))
      ZR(SC)=Z(1)
      GO TO 32
      31 ZR(2)=Z(1)

```

```

32 IF(D(I)-1) 34,33,34
33 ZR(I)=ZINF
   GO TO 35
34 IF (ZL-FC) 340,34C1,340
34C ZR(I)=Z(FL)-ZINF
   GO TO 35
3401 ZR(I)=Z(FL+1)
35 IF (RES(SC)-1) 3501,3502,3501
3501 VR(SC)=V(I)/1.74
   GO TO 3503
3502 VR(SC)=V(I)
3503 IF (SC-1) 36,38,36
36 DO 37 I=2,SC
   J=I-1
   IF (RES(J)-1) 3601,3602,3601
3601 VR(J)=V(LI(I))/1.74
   GO TO 37
3602 VR(J)=V(LI(I))
37 CONTINUE
38 IU=1
   ID=1
   IP=1
380 K=0
   L=1
3801 IF (L-SC) 39,49,39
39 IF (T(L+1)-1) 43,41,43
41 SIAN=(SIN(ANG(L)*DR))*(VR(L+1)/VR(L))
   IF (SIAN-1.0) 42,45,45
42 ANG(L+1)=ATAN2(SIAN, SQRT(1.0-(SIAN**2)))/DR
   GO TO 44
43 IF (RES(L)-1) 432,430,432
430 IF (RES(L+1)-1) 431,435,431
431 P=(SIN(ANG(L)*DR)/1.74)
   ANG(L+1) =ATAN2(P, SQRT(1.0-P**2))/DR

```

```

GO TO 44
432 IF (RES(L+1)-1) 435,433,435
433 Q=SIN(ANG(L)*DR)*1.74
IF (1.0-Q) 45,45,434
434 ANG(L+1)=ATAN2(G, SQRT(1.0-C**2))/DR
GO TO 44
435 ANG(L+1)=ANG(L)
44 L=L+1
45 K=1
I=L
SIAN=1.0-1.0E-5
ANG(I+1)=ATAN2(SIAN, SQRT(1.0-(SIAN**2)))/DR
450 IF (T(I+1)-1) 47,46,47
46 SIAN=(SIN(ANG(I+1)*DR))*(VR(I)/VR(I+1))
ANG(I)=ATAN2(SIAN, SQRT(1.0-(SIAN**2)))/DR
GO TO 48
47 IF (RES(I+1)-1) 472,470,472
470 IF (RES(I)-1) 471,474,471
471 P=SIN(ANG(I+1)*DR)/1.74
ANG(I)=ATAN2(P, SQRT(1.0-P**2))/DR
GO TO 48
472 IF (RES(I)-1) 474,473,474
473 Q=SIN(ANG(I+1)*DR)*1.74
ANG(I)=ATAN2(G, SQRT(1.0-Q**2))/DR
GO TO 48
474 ANG(I)=ANG(I+1)
48 I=I-1
IF (I) 450,39,450
C
C CALCULATE X AND SET BETWEEN LIMITS
C
49 X=C.C
DO 51 I=1,SC

```

```

51 X=X+ZR(I)*SIN(ANG(I)*DR)/COS(ANG(I)*DP)
    N=1
    IF (K) 52,54,52
52 IF (X-(XO-DELX)) 53,55,55
53 TIM=0.0
    GO TO 660
54 IF (X-(XO-DELX)) 61,55,55
55 IF (X-(XO+DELX)) 65,65,56
56 IU=IU+1
    IF (IU-1) 57,58,57
57 ID=1
    IU=1
    IP=IP+1
58 ANG(1)=ANG(1)-DELA/IP
    IF (ANG(1)) 59,380,380
59 N=N+1
    ANG(1)=ANG(1)+DELA/IP
    DELA=DELA/N
    GO TO 58
61 ID=ID+1
    IF (IU-1) 62,63,62
62 ID=1
    IU=1
    IP=IP+1
63 ANG(1)=ANG(1)+DELA/IP
    IF (ANG(1)-90.0) 380,64,64
64 N=N+1
    ANG(1)=ANG(1)-DELA/IP
    DELA=DELA/N
    GO TO 63
C
C
C
    CALCULATE T
C
65 TIM=0.0

```

```

XG=0.0
XL=0.0
DO 66 I=1,SC
  XG=XG+ZR(I)/(CCS(ANG(I)*DR))
  XL=XL+ZR(I)*SIN(ANG(I)*DR)/((CCS(ANG(I)*DR))**3)
  TIM=TIM+(ZR(I)/(COS(ANG(I)*DF)))/VR(I)
  PO=SIN(ANG(I)*DR)/VR(I)
  GF=1.0/SQRT(PX(PC)*X*XL/(LD**2))
  IF (MARK-1) 660,661,660
661 WRITE (6,662) GF
662 FORMAT(1H , ' GF = ',F20.7)
660 IF (IND-1) 67,660,67
6601 TO=TIM
      IND=2
67 AN=ANG(I)
  VAR=VR(SC)/SIN(ANG(SC)*DR)
  XT=X
  RETURN
END

```

```

C
C
C
SUBROUTINE ZVA
COMPUTE TRAVEL TIME FOR HEAD WAVE
COMMON/A2/SC
COMMON/A3/FL,ZL,FD
COMMON/A5/Z(20),V(20)
COMMON/A6/AN
COMMON/A8/T(100),D(100),L1(100),L2(100)
COMMON/A9/ZINF
COMMON/A10/XG,CELEX
COMMON/A11/TIN
COMMON/A12/TO
COMMON/A15/PES(100)
COMMON/A16/ANG(100)
COMMON/A23/ILL
COMMON/A27/AVL,MARK
COMMON/A28/XT,VAR
COMMON/A29/XG,XH,GF
COMMON/A30/UC
DIMENSION ZP(100),VR(100)
REAL KAI
INTEGER SC,FL,T,D,RES
DR=(4.0*ATAN(1.0))/180.0
I=ILL
ZR(SC)=Z(1)
IF (D(1)-1) 1,2,3
1 ZR(1)=0.0
GO TO 30
2 ZR(1)=ZINF
GO TO 30
3 ZR(1)=Z(FL)-ZINF
3) IF (SC-2) 6,6,4
4 DO 5 L=3,SC

```

```

      IF (D(L-1)) 40,401,40
40  ZR(L-1)=Z(L1(L))
      GO TO 5
401 ZR(L-1)=0.0
      5 CONTINUE
      6 IF (RES(SC)-1) 60,601,60
60  VR(SC)=V(I)/1.74
      GO TO 7
601 VR(SC)=V(1)
      7 DO 702 K=2,SC
      J=K-1
      IF (RES(J)-1) 70,701,70
70  VR(J)=V(L1(K))/1.74
      GO TO 702
701 VR(J)=V(L1(K))
702 CONTINUE
      L=I
      ANG(L)=90.0
      SIAN=VR(L+1)/VR(L)
      IF (SIAN-1.0) 80,26,26
80  ANG(L+1)=ATAN2(SIAN,SCRT(1.0-((SIAN**2)))/DF)
601 L=L+1
      IF (L-SC) 9,14,14
      9 IF (T(L+1)-1) 11,90,11
      SIAN=(SIN(ANG(L)*DF))*(VR(L+1)/VR(L))
      IF (SIAN-1.0) 80,26,26
      11 IF (RES(L)-1) 12,110,12
      110 IF (RES(L+1)-1) 1101,13,1101
1101 P=(SIN(ANG(L)*DR)/1.74)
1102 ANG(L+1)=ATAN2(P,SCRT(1.0-P**2))/DR
      GO TO 801
      12 IF (RES(L+1)-1) 13,120,13
      120 P=SIN(ANG(L)*DR)*1.74
      IF (1.0-P) 26,26,1102

```



```

      IF (X-(XC+DELX)) 23,23,26
23  XH=XC-X
      IF (XH) 24,25,25
24  XH=0.0
25  TIM=TIM+XH/VR(I)
      VAR=VR(SC)/SIN(ANG(SC)*DE)
      XT=XC
      IF (I-1) 251,27,251
251  PX=SQRT((1.0-(VR(I-1)/VR(I))**2)/(1.0-(VR(1)/VR(I))**2))
      RL=SQRT(XC*(XH**3)/(UC**4))
      KAL=(2.0*DR*180.0)*1.0/V(FL)
      IF (RL) 252,252,252
252  GF=0.0
      GO TO 27
253  GF=PX/(RL*UC*KAL)
      GO TO 27
26  TIM=0.0
27  IF (MARK-1) 28,270,28
270  WRITE (6,271) X,TIM
271  FORMAT(IH,'C.C. = ',F10.2,' TT = ',F1(.2)
      WRITE(6,272) GF
272  FORMAT(IH,' GF = ',F20.7)
28  RETURN
      END

```

```

C
C
C
SURROUTINE ALPHA
      COMPUTE AMPLITUDE AND PHASE OF COMPLETE RAY PATH
      COMMON/A2/SC
      COMMON/A5/Z(20),V(20)
      COMMON/A8/T(100),D(100),LI(100),L2(100)
      COMMON/A14/INC(100)
      COMMON/A15/RES(100)
      COMMON/A16/ANG(100)
      COMMON/A17/U(2),ANGLE,RAY,AMP,PHA
      COMMON/A19/TIMI,H
      COMMON/A26/AMPL,PHASE
      COMMON/A29/XC,XF,CF
      COMMON/A30/LD
      INTEGER SC,T,D,RES,RAY,PSCO,H
      DR=(4.0*ATAN(1.0))/180.0
      PSCO=J
      AMPL=1.0
      PHASE=0.0
      IF (D(1)) 10,11,10
10  IF (SC-1) 2,7,2
      2 DO 6 J=2,SC
      IF (D(J)) 22,21,22
21  RAY=INC(J-1)*10*2+INC(J)*10+INC(J+1)
      U(1)=V(L1(J))
      U(2)=V(L2(J))
      CALL HEAD
      IF ((XG+XH)-UD) 712,712,210
210  IF (XH-10.0) 71,71,211
211  AMPL=AMPL*AMP*GF
      PHASE=PHASE+0.0
      J=J+1
      GO TO 6

```

```

22 RAY=INC(J-1)*(10**3)+D(J)*(10**2)+T(J)*I'+RES(J)
   U(1)=V(L1(J))
   IF (L2(J)) 3,4,3
3  U(2)=V(L2(J))
   GO TO 5
4  U(2)=0.0
5  LL=J-1
   ANGLE=ANG(LL)
   CALL ZC
51  AMPL=AMPL*AMP
   PHASE=PHASE+PHA
6  CONTINUE
   IF (H-1) 610,60,610
610 IF (XG-UD) 712,712,611
611 AMPL=AMPL*GF
60  IF (PHASE) 601,8,602
601 PHASE=PHASE+360.0
   GO TO 60
602 IF (PHASE-360.0) 8,603,603
603 PHASE=PHASE-360.0
   GO TO 602
7  RAY=PSC0*(10**3)
   AMPL=AMPL*GF
   GO TO 8
71  WRITE(6,711)
711 FORMAT(1H,'NO HEAD WAVE AT CRITICAL DISTANCE')
   GO TO 714
712 WRITE(6,713)
713 FORMAT(1H,'RAY PATH LESS THAN UNIT DISTANCE')
714 AMPL=0.0
8  IF (RES(SC)-1) 88,81,88
81  S1PHI=SIN(ANG(SC)*DR)/1.74
   TTH=SIN(ANG(SC)*DR)/COS(ANG(SC)*DR)
82  C2PH=1.0-2.0*(S1PHI**2)

```

```

T2PH=SQRT(1.0-(C2PH**2))/C2PH
R=(C2PH*TTH)+2.0*(SIPHI**2)*T2PH
83 IF (RES(SC)-1) P5,831,85
831 IF (K) 84,92,84
84 AMPL=AMPL*SIN(ANG(SC)*DR)/R
GO TO 92
85 IF (R) 87,86,87
86 AMPL=C.0
GO TO 92
87 AMPL=AMPL*SIPHI*T2PH/R
GO TO 92
88 S1TH=SIN(ANG(SC)*DR)*1.74
SIPHI=SIN(ANG(SC)*DR)
IF (S1TH-1.0) 89,86,91
89 TTH=S1TH/SQRT(1.0-(S1TH**2))
GO TO 82
91 C2PH2=(1.0-2.0*(SIPHI**2))**2
T2PH2=(1.0-C2PH2)/C2PH2
TANH2TH=SIPHI/SQRT(SIPHI**2-(1.0/1.74)**2)
T2PH=SQRT(T2PH2)
IF (SIPHI-1.0) 911,86,911
911 R=SQRT(C2PH2*(TANH2TH**2)+4.0*(SIPHI**4)*T2PH2)
AMPL=AMPL*SIPHI*T2PH/R
PSH=ATAN((TANH2TH*SQRT(C2PH2))/(2.0*SIPHI**2*(SQRT(T2PH2))))
PHASE=PHASE+PSH/DR
92 RETURN
11 WRITE(6,111)
111 FORMAT(1H,/'FCCUS ON BOUNDARY - HEADWAVE NOT CALCULATED')
STOP
END

```

SUBROUTINE HEAD

C
C

```
COMMON/AA17/U(2), ANGLE, RAY, AMP, PHA  
DIMENSION RHO(2), V(2)  
INTEGER RAY, R1, P2, P3  
REAL M1, M2, K11, K21  
COMPLEX AA12, AA22, DD22, DD23, DD2, K12, K22, HPSP, HPSS, HSSP, HSSS  
CS(X)=SQRT(ABS(1.0-X**2))  
PI=4.0*ATAN(1.0)
```

```
RHO(1)=1.46+0.2375*U(1)  
RHO(2)=1.46+0.2375*U(2)  
RO=RHO(2)/RHO(1)
```

```
DO 1 I=1,2
```

```
1 V(I)=U(I)/1.74
```

```
R3=MOD(RAY,10)
```

```
R2=MOD(RAY,100)/10
```

```
R1=RAY/100
```

```
AA12=U(1)/U(2)
```

```
BB12=V(1)/V(2)
```

```
AB11=U(1)/V(1)
```

```
AB22=U(2)/V(2)
```

```
AB12=U(1)/V(2)
```

```
AB21=U(2)/V(1)
```

C

```
M1=((1.0/AB21)**2)-((RO*((1.0/AB22)**2))  
M2=(BB12**2)-FC
```

C

```
AA11=CS(AA12)  
BB11=CS(1.0/AB21)  
BB21=CS(1.0/AB22)
```

```

IF (AB12-1.0) 2,2,3
2 A12=CMPLX(CS(AB12),0.0)
GO TO 4
3 A12=CMPLX(0.0,CS(AB12))
4 A22=CMPLX(0.0,CS(AB22))
B12=CS(BB12)

```

C

```

D11=((M1+(RO-1.0)/2.0)**2)/(AB11*AB22)
D12=(RO*A11*B21)/(4.0*AB11*AA12)
D13=((M1+RO/2.0)**2)*A11*B11/(AA12*AB12)
D1=-((D11+D12+D13)**2)
D21=(AB22*((M2+(RO-1.0)/2.0)**2))/AB11
D22=(RO*A22*B12)/(4.0*AB12)
D23=((M2+RO/2.0)**2)*A12*B12/(AA12*AB12)
D2=-((D21+D22+D23)**2)

```

C

```

K11=((M1-0.5)*B21)/AB11-(((M1+RO/2.0)*B11)/AB12)/D1
K21=((M1*A11*B21)/AA12)+((M1+(RO-1.0)/2.0)/AB22)/C1
K12=((M2*A22*B12)/AB12)+((AB22*(M2+(RO-1.0)/2.0))/AB11)/O2
K22=((M2-0.5)*A22)-(((M2+RO/2.0)*A12)/AA12)/C2

```

C

```

HPSP=-((RC*(K12**2))/(2.0*AB12))
HPSS=(RC*K12*K22)/(2.0*AB12)
HSSP=(RC*K22*K12)/(2.0*AB12*(AB11**2))
HSSS=-((RC*(K22**2))/(2.0*AB12*(AB11**2)))

```

C

```

IF (P1-1) 41,41,48
41 IF (R2-1) 42,42,45
42 IF (R3-1) 43,43,44
43 AMP=(RC*(K11**2))/(2.0*AA12)
PHA=0.0

```

```

GO TO 416
44 AMP=(RO*K11*K21)/(2.0*AA12)
   PHA=0.0
GO TO 416
45 IF (R3-1) 46,46,47
46 AMP=CABS(HPSP)
   PHA=ATAN(AIMAG(HPSP)/REAL(HPSP))/(PI/180.0)
GO TO 416
47 AMP=CABS(HPSS)
   PHA=ATAN(AIMAG(HPSS)/REAL(HPSS))/(PI/180.0)
GO TO 416
48 IF (R2-1)49,49,413
49 IF (R3-1) 411,411,412
411 AMP=(RO*K21*K11)/(2.0*AA12*(AR11**2))
   PHA=0.0
GO TO 416
412 AMP=(RO*(K21**2))/(2.0*AA12*(AB11**2))
   PHA=0.0
GO TO 416
413 IF (R3-1) 414,414,415
414 AMP=CABS(HSSP)
   PHA=ATAN(AIMAG(HSSP)/REAL(HSSP))/(PI/180.0)
GO TO 416
415 AMP=CABS(HSSS)
   PHA=ATAN(AIMAG(HSSS)/REAL(HSSS))/(PI/180.0)
416 RETURN
      END

```

```

SUBROUTINE ZC
C
C   COMPUTE AMPLITUDE AND PHASE OF RESULTANT WAVE FROM
C   THAT INCIDENT ON BOUNDARY
C
COMMON/AL7/U(2),ANGLE,RAY,AMP,PHA
DIMENSION RHO(2),V(2),X(4),XI(4),Z(4,4),ZI(4,4),Y(8),W(8,8)
INTEGER RAY,INC,FES,TYPE,DIR
PI=4.0*ATAN(1.0)
C
C   DENSITY, VELOCITIES (P AND S) OF LAYERS
C
DO 106 I=1,2
IF (U(I))-2.28) 102,102,103
102 RHO(I)=0.42+0.775*U(I)
GO TO 106
103 IF (U(I))-6.27) 104,104,105
104 RHO(I)=1.84+0.155*U(I)
GO TO 106
105 RHO(I)=0.71+0.335*U(I)
106 CONTINUE
RO=RHO(2)/RHO(1)
DO 1 I=1,2
V(I)=U(I)/1.74
1 CONTINUE
C
C ANALYSING THE RAY
C
RES=MCD(RAY,10)
TYPE=(MCD(RAY,100))/10
DIR=(MOD(RAY,1000))/100
INC=RAY/1000
C
C INITIALIZE MATRICES

```

```

C
DO 5 J=1,4
X(J)=C.C
XI(J)=0.C
DO 5 K=1,4
Z(J,K)=0.C
ZI(J,K)=0.C
5 CONTINUE

C
C
C
CREATE MATRIX ELEMENTS
IF (INC-1) 51,51,52
51 CCN=SIN(ANGLE*PI/180.0)/U(1)
GO TO 53
52 CCN=SIN(ANGLE*PI/180.C)/V(1)
53 SINA=CCN*C(1)
SINB=CCN*V(1)
SINE=CCN*U(2)
SINF=CCN*V(2)
COSA=SQRT(ABS(1.0-SINA**2))
COSB=SQRT(ABS(1.0-SINB**2))
COSF=SQRT(ABS(1.0-SINE**2))
COSF=SQRT(ABS(1.0-SINF**2))
COS2A=1.0-2.0*(SINA**2)
COS2B=1.0-2.0*(SINB**2)
COS2F=1.0-2.0*(SINE**2)
SIN2A=2.0*SINA*COSA
SIN2B=2.0*SINB*COSB
SIN2E=2.0*SINE*CCSE
SIN2F=2.0*SINF*COSE
IF (TYPE) 54,86,54
54 IF(INC-1) 8,8,81

C
C
CREATE REAL MATRIX FOR INCIDENT P-WAVE

```

C

```
8 X(1)=SINA
  X(2)=COXA
  X(3)=-SIN2A
  X(4)=-CCS2B
  Z(1,1)=SINA
  Z(1,2)=-COSR
  Z(1,3)=SINE
  Z(1,4)=-CCSF
  Z(2,1)=-CCSA
  Z(2,2)=-SINB
  Z(2,3)=COSE
  Z(2,4)=SINF
  Z(3,1)=SIN2A
  Z(3,2)=-((U(1)/V(1))*CCS2B
  Z(3,3)=-RC*((V(2)/V(1))*2)*((U(1)/U(2))*SIN2E
  Z(3,4)=RQ*((V(2)/V(1))*2)*((U(1)/V(2))*CCS2F
  Z(4,1)=-CCS2B
  Z(4,2)=-((V(1)/U(1))*SIN2B
  Z(4,3)=-RC*(U(2)/U(1))*COS2F
  Z(4,4)=-RC*(V(2)/U(1))*SIN2F
```

C

CREATING IMAGINARY MATRIX FOR INCIDENT P-WAVE

C

```
9 IF (SINL-1.0) 10,10,9
  ZI(2,3)=Z(2,3)
  Z(2,3)=0.0
  ZI(3,3)=Z(3,3)
  Z(3,3)=0.0
10 IF (SINF-1.0) 12,12,11
11 ZI(1,4)=Z(1,4)
  Z(1,4)=0.0
  ZI(4,4)=Z(4,4)
  Z(4,4)=0.0
```

```

C
C
C
GO TO 12
CREATE REAL MATRIX FOR INCIDENT SV-WAVE

81 X(1)=SINB
X(2)=CCSR
X(3)=CCS2B
X(4)=-SIN2B
Z(1,1)=-CCSA
Z(1,2)=-SINB
Z(1,3)=CCSE
Z(1,4)=SINF
Z(2,1)=-SINA
Z(2,2)=CCSR
Z(2,3)=-SINE
Z(2,4)=COSF
Z(3,1)=(V(1)/U(1))*SIN2A
Z(3,2)=-CCS2B
Z(3,3)=-RC*((V(2)/U(2))**2)*(U(2)/V(1))*SIN2E
Z(3,4)=RC*(V(2)/V(1))*CCS2F
Z(4,1)=-((U(1)/V(1))*COS2R
Z(4,2)=-SIN2B
Z(4,3)=-RC*(U(2)/V(1))*COS2F
Z(4,4)=-RC*(V(2)/V(1))*SIN2F

C
C
C
CREATING IMAGINARY MATRIX FOR INCIDENT SV-WAVE

IF(SINA-1.0) 84,84,83
83 ZI(1,1)=Z(1,1)
Z(1,1)=0.0
ZI(3,1)=Z(3,1)
Z(3,1)=0.0
84 IF (SINE-1.0) 86,86,85
85 ZI(1,3)=Z(1,3)

```

```
Z(1,3)=0.0
ZI(3,3)=Z(3,3)
Z(3,3)=0.0
86 IF (SINF-1.0) 12,12,87
87 ZI(2,4)=Z(2,4)
Z(2,4)=0.0
ZI(4,4)=Z(4,4)
Z(4,4)=0.0
GO TO 12
```

C
C
C

P-WAVE INCIDENT ON FREE SURFACE

```
88 IF (INC-1) 89,89,91
89 X(1)=2.0*CCSA*SINB
X(2)=SINA*CCS2B
Z(1,2)=CCS2B
Z(2,2)=SINB*SIN2R
GO TO 92
```

C
C
C

SV-WAVE INCIDENT ON FREE SURFACE

```
91 X(1)=SINB*SIN2B
X(2)=CCS2B
Z(1,2)=SINA*CCS2B
Z(2,2)=2.0*CCSA*SINB
IF (SINA-1.0) 92,92,93
92 IF (AN) 924,921,924
921 IF (INC-1) 922,922,923
922 C=1.0
D=0.0
GO TO 925
923 C=0.0
D=1.0
GO TO 925
```

```

924 C=((Z(2,2)*X(1)-Z(1,2)*X(2))/(Z(2,2)*X(1)+Z(1,2)*X(2))
D=((2.0*X(1)*X(2))/(Z(2,2)*X(1)+Z(1,2)*X(2))
IF (INC-1) 5241,525,9241
9241 A=C
C=D
D=A
IF (D) 520, 528, 528
920 D=-D
GO TO 527
925 IF (C) 526, 528, 528
926 C=-C
927 CP=180.0
DP=180.0
GO TO 14
928 CP=0.0
DP=0.0
GO TO 14
93 C=0.0
D=1.0
CP=C.0
DP=ATAN(4.0*SQRT((1.0-(1.0/SINA)**2)))*
1((1.0/SINB)**2)-1.0)/((2.0-(1.0/SINB)**2))/(PI/180.0)
GO TO 14
C
C
C
CREATING COMPLEX MATRIX
12 DO 13 J=1,4
K=J+4
Y(J)=X(J)
Y(K)=XI(J)
DO 13 L=1,4
M=L+4
W(J,L)=Z(J,L)
W(J,M)=ZI(J,L)

```

```

W(K,L)=-Z(J,L)
W(K,M)=Z(J,L)
13 CONTINUE
C
C SOLVE LINEAR EQUATIONS
C
CALL SIMQ(W,Y,8,0)
C=SQRT(Y(1)**2+Y(5)**2)
D=SQRT(Y(2)**2+Y(6)**2)
E=SQRT(Y(3)**2+Y(7)**2)
F=SQRT(Y(4)**2+Y(8)**2)
IF ((Y(1).EQ.0.0).AND.(Y(5).EQ.0.0)) GO TO 131
CP=ATAN2(Y(5),Y(1))/(PI/180.0)
GO TO 132
121 CP=C.C
132 IF ((Y(2).EQ.0.0).AND.(Y(6).EQ.0.0)) GO TO 133
DP=ATAN2(Y(6),Y(2))/(PI/180.0)
GO TO 134
133 DP=C.C
134 IF ((Y(3).EQ.0.0).AND.(Y(7).EQ.0.0)) GO TO 135
EP=ATAN2(Y(7),Y(3))/(PI/180.0)
GO TO 136
135 EP=C.C
136 IF ((Y(4).EQ.0.0).AND.(Y(8).EQ.0.0)) GO TO 137
FP=ATAN2(Y(8),Y(4))/(PI/180.0)
GO TO 14
137 FP=C.C
14 CONTINUE
C
C OUTPUT
C
IF (TYPE-1)1000,20,1000
1000 IF (RES-1) 110,110,120
110 AMP=C

```

```
PHA=CP
GO TO 10
120 AMP=D
PHA=DP
GO TO 16
20 IF (RES-1)210,210,220
210 AMP=E
PHA=EP
GC TO 16
220 AMP=F
PHA=FP
16 CONTINUE
RETURN
END
```

```

C
C
C
PART 2 PRGRAMME FIS
COMPLEX X(64),P(64,300),Y(64)
DIMENSION F(64),PI(64),FT(64,300),PHI(64,300)
1,AMP(300),YA(64),YF(64,300),TF(9000),AMPF(9000),TIM(300),XH(300),
2PHA(300),ZZ(9000)
DOUBLE PRECISION TF,TIM,TM
DATA YES/3HYES/
DR=(4.0)*ATAN(1.0)/180.0
DO 121 JG=1,5000
121 AMPF(JG)=C.0
READ(4,1) N
1 FORMAT(I5)
2 READ(3,2) (TIM(I),AMP(I),PHA(I),XH(I),I=1,N)
2 FORMAT(11X,F14.2,20X,F15.4,F8.2,4X,F6.1)
KK=N-1
DO 20 I=1,KK
LL=I+1
DO 20 J=LL,N
IF (TIM(I)-TIM(J)) 20,20,201
201 TM=TIM(J)
AMPM=AMP(J)
PHAM=PHA(J)
XM=XH(J)
TIM(J)=TIM(I)
AMP(J)=AMP(I)
PHA(J)=PHA(I)
XH(J)=XH(I)
TIM(I)=TM
AMP(I)=AMPM
PHA(I)=PHAM
XH(I)=XM
20 CCNTINUE

```

```

NU=5
TU=0.01
M=2*#NU
READ(8,12) FIX
12 FORMAT(A3)
READ(8,11) (X(I),I=1,M)
11 FORMAT(2F10.3)
CALL NLOGN(NU,X,-1.0)
DO 3 K=1,M
F(K)=CABS(X(K))
IF ((REAL(X(K)).NE.0.0).AND.(AIMAG(X(K)).NE.0.0)) GO TO 22
21 PHI(K)=0.0
GO TO 3
22 PHI(K)=ATAN2(AIMAG(X(K)),REAL(X(K)))/DR
3 CONTINUE
DO 4 J=1,N
DO 4 L=1,M
IF (XH(J)) 31,31,32
31 FT(L,J)=F(L)*AMP(J)
GO TO 33
32 FT(L,J) =(FLCAT(M+1)/FLOAT(L))*F(L)*AMP(J)*TU
33 PHIT(L,J) =PHI(L)+PHA(J)
4 CONTINUE
DO 5 I=1,N
DO 41 J=1,M
PHIT(J,I)=PHIT(J,I)*DR
A=FT(J,I)*CCS(PHIT(J,I))
B=FT(J,I)*SIN(PHIT(J,I))
Y(J)=CMPLX(A,B)
41 CONTINUE
CALL NLOGN(NU,Y,1.0)
DO 43 J=1,M
YA(J)=CABS(Y(J))
IF ((REAL(Y(J)).NE.0.0).AND.(AIMAG(Y(J)).NE.0.0)) GO TO 42

```

```

YF(J,I)=YA(J)
GO TO 5
42 YF(J,I)=YA(J)*COS(ATAN2(AIMAG(Y(J)),REAL(Y(J))))
43 CONTINUE
5 CONTINUE
TF(I)=TIM(I)
L=1
I=1
1001 IF (DABS(TF(I)-TIM(L))-0.004) 8,8,7
8 DO 9 K=1,M
LL=K+I-1
9 AMPF(LL)=AMPF(LL)+YF(K,L)
LLF=LL
L=L+1
IF (L.GT.N) GO TO 100
IF (DABS(TIM(L)-TIM(L-1))-0.004) 1001,1001,7
7 I=I+1
TF(I)=TF(I-1)+0.01
GO TO 1001
100 DO 102 JN=1,LLF
102 AMPF(JN)=AMPF(JN)*100.0
WRITE(5,111) TF(I)
111 FORMAT(1H , /'ORIGIN AT ',F10.2,' SECS')
IF (FIX.EQ.YES) GC TO 113
CMIN=AMPF(1)
CMAX=AMPF(1)
DO 112 JJ=2,LLF
CMIN=AMIN1(AMPF(JJ),CMIN)
112 CMAX=AMAX1(AMPF(JJ),CMAX)
GO TO 115
113 READ(7,114) CMIN,CMAX
114 FORMAT(2F10.4)
115 ZZ(1)=0.0
DO 116 JJ=2,LLF

```

```

116 ZZ(JJ)=ZZ(JJ-1)+0.01
SCM=(CMAX-CMIN)/9.0
XMAX=ZZ(LLF)
XL=4.0*XMAX
CALL PLTXMX(105.0)
CALL PAXIS(1.2,0.2,8+SYN SEIS,8,9.0,90.0,CMIN,SCM,1.0)
CALL PAXIS(1.2,5.2,1H ,0,XL,0.0,0.0,1.0,1.0)
CALL PLTOFS(0.0,1.0,0.0,SCM,1.2,5.2)
CALL PLINE(ZZ(I),AMPF(I),LLF,1,0,0,1)
CALL PLTEND
IF (FIX.EC.YES) REWIND 7
WRITE(7,114) CMIN,CMAX
STOP
END

```

C
C
C

```

SUBROUTINE NLOGN(N,X,SIGN)
FAST FOURIER TRANSFORM USING COOLEY TUKEY ALGORITHM
NMAX=LARGEST VALUE OF N TO BE PROCESSED
NON DUMMY DIMENSION M(NMAX)
FOR EXAMPLE,IF NMAX=25 THEN
COMPLEX X,WK,FCLD,G
DIMENSION M(256),X(40)
LX=2**N
DO 1 I=1,N
1 M(I)=2***(N-I)
DO 4 L=1,N
NBLOCK=2***(L-1)
LBLOCK=LX/NBLOCK
LBHALF=LBLOCK/2
K=0
DO 4 IBLOCK=1,NBLOCK
FK=K

```

```

FLX=LX
V=SIGN*0.2831853*FK/FLX
AA=COS(V)
BB=SIN(V)
WK=CMPLX(AA,BB)
I=I+1
DO 2 I=1, LBHALF
  J=I*START+I
  JH=J+LBHALF
  Q=X(JH)*WK
  X(JH)=X(J)-Q
  X(J)=X(J)+Q
2 CONTINUE
DO 3 I=2,N
  II=I
  IF(K.LT.M(II)) GO TO 4
3 K=K-M(II)
4 K=K+M(II)
  K=0
DO 7 J=1,LX
  IF(K.LT.J)GO TO 5
  HOLD=X(J)
  X(J)=X(K+1)
  X(K+1)=HOLD
5 DO 6 I=1,N
  II=I
  IF(K.LT.M(II)) GO TO 7
6 K=K-M(II)
7 K=K+M(II)
  IF(SIGN.LT.0,J) GO TO 9
DO 8 I=1,LX
8 X(I)=X(II)/FLX
9 RETURN
END

```

```
$EMPTY -A
$COPY GPL7:SINC+GPL7:SUMRAYC+GPL7:DI GC+GPL7:TCLC+GPL7:PSC -A
$EMPTY -B
$COPY GPL7:ZVANGTC+GPL7:FEAC+GPL7:ZVAC+GPL7:AMPHAC+GPL7:ZDC+GPL7:Hf ACC -B
$EMPTY -C
$EMPTY -C
$EMPTY -E
$RUN -A+-B+*SSP 3=-C 4=-D 5=GPM8:DAT 6=-E
$EMPTY -FLOTF
$EMPTY -P
$RUN GPL7:FISC+*PLOTSYS 9=-PLOTf 3=-C 4=-D 6=-P 8=GPM8:D 7=-G
$EMPTY -Q
$LIST -P+-E
$PUN *DURPLCT 1=-PLOTf 2=*PUNCH* 5=*DUMMY*
```

REFERENCES

- AL-CHALABI, M. 1971. Reliability of the rotation pole in continental fitting. EARTH PLANET SCI. LETTERS 11 p. 257.
- ANDERSON, D. L. 1965. Recent evidence concerning the structure and composition of the earth's mantle. PHYS. CHEM. OF THE EARTH 6 p. 1.
- ARTEMJEV, M. E. 1971. Structure and isostasy of the
AFTYUSHKOV, E. V. Baikal Rift and the mechanism of rifting. JO. GEOPHYS. RES. 76 p. 1197.
- BACKHOUSE, R. W. 1972. Upper mantle structure using P-wave data from an East African array station. Ph.D. THESIS UNIV. OF DURHAM.
- BAILEY, D. K. 1964. Crustal warping - a possible tectonic control of alkaline magmatism. JO. GEOPHYS. RES. 69 p. 1103.
- BAKER, B. H. 1969. Structural evolution of the Rift zones in the Middle East - a comment. NATURE 224 p. 359.

- BAKER, B. H. 1971. Structure and evolution of the
WOHLENBERG, J. Kenya Rift Valley.
NATURE 229 p. 538.
- BÅTH, M. 1960. Crustal Structure of Iceland.
JO. GEOPHYS. RES. 65
p. 1793.
- BÅTH, M. 1968. Mathematical aspects of
Seismology.
ELSEVIER PUBL. CO.
AMSTERDAM.
- BERRY, M. J. 1966. Reflected and headwave
WEST, G. F. amplitudes in a medium of
several layers.
THE EARTH BENEATH THE
CONTINENTS.
AMERICAN GEOPHYS. UN.
WASH. D. C. p. 464.
- BIRCH, F. 1955. Physics of the crust.
GEOL. SOC. AM. Special
Paper 62 p. 101.
- BIRCH, F. 1960. The velocity of compressional
waves in rocks to 10 k bars. 1.
JO. GEOPHYS. RES. 65
p. 1083.
- BIRCH, F. 1961. The velocity of compressional
waves in rocks to 10 k bars. 2.
JO. GEOPHYS. RES. 66
p. 2199.
- BIRTILL, J. W. 1965. The application of phased
WHITEWAY, F. E. arrays to the analysis of
seismic body waves.
PHIL. TRANS. ROY. SOC.
LON. SERIES A 258 p. 421.

- BLOCH, S. 1969. Velocities in the crust and upper mantle of southern Africa from multimode surface wave dispersion. BULL. SEIS. SOC. AM. 59 p. 1599.
- HALES, A. L.
- LANDISMAN, M.
- BLUNDELL, D. J. 1969. A study of crustal structure beneath the Irish Sea. GEOPHYS. JO. ROY. ASTR. SOC. 17 p. 45.
- PARKS, R.
- BONJER, K. P. 1970. Crustal structure of East African Rift System from spectral response ratios of long period body waves. ZEITSCHRIFT GEOPHYS. 36 p. 287.
- FUCHS, K.
- WOHLENBERG, J.
- BOTT, M. H. P. 1965. Formation of ocean ridges. NATURE 207 p. 840.
- BREKHOVSKIKH, L. M. 1960. Waves in layered media. ACADEMIC PRESS N. Y.
- BROCK, B. B. 1965. The Rift Valley Craton. THE WORLD RIFT SYSTEM GEOL. SURV. CANADA. PAPER 66. 14 p. 99.
- BRUNE, J. 1963. Seismic waves and earth structure in the Canadian Shield. BULL. SEIS. SOC. AM. 53 p. 167.
- DORMAN, J.

- BUCHSTEIN, M. 1969. Les sources thermales et
 Le BAIL, A. thermo-minerals de la
 Republique democratique
 de Congo.
 PROC. SYM. 2, XXIII INT.
 GEOL. CONG. 19 p. 87.
- BULLARD, E. C. 1936. Gravity measurements in
 East Africa.
 PHIL. TRANS. ROY. SOC.
 LON. SERIES A. 235 p. 445.
- CERVENY, V. 1966. On dynamic properties of
 reflected and headwaves in
 the n-layered earth's crust.
 GEOPHYS. JO. ROY. ASTR.
 SOC. 11 p. 139.
- CLIFFORD, T. N. 1970. The structural framework of
 Africa.
 AFRICAN MAGMATISM and
 TECTONICS OLIVER and
 BOYD. EDIN. p. 1.
- COOK, K. L. 1962. The problem of the mantle-
 crust mix: lateral inhomogeneity
 in the uppermost part of the
 Earth's mantle.
 ADVAN. GEOPHYS. 9
 p. 295.
- COOK, K. L. 1969. Active Rift System in the
 Basin and Range Province.
 TECTONOPHYSICS 8 p. 469.
- COOLEY, J. S. 1965. An algorithm for the machine
 TUKEY, J. W. calculation of complex fourier
 series.
 MATH. COMP. 19 p. 297.

- CORBISHLEY, D. J. 1969. Measurements of the derivative of the P-wave travel time curve by means of an array network. PhD. THESIS UNIV. OF DURHAM.
- DARRACOTT, B. W. 1972. Gravity and magnetic surveys in Northern Tanzania and Southern Kenya. TECTONOPHYSICS 15 p. 131.
- FAIRHEAD, J. D.
- GIRDLER, R. W.
- DAVIES, K. A. 1951. The Uganda section of the Western Rift. GEOL. MAG. 88 p. 377.
- De BREMEACKER, J. C. L. 1959. Seismicity of the East African Rift Valley. JO. GEOPHYSICS. RES. 64 p. 1961.
- DIXEY, F. 1956. The East African Rift System. BULL. COLON. GEOL. MIN. RES. SUPPL.
- DIXON, C. G. 1969. Thermal and mineral springs in Uganda. PROC. SYM. 2 XXIII INT. GEOL. CONG. 19 p. 191.
- MORTON, W. H.
- DOPP, S. 1964. Preliminary note on the refracted P-phase in the Western Rift Valley of Africa. JO. GEOPHYS. RES. 69 p. 3027.
- DOUGLAS, A. 1967. A special purpose least squares programme. A. W. R. E. BLACKNEST REPORT No. 0-54/66.

- DRAKE, C. L. 1964. A geophysical study of the Red Sea.
GIRDLER, R. W. GEOPHYS. JO. ROY. ASTR. SOC. 8 p. 473.
- ELDER, J 1970. Quantative laboratory structures of dynamic models of igneous intrusions.
In MECHANISMS OF IGNEOUS INTRUSION
GEOL. JO. SPECIAL PAPER No. 2.
- EWING, M. E. 1956. Mid-Atlantic Ridge Seismic belt.
HEEZEN, B. C. EOS. TRANS. A. G. U. 37 p. 342.
- EVING, W. M. 1957. Elastic waves in layered media.
JARDETKY, W. S. McGRAV/ HILL BOOK COMP. N. Y.
PRESS, F.
- FAIRHEAD, J. D. 1968. The Seismicity of the East African Rift System 1955 to 1958.
M. Sc. DISSERTATION UNIV OF NEWC. UPON TYNE.
- FAIRHEAD, J. D. 1971. The seismicity of Africa.
GIRDLER, R. W. GEOPHYSICS JO. ROY. ASTR. SOC. 24 p. 610.
- FAIRHEAD, J. D. 1972. New K/Ar determinations on Rift volcanics of S. Kenya and their bearing on age of Rift faulting.
MITCHELL, J. G. NATURE PHYS. SCI. 258
WILLIAMS, L. A. J. p. 66.

- FLORENISOV, N. A. 1969. Rifts of the Baikal Mountain region.
TECTONOPHYSICS 8 p. 443.
- FRANCIS, T. J. G. 1968. The detailed seismicity of mid-ocean ridges.
EARTH PLANET SCI. LETTERS 4 p. 39.
- FREUND, R. 1970. Plate Tectonics of the Red Sea and Africa.
NATURE 228 p. 453.
- FUCHS, K. 1966. Detailed crustal investigation along a north-south section through the central part of Western Germany.
THE EARTH BENEATH THE CONTINENTS
AMERICAN GEOPHYSICS UNIV. WASH. D C. p. 433.
- GANE, P. G. 1956. Crustal structure in the Transvaal.
ATKINS, A. R. BULL. SEIS. SOC. AM.
SELLSCHOP, J. P. F. 46 p. 293.
- SELIGMAN, P. 1972. The role of magmatic processes in continental rifting and sea-floor spreading.
FOURTH TOMKIEFF MEMORIAL LECTURE. GEOL. DEPT. UNIV. OF NEWC. -UPON-TYNE.
- GASS, I. G. 1969. Structural Evolution of the Rift zones in the middle east.
GIBSON, I. L. NATURE 221 p. 926.

- GILL, R. C. O. 1973. Mechanism for the salic magma bias of continental alkaline provinces.
NATURE PHYS. SCI. 242
p. 41.
- GIRDLER, R. W. 1964. Geophysical Studies of Rift Valleys.
PHYS. CHEM. OF EARTH 5 p. 121.
- GIRDLER, R. W. 1969. Evolution of rifting in Africa.
FAIRHEAD, J. D. NATURE 224 p. 1178.
SEARLE, R. C.
- SOWERBUTTS, W. T. C.
- GREEN, D. H. 1967. The genesis of basalt magmas.
RINGWOOD, A. E. CONTR. MINERAL PETROL. 15 p. 103.
- GRIFFITHS, D. H. 1972. Some comments on the results of a seismic refraction experiment in the Kenya Rift.
TECTONOPHYSICS 15 p. 151.
- GRIFFITHS, D. H. 1971. Seismic refraction line in the Gregory Rift.
KING, R. F. NATURE 229 p. 69.
KHAN, M. A.
- BLUNDELL, D. J.
- GUMPER, F. 1970. Seismic wave velocities and earth structure on the African continent.
POMEROY, P. W. BULL. SEIS. SOC. AM. 60 p. 651.
- GUTENBERG, B. 1954. Effects of low velocity layers.
GEOFIS. PURA. APPL. 28 p. 1.

- GUTENBERG, B. 1955. Wave velocities in the earth's crust.
In THE CRUST OF THE EARTH
GEOL. SOC. AM. SPECIAL
PAPER No. 62 p. 19.
- HALES, A L.
SACKS, I. S. 1959. Evidence for an intermediate
layer from crustal structure
studies in Eastern Transvaal.
GEOPHYS. JO. ROY. ASTR.
SOC. 2 p. 15.
- HARRIS, P. G. 1969. Basalt type and rift valley
tectonism.
TECTONOPHYSICS 8 p. 427.
- HARRIS, P. G. 1970. Convection and magmatism
with reference to the African
continent.
In AFRICAN MAGMATISM
AND TECTONICS.
OLIVER AND BOYD EDIN.
p. 419.
- HAST, N. 1969. The state of stress in the
upper part of the earth's crust.
TECTONOPHYSICS 8 p. 169.
- HEPVORTH, J. V.
KENNERLEY, J. B. 1970. Photogeology and structure of
the Mozambique orogenic
front near Kolo, northeast
Tanzania.
GEOL. SOC. LON. PROC.
No. 1662 p. 62.

- HERRIN, E. 1969. Regional variations of P-wave velocity in the upper mantle beneath North America. In THE EARTH'S CRUST AND UPPER MANTLE AMERICAN GEOPHYS. UNIV. WASH. D C. p. 242.
- HERRIN, E. 1968. Regional variations in P TAGGART, J. travel times. BULL. SEIS. SOC. AM. 58 p. 1325.
- HILLER, W. 1967. La seismicite du Fosse ROTHE, J. P. Rhenan. ABHANDL GEOL. LANDESAMTES SCHNEIDER, G. BADEN-WURTTEMBERG 6 p. 98.
- ILLIES, J. H. 1969. An intercontinental belt of the World Rift System. TECTONOPHYSICS 8 p. 5.
- JACOB, A. W. B. 1969. Crustal phase velocities observed at the Eskdalemuir seismic array. GEOPHYS. JO. ROY. ASTR. SOC. 18 p. 189.
- JENNINGS, D. J. 1964. Geology of the Kapsabet Plateau Area. GEOL. SURVEY KENYA REPORT No. 63.
- KELLY, E. J. 1964. Limited network processing of seismic signals. M. I. T. LINCOLN LAB. GROUP REPORT 44.

- KHAN, M. A. 1971. Gravity measurements in the Gregory Rift. NATURE 229 p. 72.
- MANSFIELD, J.
- KING, B. C. 1970. Vulcanicity and Rift tectonics in East Africa. In AFRICAN MAGMATISM AND TECTONICS OLIVER AND BOYD EDIN. p. 263.
- KING, B. C. 1972. Volcanism of the Kenya Rift Valley. PHIL. TRANS. ROY. SOC. LON. SERIES A. 271 p. 185.
- CHAPMAN, G. R.
- KNOPOFF, L. 1957. Surface Amplitudes of reflected body waves. GEOPHYSICS 22 p. 842.
- FREDERICKS, R. V.
- GANGI, A. F.
- PORTER, L. D.
- KNOPOFF, L. 1972. Rayleigh Wave Phase Velocities for the path Addis Ababa-Nairobi. TECTONOPHYSICS 15 p. 157.
- SCHLUE, J. V.
- KOLSKY, H. 1963. Stress waves in solids. DOVER PUBL. INC.
- LANDISMAN, M. 1966. Seismic Studies of the earth's crust in continents Part 2. Evidence for a low velocity zone in the upper part of the lithosphere. GEOPHYS. JO. ROY. ASTR. SOC. 10 p. 525.
- MUELLER, ST.

- LANDISMAN, M. 1966. Seismic studies of the earth's crust in continents Part 2. Analysis of wave propagation in continents and adjacent shelf areas. GEOPHYS. JO. ROY. ASTR. SOC. 10 p. 539.
- MUELLER, ST.
- LILWALL, R. C. 1970. Estimation of P-wave travel times using the joint epicentre method. GEOPHYS. JO. ROY. ASTR. SOC. 19 p. 165.
- DOUGLAS, A.
- Le BAS, M. J. 1971. Per-alkaline volcanism, crustal swelling and rifting. NATURE PHYS. SCI. 230 p. 85.
- Le PICHON, X. 1968. Sea floor spreading and continental drift. JO. GEOPHYS. RES. 73 p. 3661.
- Le PICHON, X 1965. Crustal structure of the mid ocean ridges (1). Seismic refraction measurements. JO. GEOPHYS. RES. 70 p. 319.
- HOUTZ, R. E.
- DRAKE, C. L.
- NAFE, J. E.
- LOGATCHEV, N. A. 1972. East African Rift development. TECTONOPHYSICS 15 p. 71.
- BELOUSSOV, V. V.
- MILANOVSKY, E. E.
- LONG, R. E. 1968. Temporary seismic array stations. GEOPHYS. JO. ROY. ASTR. SOC. 16 p. 37.

- LONG, R. E. 1972. The structure of East Africa using surface wave dispersion and Durham seismic array data.
TECTONOPHYSICS 15 p. 165.
- BACKHOUSE, R. V.
MAGUIRE, P. K. H.
SUNDARALINGHAM, K.
- LONG, R. E. 1969. Teleseismic P-wave delay time in Iceland.
GEOPHYS. JO. ROY. ASTR. SOC. 20 p. 41.
- MITCHELL, M. G.
- MAASHA, N. 1972. Earthquake fault parameters and tectonics in Africa.
JO. GEOPHYS. RES. 77
p. 5731.
- MOLNAR, P.
- MAGNITSKY, V. A. 1970. Problem of phase transitions in the upper mantle and its connection with the Earth's crustal structure.
JO. GEOPHYS. RES. 75
p. 877.
- KALASHNIKOVA, N.
- MALZER, H. 1967. Studies of relative vertical earth crustal movements in the Rhinegraben from Rastatt to Basel.
ABHANDL. GEOL. LANDESAMTES BADEN. WURTTEMBERG
6 p. 20.
- McCALL, G. J. H. 1967. Geology of the Nakuru-Thomson's Falls - Lake Hannington area.
GEOL. SURVEY KENYA REPORT No. 78.

- McCAMY, K. 1964. A correlation method of
MEYER, R. P. apparent velocity measurement.
JO. GEOPHYS. RES. 69
p. 691.
- McCONNELL, R. B. 1972. Geological development of the
Rift System of East Africa.
GEOL. SOC. AM. BULL.
83 p. 2549.
- McKENZIE, D. P. 1970. Plate tectonics of the Red Sea
and East Africa.
DAVIES, D. NATURE 226 p. 243.
MOLNAR, P.
- MEISSNER, R. 1967. Seismic refraction measurements
BECKHEMER, H. in the northern Rhinegraben.
ABHANDL. GEOL.
LANDESAMTES BADEN-
WURTEMBERG 6 p. 105.
- MOHR, P. A. 1970. Plate Tectonics of the Red
Sea and East Africa.
NATURE 228 p. 547.
- MOLNAR, P. 1971. A microearthquake survey in
AGGARWAL, Y. P. Kenya.
BULL. SEIS. SOC. AM.
61 p. 195.
- MOLNAR, P. 1969. Lateral variations of
OLIVER, J. attenuation in the upper mantle
and discontinuities in the
lithosphere.
JO. GEOPHYS. RES. 74 p. 2648.
- MUELLER, ST. 1969. Crustal structure beneath the
PETERSCHMITT, E. Rhinegraben from seismic
FUCHS, K. refraction and reflection
ANSORGE, J. measurements.
TECTONOPHYSICS 8 p. 529.

- | | | |
|-----------------------------|------|--|
| MUIRHEAD, K. J. | 1968 | The reduction and analysis of seismic data using digital computers.
Ph. D. THESIS A. N. U. |
| MULLER, G. | 1968 | Theoretical seismograms for some types of point sources in layered media. Part 1 Theory.
ZEITSCHRIFT GEOPHYSIK <u>34</u> p. 15. |
| NAFE, J. E.
DRAKE, C. L. | 1963 | Physical properties of marine sediments.
THE SEA <u>3</u> p. 794
INTERSCIENCE PUBL. N. Y. |
| O'BRIEN, P. N. S. | 1964 | Seismic waves observed 20 km from explosions in a Lake.
B. P. RES. CENTRE REP. 140. |
| O'BRIEN, P. N. S. | 1965 | Analysis of the Bormio and Raile refraction records of the 1962 Lake Lagorai explosions.
B. P. RES. CENTRE REP. 144. |
| OSMASTON, M. F. | 1971 | Genesis of ocean ridge median valleys and continental rift valleys.
TECTONOPHYSICS <u>11</u> p. 387. |
| REEVES, W. H. | 1969 | Thermal and mineral waters of Zambia.
PROC. SYM. <u>2</u> XXIII INT. GEOL. CONG. <u>19</u> p. 215. |
| RICHTER, C. F. | 1958 | Elementary seismology.
H. FREEMAN and CO. INC. |

- ROBERTS, D. G. 1969. Structural evolution of the Rift zones in the Middle East. NATURE 223 p. 55.
- ROBINSON, E. A. 1967. Multichannel time series analysis with digital computer programmes. HOLDEN-DAY. SAN-FRANCISCO.
- ROTHE, J. P. 1954. La zone seismique mediane Indo-Atlantique. PROC. ROY. SOC. LON. SERIES A 222 p. 389.
- RYKOUNOV, L. N. 1972. Study of microearthquakes in the Rift zones of East Africa. SEDOV, V. V. TECTONOPHYSICS 15 p. 123.
- SAVRINA, L. A.
- BOURMIN, V. J. U.
- SANDERS, L. D. 1964. Geology of the Eldoret area. GEOL. SURVEY KENYA REP. 64.
- SEARLE, R. C. 1970. Evidence from gravity anomalies for thinning of the lithosphere beneath the Rift Valley of Kenya. GEOPHYS. JO. ROY. ASTR. SOC. 21 p. 13.
- SOWERBUTTS, W. T. C. 1969. Crustal structure of the East African Plateau and Rift Valleys from gravity measurements. NATURE 223 p. 143.
- SPENCER, T. W. 1960. The method of generalized reflection and transmission coefficients. GEOPHYSICS 25 p. 625.

- STEINHART, J. S. 1962. The Earth's crust.
GREEN, R. CARNEGIE INST. WASH.
ASADA, T. YEAR BOOK 61 p. 221.
RODRIGUEZ, A.
ALDRICH, L. T.
TUVE, M. A.
- SUNDARALINGHAM, K. 1971. Seismic investigation of the
crust and upper mantle of
East Africa.
PhD. THESIS UNIV OF DURHAM.
- SUTTON, G. H. 1958. Seismological studies of the
Western Rift Valley of Africa.
BERG, E. TRANS. AMER. GEOPHYS.
UNION 39 p. 474.
- SYKES, L. R. 1967. Mechanism of earthquakes
and nature of faulting on the
mid oceanic ridges.
JO. GEOPHYS. RES. 72
p. 2131.
- SYKES, L. R. 1964. The seismicity of East Africa,
LANDISMAN, M. the Gulf of Aden, and the
Arabian and Red Seas.
BULL. SEIS. SOC. AM.
54 p. 1927.
- TALWANI, M. 1965. Crustal structure of the Mid-
ocean Ridges (2). Computed
Le PICHON, X. model from gravity and seismic
EWING, M. refraction data.
JO. GEOPHYS. RES. 70 p. 341.
- THOMPSON, A. O. 1963. Geology of the Naivasha area.
DODSON, R. G. GEOL. SURVEY KENYA
REPORT No. 55.

- TOBIN, D. G. 1969. Microearthquakes in the
 Rift Valley of Kenya.
 BULL. GEOL. SOC. AM.
80 p. 2043.
- WARD, P. L.
 DRAKE, C. L.
- VON HERZEN, R. P. 1967. Terrestrial heat flow in
 Lake Malawi, Africa.
 JO. GEOPHYS. RES. 72
 p. 4221.
- VACQUIER, V.
- WALKER, B. G. 1969. Springs of deepseated origin
 in Tanzania.
 PROC. SYM. 2 XXIII INT.
 GEOL. CONG. 19 p. 171.
- WARD, P. L. 1969. Microearthquake survey and
 the Mid-Atlantic Ridge in
 Iceland.
 JO. GEOPHYS. RES. 74
 p. 665.
- PALMASON, G.
 DRAKE, C.
- WATSON, G. N. 1952. A treatise on the theory of
 Bessel functions.
 CAMBRIDGE UNIV. PRESS, N. Y.
- WAYLAND, E. J. 1935. Notes on thermal and hot
 springs in Ugan 'a.
 BULL. GEOL. SURVEY.
 UGANDA 2 p. 144.
- WILLIAMS, L. A. J. 1969. Volcanic associations in the
 Gregory Rift Valley, East
 Africa.
 NATURE 224 p. 61.
- WILLIAMS, L. A. J. 1970. The volcanics of the Gregory
 Rift, East Africa.
 BULL. VOLCAN. XXXIV-2
 p. 439.

- WILLIAMS, L. A. J. 1972. The Kenya Rift volcanics
A note on volumes and chemical
composition.
TECTONOPHYSICS 15 p. 83.
- WILLIS, B. 1936. East African Plateau and Rift
Valleys.
CARNEGIE.
- WILLMORE, P. L. 1952. Seismic investigation of
HALES, A. L. crustal structure in the
GANE, P. G. Western Transvaal.
BULL. SEIS. SOC. AM. 42
p. 58.
- WOHLENBERG, J. 1970. On the seismicity of the East
African Rift System.
In GRABEN PROBLEMS
IUMP SCIEN. REPORT 27
p. 289.
- WOHLENBERG, J. 1972. Report on airmagnetic surveys
BHATT, N. V. of two areas in the Kenya Rift
Valley.
TECTONOPHYSICS 15 p. 143.
- WRIGHT, J. B. 1965. Petrographic subprovinces in
the Tertiary to Recent
volcanics of Kenya.
GEOL. MAG. 102 p. 541.

